

University of Bielefeld
Theoretical Physics

Diploma thesis

Algorithmic approach to finite-temperature QCD

Jan Möller

Presented to: Dept. of Physics, University of Bielefeld
Date: 9th April, 2009

PD Dr. YORK SCHRÖDER (1st corrector)
Prof. Dr. MIKKO LAINE (2nd corrector)

Abstract

In this thesis we describe an approach to deal with high-order loop corrections in a systematic way. We apply this approach to determine the $\mathcal{O}(g^6)$ contribution to the electric screening mass m_E^2 and $\mathcal{O}(g^8)$ correction to the effective gauge coupling g_E^2 appearing as matching coefficients in so-called EQCD, which acts as a large-distance effective theory for the theory of strong interactions at finite-temperature. The first chapter summarises the theoretical tools needed in order to simplify this task. The second chapter illustrates the necessity of using computer algebra systems (CAS) to deal with very large algebraic expressions and the concrete implementation of our calculation in FORM. In chapter three we evaluate basketball-like sum-integrals by methods originally introduced by Arnold & Zhai. The fourth chapter concludes with results from the three-loop computation and an outlook about what has to be done to complete the calculation.

Zusammenfassung

In dieser Diplomarbeit beschreiben wir einen systematischen Ansatz für Schleifen-Korrekturen höherer Ordnung. Dieses wenden wir an um den $\mathcal{O}(g^6)$ Beitrag zur elektrischen Abschirm-Masse m_E^2 und die $\mathcal{O}(g^8)$ Korrektur zur effektiven Eichkopplung g_E^2 zu berechnen. Beide treten als Matching-Koeffizienten in der sogenannten EQCD, einer effektive Theorie der starken Wechselwirkung bei endlicher Temperatur, auf. Das erste Kapitel umfasst theoretische Hilfsmittel um diese Aufgabe zu vereinfachen. Im zweiten Kapitel illustrieren wir die Notwendigkeit der Nutzung von Computer-Algebra-Systemen um mit langen algebraischen Ausdrücken umzugehen. In Kapitel drei berechnen wir Basketball-ähnliche Summenintegrale mit Methoden von Arnold & Zhai. Im vierten Kapitel diskutieren wir die Ergebnissen der Drei-Schleifen-Rechnung und geben einen Ausblick darüber was noch getan werden muss um die Rechnung zu vervollständigen.

Contents

Preface	3
1 Introduction and theoretical tools	5
1.1 Partition function and path integral	5
1.2 Free scalar field	7
1.3 Interacting scalar field	7
1.4 Green's functions and generating functionals	11
1.5 Background field method	14
1.6 QCD Feynman rules and renormalisation	15
1.7 QCD at high temperatures	18
1.8 Matching computation	20
1.9 Spatial string tension	22
2 Framework: Automated loop computations	23
2.1 One-loop evaluation by hand	23
2.2 Two-loop	29
2.3 Some preparations	30
2.4 Integration by parts relations and shifts	35
2.5 Reduction: Laporta algorithm and decompositions	38
2.6 Implementation of the Laporta algorithm	43
3 Evaluation of master integrals	47
3.1 Bosonic basketball S_3^{bb}	48
3.2 Bosonic basketball $S_{3,1}^{bb}$	56
3.3 Mixed basketball $S_{2,1}^{bf}$	58
4 Results and discussion	63
4.1 Π_{E3} and Π'_{T3} reduction	63
4.2 Conclusions and Outlook	66
A Appendix	67
A.1 Taylor coefficients	67
A.2 Vertices of QCD in background field gauge	69
A.3 Selected three-loop self-energy diagrams	69
A.4 Computation details	70
A.5 Example Code	72

Acknowledgements	73
Erklärung	75
Bibliography	77

Preface

Due to the impressive experimental precision reached in the recent years at present colliders and at the LHC in the near future, accurate predictions from the theoretical side are required. Perturbative calculations in quantum field theories and especially in the Standard Model (SM) of particle physics become more and more complicated as the number of loops and/or external legs gets larger. At some point, the number of diagrams and large expressions in the intermediate steps forbid a calculation completely by hand and necessitate the usage of computer algebra. The first attempt was made by M. Veltman in 1967 with `SCHOONSHIP` [1], which was primarily designed for the evaluation of fermion traces. In the early 1980s more general programs like `REDUCE` [2] or `SMP` [3] were introduced by particle physicists. Nowadays the algebraic manipulator `FORM` [4] is widely used in particle physics and is a direct descendant of M. Veltman's `SCHOONSHIP`.

Any perturbative calculation consists of a combinatoric, algebraic and analytic part. The former parts are well suited problems for automatisation and by now efficient algorithms have been implemented. The usual approach to deal with the analytic part i.e. with Feynman integrals is to reduce them algebraically to a small set of so-called master integrals with techniques like integration-by-parts [5] and/or a more recent approach via Gröbner-, s-bases [6, 7]. An important algorithm based on the systematic use of integration-by-parts relations was proposed by S. Laporta [8] and a public implementation is e.g. `AIR` [9]. A combined strategy of the s-bases approach and Laporta's method has been implemented recently in `FIRE` [10].

At least at this point, human intervention is unavoidable in order to evaluate the remaining master integrals. Fortunately, at least for zero-temperature physics, recent developments in the field of sector decomposition (for a concise review see [11]) has resulted in programs like `FIESTA` [12] capable to solve multi-loop integrals up to 11 propagators numerically. On the other hand, at finite temperature, surprisingly little is currently known [13]. Up to now, no systematic approach for the evaluation of multi-loop sum-integrals exists.

As we will see in this thesis, the relevant master integrals which remain in this calculation are basketball-like sum-integrals and fortunately the evaluation of those is solely a question of man-power.

1 Introduction and theoretical tools

This chapter consists of a brief review of some important topics in thermal field theory and theoretical tools to simplify the perturbative calculation.

1.1 Partition function and path integral

The fundamental quantity in statistical mechanics is the partition function \mathcal{Z} . In the canonical ensemble and with $k_B = 1 \Rightarrow \beta \equiv \frac{1}{T}$ we have

$$\mathcal{Z}(T) \equiv \text{Tr}[\exp(-\beta H)] , \quad (1.1)$$

with T the temperature and H the Hamiltonian of our quantum mechanical system. From this point on, we can easily compute further observables like the free energy F , average energy E or the entropy S via

$$\begin{aligned} F &= -T \ln \mathcal{Z} , \\ E &= \frac{1}{\mathcal{Z}} \text{Tr}[H \exp(-\beta H)] , \\ S &= \frac{\partial F}{\partial T} . \end{aligned} \quad (1.2)$$

In the majority of cases, it is difficult to evaluate the partition function via (1.1). A more convenient way to express the partition function is given by the path integral representation. In order to derivate the path integral, we recall some basics of quantum mechanics ($\hbar = 1$):

$$\langle x|p|p\rangle = p\langle x|p\rangle = -i\partial_x\langle x|p\rangle \Rightarrow \langle x|p\rangle = Ae^{ipx} , \quad (1.3)$$

and with the completeness relations for x and p which can be written as

$$\begin{aligned} \int dx |x\rangle\langle x| &= \mathbb{1} , \\ \int \frac{dp}{B} |p\rangle\langle p| &= \mathbb{1} , \end{aligned} \quad (1.4)$$

we obtain the relation $B = 2\pi|A|^2$. If we choose $A \equiv 1$ it follows $B = 2\pi$. In the following we evaluate the partition function in x -basis and obtain

$$\mathcal{Z} = \text{Tr}[e^{-\beta H}] = \int dx \langle x|e^{-\beta H}|x\rangle = \int dx \langle x|e^{-\epsilon H} \dots e^{-\epsilon H}|x\rangle , \quad (1.5)$$

with $\epsilon \equiv \frac{\beta}{N}$. In the last expression we have split the exponential $e^{-\beta H}$ into N parts. The standard procedure is now to insert alternately

$$\int \frac{dp_i}{B} |p_i\rangle \langle p_i| = \mathbb{1}, \quad i = 1, \dots, N, \quad (1.6)$$

and

$$\int dx_i |x_i\rangle \langle x_i| = \mathbb{1}, \quad i = 1, \dots, N, \quad (1.7)$$

to simplify (1.5) to objects like

$$\begin{aligned} \langle x_{i+1} | p_i \rangle \langle p_i | e^{-\epsilon H(x,p)} | x_i \rangle &= e^{ip_i x_{i+1}} \langle p_i | e^{-\epsilon H(p_i, x_i) + \mathcal{O}(\epsilon^2)} | x_i \rangle \\ &= \exp \left\{ -\epsilon \left[\frac{p_i^2}{2m} - ip_i \frac{x_{i+1} - x_i}{\epsilon} + V(x_i) + \mathcal{O}(\epsilon) \right] \right\}. \end{aligned} \quad (1.8)$$

On the very right we get

$$\langle x_1 | x \rangle = \delta(x_1 - x), \quad (1.9)$$

and after integration over x we have $\langle x | = \langle x_1 |$. By sending $N \rightarrow \infty$ the correction $\mathcal{O}(\epsilon)$ in Eq. (1.8) goes to zero and we get for the partition function

$$\mathcal{Z} = \lim_{N \rightarrow \infty} \int \left[\prod_{i=1}^N \frac{dx_i dp_i}{2\pi} \right] \exp \left\{ - \sum_{j=1}^N \epsilon \left[\frac{p_j^2}{2m} - ip_j \frac{x_{j+1} - x_j}{\epsilon} + V(x_j) \right] \right\} \Big|_{x_{N+1} \equiv x_1, \epsilon \equiv \frac{\beta}{N}}. \quad (1.10)$$

The momentum integrations over p_i can be carried out explicitly

$$\int_{-\infty}^{\infty} \frac{dp_i}{2\pi} \exp \left\{ -\epsilon \left[\frac{p_j^2}{2m} - ip_j \frac{x_{j+1} - x_j}{\epsilon} \right] \right\} = \sqrt{\frac{m}{2\pi\epsilon}} \exp \left[\frac{m(x_{i+1} - x_i)^2}{2\epsilon} \right]. \quad (1.11)$$

Then we obtain from Eq. (1.10)

$$\mathcal{Z} = \lim_{N \rightarrow \infty} \int \left[\prod_{i=1}^N \frac{dx_i}{\sqrt{2\pi\epsilon/m}} \right] \exp \left\{ - \sum_{j=1}^N \epsilon \left[\frac{m}{2} \left(\frac{x_{j+1} - x_j}{\epsilon} \right)^2 + V(x_j) \right] \right\} \Big|_{x_{N+1} \equiv x_1, \epsilon \equiv \frac{\beta}{N}}, \quad (1.12)$$

and the continuum version of the path integral

$$\mathcal{Z} = C \int_{x(\beta)=x(0)} \mathcal{D}x \exp \left\{ - \int_0^\beta d\tau \left[\frac{m}{2} \left(\frac{dx(\tau)}{d\tau} \right)^2 + V(x(\tau)) \right] \right\}, \quad (1.13)$$

with

$$C \equiv \left(\frac{m}{2\pi\epsilon} \right)^{N/2} = \exp \left[\frac{N}{2} \ln \left(\frac{mN}{2\pi\beta} \right) \right]. \quad (1.14)$$

We can ask now how is it possible to bring Eq.(1.13) in a form comparable to the usual path integral with the exponential

$$\exp \left(i \int dt \mathcal{L}_M \right), \quad \mathcal{L}_M = \frac{m}{2} \left(\frac{dx}{dt} \right)^2 - V(x). \quad (1.15)$$

The first step for this task is to perform a Wick rotation i.e. $t \rightarrow \tau \equiv it$ and introduce the Euclidean Lagrangian

$$\mathcal{L}_E \equiv -\mathcal{L}_M(t = -i\tau) = \frac{m}{2} \left(\frac{dx}{d\tau} \right)^2 + V(x) . \quad (1.16)$$

Then we restrict τ to the interval $0 \dots \beta$ and demand periodicity over τ and obtain for the exponential in Eq. (1.13)

$$\exp(-S_E) \equiv \exp \left(- \int_0^\beta d\tau \mathcal{L}_E \right) . \quad (1.17)$$

It should be noted that this derivation of the path integral also works in field theory with minimal modifications [14].

1.2 Free scalar field

We start with the usual Minkowskian Lagrangian for the free scalar field

$$\mathcal{L}_M = \frac{1}{2} (\partial^\mu \phi) (\partial_\mu \phi) - V(\phi) . \quad (1.18)$$

If we follow the procedure of the previous chapter in order to evaluate the path integral for the Lagrangian (1.18), and consider

$$\begin{aligned} x &\rightarrow \phi(\mathbf{x}), \quad p \rightarrow \pi(\mathbf{x}), \\ \langle \phi | \pi \rangle &= \exp \left(i \int d^3 \mathbf{x} \pi(\mathbf{x}) \phi(\mathbf{x}) \right), \end{aligned} \quad (1.19)$$

it leads us to

$$\mathcal{Z} = \int_{\phi(\beta, \mathbf{x}) = \phi(0, \mathbf{x})} \prod_{\mathbf{x}} [C \mathcal{D} \phi(\tau, \mathbf{x})] \exp \left\{ - \int_0^\beta d\tau \int d^d \mathbf{x} \mathcal{L}_E \right\}, \quad (1.20)$$

with

$$\mathcal{L}_E = -\mathcal{L}_M(t = -i\tau) = \frac{1}{2} (\partial_\mu \phi) (\partial_\mu \phi) + V(\phi) . \quad (1.21)$$

Eq. (1.19) reflects the fact that we go from an finite number of degrees of freedom (DOF) in quantum mechanics to an infinite number of DOF in quantum field theory.

1.3 Interacting scalar field

When the Lagrangian (1.21) contains terms higher than quadratic in the fields, it is generally not possible to evaluate the path integral (1.20) analytically. Therefore one has to develop a technique to approximate the path integral in the interacting case. For the following procedure it is economical to introduce an abbreviated form of Eq. (1.20):

$$\mathcal{Z} = N' \int [d\phi] e^{-S}, \quad (1.22)$$

with $S = S_0 + S_I$ where S_0 is quadratic in the fields and S_I contains higher orders in ϕ . It seems resonable to expand the exponential in Eq. (1.22) in a power series

$$\mathcal{Z} = N' \int [d\phi] e^{-S_0} \sum_{l=0}^{\infty} \frac{(-S_I)^l}{l!}, \quad (1.23)$$

and after taking the logarithm we obtain

$$\begin{aligned} \ln \mathcal{Z} &= \ln \left(N' \int [d\phi] e^{-S_0} \right) + \ln \left(1 + \sum_{l=1}^{\infty} \frac{(-1)^l}{l!} \frac{\int [d\phi] e^{-S_0} S_I^l}{\int [d\phi] e^{-S_0}} \right) \\ &\equiv \ln \mathcal{Z}_0 + \ln \mathcal{Z}_I. \end{aligned} \quad (1.24)$$

With the notation

$$\langle \dots \rangle_0 \equiv \frac{\int [d\phi] (\dots) e^{-S_0}}{\int [d\phi] e^{-S_0}}, \quad (1.25)$$

we are able to write the interacting part of Eq. (1.24) in the following short form

$$\ln \mathcal{Z}_I = \ln \left(1 + \sum_{l=1}^{\infty} \frac{(-1)^l}{l!} \langle S_I^l \rangle_0 \right). \quad (1.26)$$

Eq. (1.24) separates the contributions from interactions, $\ln \mathcal{Z}_I$, and the well-known ideal gas contribution $\ln \mathcal{Z}_0$. After these preparations the relevant quantity is Eq. (1.26). In order to compute Eq. (1.26) we expand the logarithm in a power series

$$\begin{aligned} \ln \mathcal{Z}_I &= \sum_{k=0}^{\infty} \frac{(-1)^k}{k+1} \left(\sum_{l=1}^{\infty} \frac{(-1)^l}{l!} \langle S_I^l \rangle_0 \right)^{k+1} \\ &= \sum_{k=0}^{\infty} \frac{(-1)^k}{k+1} \left(-\langle S_I \rangle_0 + \frac{1}{2} \langle S_I^2 \rangle_0 - \frac{1}{6} \langle S_I^3 \rangle_0 + \dots \right)^{k+1} \\ &= -\langle S_I \rangle_0 + \frac{1}{2} [\langle S_I^2 \rangle_0 - \langle S_I \rangle_0^2] - \frac{1}{6} [\langle S_I^3 \rangle_0 - 3\langle S_I \rangle_0 \langle S_I^2 \rangle_0 + 2\langle S_I \rangle_0^3] + \dots, \end{aligned} \quad (1.27)$$

and if we assume λ is the coupling constant, then the first term is of order λ and the second and third of order, $\mathcal{O}(\lambda^2)$ and $\mathcal{O}(\lambda^3)$, respectively. Moreover, the first, second and third term are associated with **connected** diagrams. The corresponding diagrams in ϕ^4 theory up to $\mathcal{O}(\lambda^2)$ are:

$$= 3 \bigcirc \bigcirc + 36 \bigcirc \bigcirc \bigcirc + 12 \bigcirc \bigcirc + \mathcal{O}(\lambda^3).$$

It turns out that at arbitrary order N in the perturbative expansion all **disconnected** contributions cancel. Formally $\ln \mathcal{Z}_I$ can be written as

$$\ln \mathcal{Z}_I = \sum_{N=1}^{\infty} \ln \mathcal{Z}_N, \quad (1.28)$$

where $\ln \mathcal{Z}_N$ is $\sim \lambda^N$. A comparison of Eq. (1.24) and (1.25) yields

$$\mathcal{Z}_I = \sum_{l=0}^{\infty} \frac{(-1)^l}{l!} \langle S_I^l \rangle_0. \quad (1.29)$$

Furthermore, $\langle S_I^l \rangle_0$ can be expressed as a sum of terms and each of them are products of connected diagrams:

$$\langle S_I^l \rangle_0 = \sum_{a_1, a_2, \dots=0}^{\infty} \frac{l!}{a_1! a_2! (2!)^{a_2} a_3! (3!)^{a_3} \dots} \langle S_I \rangle_{0,c}^{a_1} \langle S_I^2 \rangle_{0,c}^{a_2} \dots \delta_{a_1+2a_2+3a_3+\dots, l}. \quad (1.30)$$

The subscript c in $\langle S_I^i \rangle_{0,c}^{a_i}$ indicates connected diagrams and the Kronecker delta ensures that the contribution is of order λ^l . Finally, substituting Eq. (1.30) in (1.29) we obtain

$$\begin{aligned} \mathcal{Z}_I &= \sum_{a_1, a_2, \dots=0}^{\infty} \sum_{l=0}^{\infty} \frac{(-1)^l}{a_1! a_2! (2!)^{a_2} a_3! (3!)^{a_3} \dots} \langle S_I \rangle_{0,c}^{a_1} \langle S_I^2 \rangle_{0,c}^{a_2} \dots \delta_{a_1+2a_2+3a_3+\dots, l} \\ &= \sum_{a_1, a_2, \dots=0}^{\infty} \frac{(-1)^{a_1} \langle S_I \rangle_{0,c}^{a_1}}{a_1!} \frac{(-1)^{2a_2} \langle S_I^2 \rangle_{0,c}^{a_2}}{a_2! (2!)^{a_2}} \dots = \exp \left(\sum_{n=1}^{\infty} \frac{(-1)^n}{n!} \langle S_I^n \rangle_{0,c} \right). \end{aligned} \quad (1.31)$$

Another important quantity is the so called **self-energy** $\Pi(\omega_n, \mathbf{p})$ which is defined by

$$\mathcal{D}(\omega_n, \mathbf{p}) = [\omega_n^2 + \mathbf{p}^2 + m^2 + \Pi(\omega_n, \mathbf{p})]^{-1}, \quad (1.32)$$

where $\mathcal{D}(\omega_n, \mathbf{p})$ is the full two-point propagator in frequency-momentum space and ω_n the **Matsubara frequencies**

$$\omega_n \equiv \begin{cases} 2\pi nT & \text{bosonic} \\ (2n+1)\pi T & \text{fermionic} \end{cases} \quad (1.33)$$

This case differentiation reflects the fact that we require periodicity $\phi(\mathbf{x}, 0) = \phi(\mathbf{x}, \beta)$ for the bosonic field, cf. Eq. (1.20) and antiperiodicity $\psi_\alpha(\mathbf{x}, 0) = -\psi_\alpha(\mathbf{x}, \beta)$ for fermionic fields, respectively. We can write Eq. (1.32) in terms of the free-particle propagator \mathcal{D}_0

$$\mathcal{D}_0 = \frac{1}{\omega_n^2 + \mathbf{p}^2 + m^2}, \quad (1.34)$$

and find the expression

$$\mathcal{D}(\omega_n, \mathbf{p}) = (1 + \mathcal{D}_0 \Pi)^{-1} \mathcal{D}_0. \quad (1.35)$$

Our goal is to establish a relationship between the full two-point propagator $\mathcal{D}(\omega_n, \mathbf{p})$ and the functional derivative of $\ln Z_I$ with respect to $\mathcal{D}_0(\omega_n, \mathbf{p})$. For this task it is necessary to inspect the full two-point propagator $\mathcal{D}(\omega_n, \mathbf{p})$ a little bit more in detail

$$\begin{aligned} \mathcal{D}(\omega_n, \mathbf{p}) &= \int_0^\beta d\tau \int d^3x e^{-i(\mathbf{p} \cdot \mathbf{x} + \omega_n \tau)} \mathcal{D}(\mathbf{x}, \tau) \\ &= \sum_{n_1, n_2} \sum_{\mathbf{p}_1, \mathbf{p}_2} \frac{\beta}{V} \langle \tilde{\phi}_{n_1}(\mathbf{p}_1) \tilde{\phi}_{n_2}(\mathbf{p}_2) \rangle \int_0^\beta d\tau \int d^3x e^{i(\mathbf{p}_1 - \mathbf{p}) \cdot \mathbf{x}} e^{i(\omega_{n_1} - \omega_n) \cdot \tau}, \end{aligned} \quad (1.36)$$

where we make use of translational invariance of the finite-temperature propagator in position space $\mathcal{D}(\mathbf{x}_1, \tau_1, \mathbf{x}_2, \tau_2) \equiv \langle \phi(\mathbf{x}_1, \tau_1) \phi(\mathbf{x}_2, \tau_2) \rangle = \mathcal{D}(\mathbf{x}_1 - \mathbf{x}_2, \tau_1 - \tau_2)$ and $\mathbf{x}_1 = \mathbf{x}, \mathbf{x}_2 = 0, \tau_1 = \tau, \tau_2 = 0$. The ensemble average

$$\langle \tilde{\phi}_{n_1}(\mathbf{p}_1) \tilde{\phi}_{n_2}(\mathbf{p}_2) \rangle = \frac{\int [d\phi] \tilde{\phi}_{n_1}(\mathbf{p}_1) \tilde{\phi}_{n_2}(\mathbf{p}_2) e^{-S}}{\int [d\phi] e^{-S}} \quad (1.37)$$

vanishes unless $\mathbf{p}_1 = -\mathbf{p}_2, n_1 = -n_2$. Hence we obtain from Eq. (1.36)

$$\mathcal{D}(\omega_n, \mathbf{p}) = \beta^2 \frac{\int [d\phi] \tilde{\phi}_n(\mathbf{p}) \tilde{\phi}_{-n}(-\mathbf{p}) e^{-S}}{\int [d\phi] e^{-S}}. \quad (1.38)$$

In the next step we examine the Lagrangian $\mathcal{L}_E = \frac{1}{2} (\partial_\mu \phi) (\partial_\mu \phi) + \frac{1}{2} m^2 \phi^2$. The corresponding action follows after integration by parts and using periodicity of ϕ to

$$\begin{aligned} S &= -\frac{1}{2} \int_0^\beta d\tau \int d^3x \phi \left(-\frac{\partial^2}{\partial \tau^2} - \nabla^2 + m^2 \right) \phi \\ &= -\frac{1}{2} \beta^2 \sum_n \sum_{\mathbf{p}} (\omega_n^2 + \omega^2) \tilde{\phi}_n(\mathbf{p}) \tilde{\phi}_{-n}(-\mathbf{p}), \end{aligned} \quad (1.39)$$

where $\omega = \sqrt{\mathbf{p}^2 + m^2}$. In Eq. (1.39) we also make use of the Fourier expansion

$$\phi(\mathbf{x}, \tau) = \sqrt{\frac{\beta}{V}} \sum_n \sum_{\mathbf{p}} e^{i(\mathbf{p} \cdot \mathbf{x} + \omega_n \tau)} \tilde{\phi}_n(\mathbf{p}), \quad (1.40)$$

for the field ϕ . With Eq. (1.39), (1.38) and (1.24) we obtain the important relation

$$\mathcal{D}(\omega_n, \mathbf{p}) = -2 \frac{\delta \ln Z}{\delta \mathcal{D}_0^{-1}} = 2 \mathcal{D}_0^2 \frac{\delta \ln Z}{\delta \mathcal{D}_0}, \quad (1.41)$$

and therefore

$$(1 + \mathcal{D}_0 \Pi)^{-1} = 2 \mathcal{D}_0 \frac{\delta \ln Z}{\delta \mathcal{D}_0}. \quad (1.42)$$

This leads to our final result

$$(1 + \mathcal{D}_0 \Pi)^{-1} = 1 + 2 \mathcal{D}_0 \frac{\delta \ln Z_I}{\delta \mathcal{D}_0}, \quad (1.43)$$

via

$$\frac{\delta \ln Z_0}{\delta \mathcal{D}_0(\omega_n, \mathbf{p})} = \frac{1}{2} \mathcal{D}_0^{-1}(\omega_n, \mathbf{p}). \quad (1.44)$$

Now we write the self-energy $\Pi(\omega_n, \mathbf{p})$ in the same way as we proceeded with $\ln Z$ in Eq. (1.29)

$$\Pi = \sum_{l=1}^{\infty} \Pi_l, \quad (1.45)$$

where Π_l is proportional to λ^l . Inserting Eq. (1.45) in Eq. (1.43) and expanding to first order yields

$$\begin{aligned}
1 - \mathcal{D}_0 \Pi_1 &= 1 + 2\mathcal{D}_0 \frac{\delta \ln Z_1}{\delta \mathcal{D}_0} \\
&= 1 + 2\mathcal{D}_0 \frac{\delta}{\delta \mathcal{D}_0} \left(3 \text{---} \bigcirc \text{---} \bigcirc \text{---} \right) \\
&= 1 + 12\mathcal{D}_0 \text{---} \bigcirc \text{---} .
\end{aligned} \tag{1.46}$$

This means that a functional differentiation with respect to \mathcal{D}_0 is equivalent to cutting one line in the diagram. A factor of 2 occurs because both possible cuts are equivalent. Hence

$$\Pi_1 = -12 \text{---} \bigcirc \text{---} . \tag{1.47}$$

The second-order contribution to Π is

$$\begin{aligned}
-\mathcal{D}_0 \Pi_2 + \mathcal{D}_0 \Pi_1 \mathcal{D}_0 \Pi_1 &= 2\mathcal{D}_0 \frac{\delta \ln Z_2}{\delta \mathcal{D}_0} \\
&= 2\mathcal{D}_0 \frac{\delta}{\delta \mathcal{D}_0} \left(36 \text{---} \bigcirc \text{---} \bigcirc \text{---} \bigcirc \text{---} + 12 \text{---} \bigcirc \text{---} \bigcirc \text{---} \right) \\
&= 144\mathcal{D}_0 \text{---} \bigcirc \text{---} \bigcirc \text{---} + 96\mathcal{D}_0 \text{---} \bigcirc \text{---} + 144\mathcal{D}_0 \text{---} \bigcirc \text{---} \bigcirc \text{---} .
\end{aligned} \tag{1.48}$$

The second term on the left cancels with the last on the right. Those diagrams are called **one-particle reducible**. Thus

$$\Pi_2 = -144 \text{---} \bigcirc \text{---} \bigcirc \text{---} - 96 \text{---} \bigcirc \text{---} . \tag{1.49}$$

It can be shown, at arbitrary order N in the perturbative expansion, that all one-particle reducible contributions cancel and only the so called **one-particle irreducible** (1PI) diagrams are left

$$\Pi = -2 \left(\frac{\delta \ln Z_I}{\delta \mathcal{D}_0} \right)_{\text{1PI}} . \tag{1.50}$$

1.4 Green's functions and generating functionals

This section consists of a short review of some basic functional methods in field theory which are required for the background field formalism considered in Sec. 1.5. The generating functional is given by

$$Z[J] = \int [dQ] \exp \left[i \left(S[Q] + J \cdot Q \right) \right] , \tag{1.51}$$

whereas Q is a generic scalar field with action $S[Q]$ and $J \cdot Q \equiv \int d^4x J Q$. The n -**point Green's functions** are defined by

$$G^{(n)}(Q, \dots, Q) \equiv \langle 0 | T \{ \underbrace{Q \dots Q}_{n\text{-times}} \} | 0 \rangle = \int [dQ] (Q \dots Q) \exp i S[Q] , \quad (1.52)$$

and with Eq. (1.51) we are able to express $G^{(n)}$ via the n -th functional derivative with respect to the source J of $Z[J]$:

$$G^{(n)}(Q, \dots, Q) = \left(\frac{1}{i} \frac{\delta}{\delta J} \right)^n Z[J] \Big|_{J=0} . \quad (1.53)$$

The Green's functions introduced in (1.52) are **disconnected** Green's functions (Fig. 1.1a).

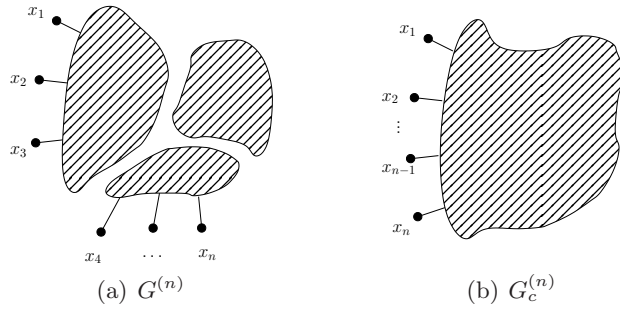


Figure 1.1: Disconnected $G^{(n)}$ and connected $G_c^{(n)}$ Green's functions

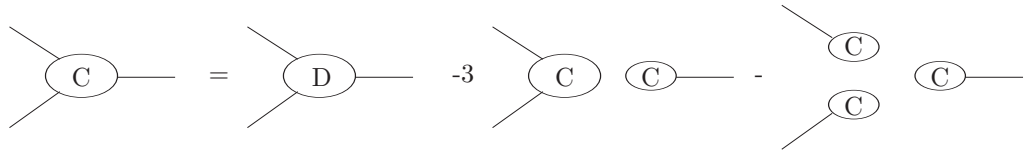
We have already seen that contributions from disconnected Green's functions do not contribute to $\ln Z$ or Π . Hence we work from now on only with **connected** Green's functions. These functions are generated by taking functional derivatives of

$$W[J] \equiv -i \ln Z[J] . \quad (1.54)$$

Let us inspect the first three derivatives with respect to J :

$$\begin{aligned} \left. \frac{\delta W}{\delta J} \right|_{J=0} &= \frac{\langle 0 | Q | 0 \rangle}{\langle 0 | 0 \rangle} , \\ \left. \frac{1}{i} \frac{\delta^2 W}{\delta J^2} \right|_{J=0} &= \left[\frac{\langle 0 | T \{ Q Q \} | 0 \rangle}{\langle 0 | 0 \rangle} - \left(\frac{\langle 0 | Q | 0 \rangle}{\langle 0 | 0 \rangle} \right)^2 \right] , \\ \left(\frac{1}{i} \right)^2 \left. \frac{\delta^3 W}{\delta J^3} \right|_{J=0} &= \frac{\langle 0 | T \{ Q Q Q \} | 0 \rangle}{\langle 0 | 0 \rangle} - 3 \frac{\langle 0 | T \{ Q Q \} | 0 \rangle \langle 0 | Q | 0 \rangle}{\langle 0 | 0 \rangle^2} + 2 \left(\frac{\langle 0 | Q | 0 \rangle}{\langle 0 | 0 \rangle} \right)^3 . \end{aligned} \quad (1.55)$$

The last equation reads diagrammatically:



A comparison of Eq. (1.27) and (1.55) reveals a strong similarity. A further simplification is to express the connected Green's functions in terms of **one-particle irreducible** (1PI) Green's functions which are generated by

$$\Gamma[\bar{Q}] = W[J] - J \cdot \bar{Q}, \quad \bar{Q} \equiv \frac{\delta W}{\delta J}, \quad (1.56)$$

the so-called **effective action**. \bar{Q} can be understood as the vacuum expectation value of Q in presence of the source J cf. (1.55). It turns out that the most economical way to determine connected Green's functions is to compute 1PI graphs and string these together. A few examples below will show how this works in practice. Let us inspect the first three derivatives of (1.56) with respect to \bar{Q} :

$$\frac{\delta \Gamma}{\delta \bar{Q}} = -J. \quad (1.57)$$

This field equation replaces the classical field equation $\delta S / \delta Q = -J$ in the quantized theory. Taking the second derivative yields

$$\frac{\delta^2 \Gamma}{\delta \bar{Q}^2} = -\frac{\delta J}{\delta \bar{Q}} = \left[-\frac{\delta \bar{Q}}{\delta J} \right]^{-1} = \left[-\frac{\delta^2 W}{\delta J^2} \right]^{-1} \stackrel{(1.55)}{=} iD^{-1}, \quad (1.58)$$

where D stands for the full propagator. After multiplying Eq. (1.58) from the left and right with D we obtain

$$D \frac{1}{i} \frac{\delta^2 \Gamma}{\delta \bar{Q}^2} D = D, \quad (1.59)$$

or diagrammatically:

This means that the full two-point propagator can be constructed by dressing the two external lines with propagators. In addition to this result we can use Eq. (1.58) to find the following identity

$$\frac{\delta}{\delta \bar{Q}} = \frac{\delta J}{\delta \bar{Q}} \frac{\delta}{\delta J} = D^{-1} \frac{1}{i} \frac{\delta}{\delta J}. \quad (1.60)$$

The equation above allows us to understand why Eq. (1.56) generates the 1PI-Green's functions. When operating with Eq. (1.60) on $\Gamma[\bar{Q}]$, $\delta / \delta J$ adds an external leg and D^{-1} removes the propagator from this leg. The continuous adding and removing of propagators (= amputation) keeps diagrams 1PI. Finally, let us compute the third derivative:

$$\frac{\delta^3 \Gamma}{\delta \bar{Q}^3} = D^{-1} \frac{1}{i} \frac{\delta}{\delta J} \left[-\frac{\delta^2 W}{\delta J^2} \right]^{-1} = iD^{-3} \frac{\delta^3 W}{\delta J^3}. \quad (1.61)$$

1.5 Background field method

The background field method allows us to quantize gauge theories without losing explicit gauge invariance. Furthermore, this approach makes a lot of computations much easier and helps for a better understanding of gauge theories. The usual approach in gauge field theory starts with a gauge invariant Lagrangian. For the purpose of quantization, we have to choose a gauge. At that time, the Lagrangian consists of the classical Lagrangian, gauge fixing and ghost terms. In the background field gauge we retain explicit gauge invariance in the original Lagrangian with gauge fixing and ghost terms. From this it follows that, among other things, even quantities like divergent counterterms take a gauge invariant structure. The generating functional for gauge theory reads

$$Z[J] = \int [dQ] \det \left[\frac{\delta G^a}{\delta \omega^b} \right] \exp \left[i \left(S[Q] - \frac{1}{2\xi} G \cdot G + J \cdot Q \right) \right], \quad (1.62)$$

where Q is a short notation for Q_μ^a and

$$\begin{aligned} J \cdot Q &\equiv \int d^4x J_\mu^a Q_\mu^a, \\ G \cdot G &\equiv \int d^4x G^a G^a. \end{aligned} \quad (1.63)$$

In the following we consider the gauge field action

$$S = -\frac{1}{4} \int d^4x F_{\mu\nu}^a F_{\mu\nu}^a, \quad (1.64)$$

with

$$F_{\mu\nu}^a = \partial_\mu Q_\nu^a - \partial_\nu Q_\mu^a + g f^{abc} Q_\mu^b Q_\nu^c. \quad (1.65)$$

G^a represents the gauge fixing term and $\delta G^a / \delta \omega^b$ the derivative with respect to the parameterisation ω^b of the infinitesimal gauge transformation

$$Q_\mu^a \rightarrow Q_\mu^a + \partial_\mu \omega^a + g f^{abc} \omega^b Q_\mu^c. \quad (1.66)$$

Then we introduce the background field generating functional which is defined by

$$\tilde{Z}[J, A] = \int [dQ] \det \left[\frac{\delta \tilde{G}^a}{\delta \omega^b} \right] \exp i \left[S[Q + A] - \frac{1}{2\xi} \tilde{G} \cdot \tilde{G} + J \cdot Q \right], \quad (1.67)$$

with background field A_μ^a and as above $\delta \tilde{G}^a / \delta \omega^b$ the derivative of gauge fixing \tilde{G}^a under gauge transformation

$$Q_\mu^a \rightarrow Q_\mu^a + \partial_\mu \omega^a + g f^{abc} \omega^b (Q_\mu^c + A_\mu^c). \quad (1.68)$$

In order to perform computations in background field gauge we need a relation between the conventional approach via Eq. (1.56) and the background field effective action

$$\tilde{\Gamma}[\tilde{Q}, A] = \tilde{W}[J, A] - J \cdot \tilde{Q}, \quad \tilde{Q} \equiv \frac{\delta \tilde{W}}{\delta J}, \quad (1.69)$$

with

$$\widetilde{W} \equiv -i \ln \widetilde{Z}[J, A] . \quad (1.70)$$

Shifting the integration variable $Q \rightarrow Q - A$ in Eq. (1.67) and using of Eqs. (1.70) and (1.69) yields

$$\widetilde{\Gamma}[\widetilde{Q}, A] = \Gamma[\widetilde{Q} + A], \quad \widetilde{Q} = Q - A . \quad (1.71)$$

In the special case $\widetilde{Q} = 0$ we find

$$\widetilde{\Gamma}[0, A] = \Gamma[A] . \quad (1.72)$$

This result tells us that computations with $\widetilde{\Gamma}[0, A]$ and gauge fixing $\widetilde{G}^a = \widetilde{G}^a(Q, A)$ provide the same result as the conventional approach via $\Gamma[\widetilde{Q}]$ evaluated at $\widetilde{Q} = A$ with gauge fixing $G^a = \widetilde{G}^a(Q - A, A)$. However, the unusual gauge fixing $G^a = \widetilde{G}^a(Q - A, A)$ results in different Green's functions compared to those obtained in a conventional gauge. But in the end gauge independence of physical quantities guarantees the correct result.

Let us focus our attention on the explicit gauge invariance of $\widetilde{\Gamma}[0, A]$ in A . For this task it is necessary to choose the correct gauge fixing term and it turns out that

$$\widetilde{G}^a = \partial_\mu Q_\mu^a + g f^{abc} A_\mu^b Q_\mu^c \quad (1.73)$$

makes Eq. (1.67) invariant under gauge transformations

$$\begin{aligned} A_\mu^a &\rightarrow A_\mu^a + \partial_\mu \omega^a + g f^{abc} \omega^b A_\mu^c , \\ J_\mu^a &\rightarrow J_\mu^a + g f^{abc} \omega^b J_\mu^c . \end{aligned} \quad (1.74)$$

The proof of this proposition can be found in [15, 16] or [17].

1.6 QCD Feynman rules and renormalisation

In order to compute the background field effective action $\widetilde{\Gamma}[0, A]$ we need to sum all one-particle irreducible diagrams. There are restrictions on the diagrams, only diagrams with external fields A (since $\widetilde{Q} = 0$) and Q fields inside the loops (because there is no functional integration over A cf. Eq. (1.67)) contribute. From here on we need Feynman rules to translate the graphical notation into a mathematical expression. We start with the action for finite temperature QCD, corresponding to a gauge group $SU(N_c)$ and N_f flavours of quarks

$$S_E^{\text{QCD}} = \int_0^\beta d\tau \int d^{3-2\epsilon} \mathbf{x} \left[\frac{1}{4} F_{\mu\nu}^a F_{\mu\nu}^a - \frac{1}{2\xi} G^a G^a + \bar{c}^a \left(\frac{\delta G^a}{\delta \omega^b} \right) c^b + \bar{\psi} (\gamma_\mu D_\mu + m) \psi \right], \quad (1.75)$$

where the subscript E stands for Euclidian space-time and $\mu = 0, \dots, 3$, $D_\mu = \partial_\mu - ig Q_\mu$, $Q_\mu = Q_\mu^a T^a$, $\text{Tr}[T^a T^b] = \delta^{ab}/2$, $\{\gamma_\mu, \gamma_\nu\} = 2\delta_{\mu\nu}$. The Dirac fields $\psi, \bar{\psi}$ are treated as vectors in Dirac space. The Faddeev-Popov determinant in Eq. (1.62) is written in terms of an anticommutating scalar ghost field. We express the gauge fixing term,

Eq. (1.73), and the functional derivative in a more convenient way and introduce the **covariant derivative in the adjoint representation**

$$\mathcal{D}_\mu^{ab}(Q) = \partial_\mu \delta^{ab} + g f^{abc} Q_\mu^c, \quad (1.76)$$

in terms of which

$$\begin{aligned} \tilde{G}^a &= \mathcal{D}_\mu^{ab}(A) Q_\mu^b, \\ \frac{\delta \tilde{G}^a}{\delta \omega_b} &= \mathcal{D}_\mu^{ac}(A) \mathcal{D}_\mu^{cb}(Q + A). \end{aligned} \quad (1.77)$$

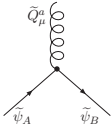
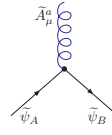
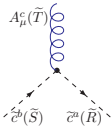
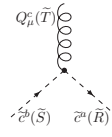
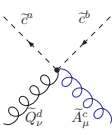
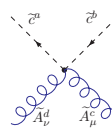
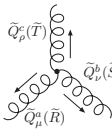
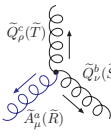
Now we are able to express the action (1.75) in Fourier representation. Then we split the action into a quadratic part and a part which contains all higher orders in the fields. Inverting the matrices appearing in the quadratic part provides us with the propagators

$$\langle \tilde{Q}_\mu^a(\tilde{R}) \tilde{Q}_\nu^b(\tilde{S}) \rangle_0 = \delta^{ab} \delta(\tilde{R} + \tilde{S}) \left[\frac{\delta_{\mu\nu} - \frac{\tilde{R}_\mu \tilde{R}_\nu}{\tilde{R}^2}}{\tilde{R}^2} + \frac{\xi \frac{\tilde{R}_\mu \tilde{R}_\nu}{\tilde{R}^2}}{\tilde{R}^2} \right], \quad (1.78a)$$

$$\langle \tilde{c}^a(\tilde{R}) \tilde{c}^b(\tilde{S}) \rangle_0 = \delta^{ab} \delta(\tilde{R} - \tilde{S}) \frac{1}{\tilde{R}^2}, \quad (1.78b)$$

$$\langle \tilde{\psi}_A(\tilde{R}) \tilde{\psi}_B(\tilde{S}) \rangle_0 = \delta_{AB} \delta(\tilde{R} - \tilde{S}) \frac{-i \tilde{\not{R}} + m}{\tilde{R}^2 + m^2}, \quad (1.78c)$$

and everything else gives the Feynman rules in QCD in background field gauge. The subscript in Eq. (1.78c) contains quark flavour and colour. After symmetrization as far as possible via integration by parts and changing summation indices we have:

	= -ig\gamma_\mu T_{AB}^a,		= -ig\gamma_\mu T_{AB}^a,
	= -igf^{acb}(\tilde{R}_\mu + \tilde{S}_\mu),		= -igf^{abc}\tilde{R}_\mu,
	= -g^2 f^{ace} f^{edb} \delta_{\mu\nu},		= -g^2 (f^{ace} f^{edb} + f^{ade} f^{ecb}) \delta_{\mu\nu},
	= igf^{abc} [\delta_{\mu\rho}(\tilde{R}_\nu - \tilde{T}_\nu) + \delta_{\rho\nu}(\tilde{T}_\mu - \tilde{S}_\mu) + \delta_{\nu\mu}(\tilde{S}_\rho - \tilde{R}_\rho)],		
	= igf^{abc} [\delta_{\mu\rho}(\tilde{R}_\nu - \tilde{T}_\nu - \frac{1}{\xi} \tilde{S}_\nu) + \delta_{\rho\nu}(\tilde{T}_\mu - \tilde{S}_\mu) + \delta_{\nu\mu}(\tilde{S}_\rho - \tilde{R}_\rho + \frac{1}{\xi} \tilde{T}_\rho)],		

Solid lines represent fermions, dashed lines ghosts and curly lines stand for gluons. It should be noted that we are not able to determine the propagator for the background field A because the A field gauge invariance has not been broken. In addition, the above vertices are only those with two or more Q lines (fermions, ghosts or gluons). This is reasonable because we are only interested in 1PI graphs. For completeness, in Fig. A.1 all vertices are shown which can be extracted from the action (1.75) with (1.77).

In the calculation process of $\tilde{\Gamma}[0, A]$ divergences will arise and must be renormalised. As usual, we introduce renormalisation constants

$$(A_\mu)_B = Z_A^{1/2} A_\mu, \quad (1.79a)$$

$$g_B = Z_g g, \quad (1.79b)$$

$$\xi_B = Z_\xi \xi, \quad (1.79c)$$

where the subscript B stands for bare quantities. The ghost field c , quantum field Q and fermion field ψ are only internal fields and therefore do not have to be renormalised. As mentioned above, the great advantage in background field gauge is that, in particular, the renormalisation factors Z_A and Z_g are associated with each other. Due to the fact that gauge invariance is retained, the divergences arising in $\tilde{\Gamma}[0, A]$ must have a structure of a divergent constant times $(F_{\mu\nu}^a)^2$. With Eq. (1.79a) and (1.79b) the renormalised $(F_{\mu\nu}^a)_B$ reads

$$(F_{\mu\nu}^a)_B = Z_A^{1/2} \left[\partial_\mu A_\nu^a - \partial_\nu A_\mu^a + Z_g Z_A^{1/2} g f^{abc} A_\mu^b A_\nu^c \right]. \quad (1.80)$$

The only way to bring Eq. (1.80) in a gauge invariant form times a divergent constant is if

$$Z_g = Z_A^{-1/2}. \quad (1.81)$$

For our purposes, the most convenient way to renormalise the theory is dimensional regularisation in the **modified minimal subtraction** ($\overline{\text{MS}}$) scheme. Therefore all integrals appearing during the calculation are carried out in $3 - 2\epsilon$ dimensions. The

renormalisation constants introduced in Eq. (1.79a - 1.79c) can be written as a sum over poles in ϵ , e.g.:

$$Z_A = 1 + \sum_{n=1}^{\infty} \frac{Z_A^{(n)}}{\epsilon^n}. \quad (1.82)$$

If we perform our calculation up to n -loop, we will get contributions $1/\epsilon \dots 1/\epsilon^n$. Furthermore, in dimensional regularisation the bare coupling g_B is no longer dimensionless. Considering the $F_{\mu\nu}^a F_{\mu\nu}^a$ term in (1.75) and keeping in mind that the action is dimensionless gives

$$\left. \begin{aligned} & \int d^{3-2\epsilon}x (\partial_\mu A_\nu)^2 \\ & \int d^{3-2\epsilon}x g_B^2 (A_\mu A_\nu)^2 \end{aligned} \right\} \Rightarrow g_B \sim (\text{mass})^\epsilon. \quad (1.83)$$

We introduce an arbitrary mass parameter μ such that the combination $\mu^{-2\epsilon} g^2$ is dimensionless. In this framework the usual sum-integral becomes to

$$\oint_P \rightarrow \mu^{2\epsilon} T \sum_{p_0} \int \frac{d^{3-2\epsilon}p}{(2\pi)^{3-2\epsilon}}. \quad (1.84)$$

Working in the $\overline{\text{MS}}$ scheme corresponds to doing common **minimal subtraction** (MS) scheme and then changing to the $\bar{\mu}$ scale parameter by $\mu^2 \equiv \bar{\mu}^2 e^{\gamma_E}/4\pi$.

1.7 QCD at high temperatures

The perturbation theory outlined in Section 1.3 is the so-called weak-coupling expansion. It is obvious that, only if the coupling is small, an expansion therein is justified. A weak-coupling expansion in QCD at high temperatures is justified because we have *asymptotic freedom*. This means, at sufficiently high temperatures the coupling is small and an expansion converges. However, at realistic temperatures the convergence can still be very slow (see e.g. [18, 19]). Hence we need high order computations in QCD to get accurate results. Unfortunately, a naive perturbative expansion in g^2 does not work, due to the fact that we are faced with a *multi-scale system* [20, 21]. The coupling is treated as a small parameter, but $g(\bar{\mu})$ varies with the momentum scale $\bar{\mu}$. QCD at high temperature exhibits three different momentum scales T , gT and g^2T [22]. Perturbation theory, restricted to the momentum scale T^1 can be treated with conventional methods. But at higher order in perturbation theory, the other momentum scales gT and g^2T enter the stage and can contribute to observables. In contrast to the momentum scale T , these low momentum scales are only accessible through improved analytic methods or non-perturbatively via lattice simulations, as is especially the case for the g^2T scale.

As an example we consider the free energy of QCD at high temperature. The free energy can be decomposed into contributions of the different momentum scales and it

¹The typical momentum of a particle in the plasma with temperature T

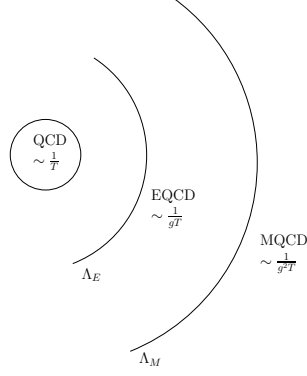


Figure 1.2: Different length scales in hot QCD

turns out that the scale T is a power series in g^2 , the scale gT a power series in g , entering at order g^3 and the contribution of $g^2 T$ beginning at g^6 . In the following we construct a sequence of two effective theories in order to separate the different momentum scales [23, 24]. The first theory (called EQCD) is constructed by integrating out the hard scale T and reproduces static properties of thermal QCD at length scales of $1/gT$ or greater. We obtain the second effective theory (MQCD) by integrating out the scale gT from the first. MQCD reproduces the behavior of full QCD at length scales of order $1/g^2 T$ or larger. The idea behind this simplification is the following: Before gauge fixing, the QCD Lagrangian, taken from Eq. (1.75), with vanishing mass matrix reads

$$\mathcal{L}_{QCD} = \frac{1}{4} F_{\mu\nu}^a F_{\mu\nu}^a + \bar{\psi} \gamma_\mu D_\mu \psi . \quad (1.85)$$

We know from Section 1.3 that bosonic fields are periodic in imaginary time τ . Thus the fields $Q_\mu^a(\mathbf{x})$ can be expanded into their Fourier modes $Q_{\mu,n}^a \exp[i2\pi n T \tau]$ with the corresponding propagators $[\mathbf{p}^2 + (2\pi n T)^2]^{-1}$. For nonstatic modes, $2\pi n T$ acts like a mass and at sufficiently high temperature T these modes decouple like infinitely heavy particles from the theory. In contrast to zero-temperature field theories with heavy particles, the decoupling is not ‘complete’. In addition to \mathcal{L}_{EQCD}^0 there are corrections that cannot be ignored

$$S_{EQCD} = \int d^{3-2\epsilon} x \mathcal{L}_{EQCD} , \quad (1.86)$$

$$\mathcal{L}_{EQCD} = \underbrace{\frac{1}{4} F_{ij}^a F_{ij}^a + \text{Tr}[D_i, A_0]^2 + m_E^2 \text{Tr}[A_0^2]}_{\mathcal{L}_{EQCD}^0} + \lambda_E^{(1)} (\text{Tr}[A_0^2])^2 + \lambda_E^{(2)} \text{Tr}[A_0^4] + \dots , \quad (1.87)$$

with $i = 1, \dots, 3$, $F_{ij}^a = \partial_i A_j^a - \partial_j A_i^a + g_E f^{abc} A_i^b A_j^c$ and $D_i = \partial_i - ig_E A_i$. The electrostatic gauge field $A_0^a(\mathbf{x})$ and magnetostatic gauge field $A_i^a(\mathbf{x})$ appearing in the theory can be related (up to normalisation) to the zero modes of $Q_\mu^a(\mathbf{x})$ in thermal QCD. The derivation of \mathcal{L}_{EQCD}^0 can be found in [25] and for higher operators see [26]. The largest contribution that higher-order operators, omitted in Eq. (1.87), could give (e.g. in the case of the thermodynamic pressure) is $\sim g^7$. This can be shown by dimensional analysis [27].

1.8 Matching computation

In order to determine the coefficients emerging in (1.87) we have to perform a matching computation. This means we require the same result on the QCD and EQCD side within the domain of validity. A convenient way to perform the matching computation is by using a strict perturbation expansion in g^2 . On both sides, the expansion is afflicted with infrared divergences. These divergences are screened by plasma effects and can be taken into account (at least for electrostatic gluons) by resumming an infinite set of diagrams (see e.g. [14]). Screening of magnetostatic gluons is completely a non-perturbative effect. For the matching computation, it is not necessary to worry about the infrared divergences because the matching parameters are only sensitive to the effects of large momenta. All infrared divergences appearing during matching computation can be removed by choosing a convenient infrared cutoff. It is essential to choose the same infrared cutoff in both theories. At leading order, the effective gauge coupling g_E , related to g_B , in the full theory reads

$$g_E^2 = g_B^2 T. \quad (1.88)$$

This can be seen by substituting $Q_0(\mathbf{x}, \tau) \rightarrow \sqrt{T} Q_0(\mathbf{x})$ in (1.85) and comparing $\int_0^\beta d\tau \mathcal{L}_{QCD}$ and (1.87). The mass parameter m_E^2 in (1.87) can be understood as the large momentum contribution to the electric screening mass m_{el}^2 in the full theory. The screening mass m_{el} is defined² by the pole of the propagator for $A_0^a(\tau, \mathbf{x})$ at $\mathbf{p}^2 = -m_{el}^2$ and $p_0 = 0$

$$p^2 + \Pi(p^2) = 0, \quad (1.89)$$

with $\Pi(p^2) \equiv \Pi_{00}(p^2)$. On the EQCD side, the mass parameter m_E is defined in a similar way by

$$p^2 + m_E^2 + \Pi_{\text{EQCD}}(p^2) = 0, \quad (1.90)$$

evaluated at $p^2 = -m_{el}^2$, and Π_{EQCD} denotes the self-energy on EQCD side. In the following we expand the self energy $\Pi(\mathbf{p}^2)$ in a Taylor series and obtain

$$\begin{aligned} \Pi(\mathbf{p}^2) &= \Pi(0) + \mathbf{p}^2 \Pi'(0) + \dots \\ &\equiv \sum_{n=1}^{\infty} \Pi_n(0) (g_B^2)^n + \mathbf{p}^2 \sum_{n=1}^{\infty} \Pi'_n(0) (g_B^2)^n + \dots \end{aligned} \quad (1.91)$$

With Eq. (1.89) and (1.91) we express the electric screening mass m_{el} in terms of Taylor coefficients up to next-to-next to leading order

$$\begin{aligned} m_{el}^2 &= g_B^2 \Pi_1(0) + g_B^4 [\Pi_2(0) - \Pi'_1(0) \Pi_1(0)] + g_B^6 [\Pi_3(0) - \Pi'_1(0) \Pi_2(0) - \\ &\quad - \Pi'_2(0) \Pi_1(0) + \Pi''_1(0) \Pi_1^2(0) + \Pi_1(0) \Pi_1'^2(0)] + \mathcal{O}(g_B^8). \end{aligned} \quad (1.92)$$

In this expansion we treated the deviation of p^2 from 0 as a perturbation in g^2 . To complete the matching for m_E we have to compute Π_{EQCD} on the EQCD side in a strict perturbation in g_B^2 . The only scale in $\Pi_{\text{EQCD}}(p^2)$ is p^2 and after Taylor expansion

²In presence of an infrared cut-off, otherwise a non-perturbative definition is needed.

the dimensionally regularised integrals vanishing identically. With Eq. (1.90) we find immediately

$$m_E^2 = m_{el}^2. \quad (1.93)$$

In order to match the effective gauge coupling g_E we make use of background field method introduced in Section 1.5. Symbolically, Eq. (1.87) can be written as

$$\mathcal{L}_{\text{eff}} \sim c_2 A^2 + c_3 g A^3 + c_4 g^2 A^4 + \dots, \quad (1.94)$$

where A denotes the background field potential and $c_i = 1 + \mathcal{O}(g^2)$. With $A_{\text{eff}}^2 \equiv c_2 A^2$ Eq. (1.94) becomes

$$\mathcal{L}_{\text{eff}} \sim A_{\text{eff}}^2 + c_3 c_2^{-3/2} g A_{\text{eff}}^3 + c_4 c_2^{-2} g^2 A_{\text{eff}}^4 + \dots, \quad (1.95)$$

and under consideration of the gauge invariant structure (cf. Eq. (1.80)) in terms of the effective background potential we obtain

$$g_E = c_3 c_2^{-3/2} g = c_4^{1/2} c_2^{-1} g. \quad (1.96)$$

In addition, gauge invariance in the original potential A and Eq. (1.94) yields $c_3 = c_2 = c_4$ and

$$g_E = c_2^{-1/2} g. \quad (1.97)$$

This means that the background field method simplifies this task from two independent calculations of a 3-point or 4-point function in combination with a two-point function in the case of Eq. (1.96) to calculating a single two-point function in the case of Eq. (1.97).

At this point it is helpful to recall Eq. (1.35). The gluon self-energy $\Pi_{\mu\nu}$ can be expressed through the inverses of the full and free propagators

$$\Pi_{\mu\nu} = \mathcal{D}_{\mu\nu}^{-1} - \mathcal{D}_{0\mu\nu}^{-1}. \quad (1.98)$$

There are two constraints concerning the full propagator $\mathcal{D}_{\mu\nu}$ and self-energy $\Pi_{\mu\nu}$

$$p^\mu \Pi_{\mu\nu} = 0, \quad (1.99a)$$

$$p^\mu p^\nu \mathcal{D}_{\mu\nu} = \xi, \quad (1.99b)$$

where p^μ denotes the gluon four-momentum and ξ a general gauge parameter. The corresponding proofs can be found in [14] and [28]. In general, $\Pi_{\mu\nu}$, $\mathcal{D}_{\mu\nu}$ and $\mathcal{D}_{\mu\nu}^{-1}$ are symmetric second-rank tensors made up of $g_{\mu\nu}$, $p_\mu p_\nu$, $u_\mu u_\nu$ and $p_\mu u_\nu + p_\nu u_\mu$ where $u_\mu = (1, \mathbf{0})$ describes the rest frame of the thermal bath. With Eq. 1.98-1.99b we obtain

$$\Pi_{00}(\mathbf{p}) \equiv \Pi_E(\mathbf{p}^2), \quad (1.100a)$$

$$\Pi_{ij}(\mathbf{p}) \equiv \left(\delta_{ij} - \frac{p_i p_j}{\mathbf{p}^2} \right) \Pi_T(\mathbf{p}^2) + \frac{p_i p_j}{\mathbf{p}^2} \Pi_L(\mathbf{p}^2), \quad (1.100b)$$

while Π_{0i} , Π_{i0} and Π_L are vanishing. A Taylor expansion according to Eq. (1.97) yields

$$g_E^2 = T \left\{ g_B^2 - g_B^4 \Pi'_{T1}(0) + g_B^6 \left[\left(\Pi'_{T1}(0) \right)^2 - \Pi'_{T2}(0) \right] + g_B^8 \left[\Pi'_{T1}(0) \Pi'_{T2}(0) - \left(\Pi'_{T1}(0) \right)^3 - \Pi'_{T3}(0) \right] + \mathcal{O}(g_B^{10}) \right\}. \quad (1.101)$$

1.9 Spatial string tension

The spatial string tension is defined by

$$\sigma_s \equiv \lim_{R_1 \rightarrow \infty} \frac{V_s(R_1)}{R_1}, \quad (1.102)$$

with the potential

$$V_s(R_1) = - \lim_{R_2 \rightarrow \infty} \frac{1}{R_2} \ln W_s(R_1, R_2), \quad (1.103)$$

where $W_s(R_1, R_2)$ is a rectangular Wilson loop of size $R_1 \times R_2$ in the (x_1, x_2) -plane.

In three dimensional SU(3) gauge theory (MQCD) the same observable exists and is directly related to the corresponding gauge coupling g_M^2 due to its dimensionality

$$\sigma_s = c \times g_M^4, \quad (1.104)$$

where c stands for a numerical proportionality constant. The coefficient has been determined by 3d quenched lattice simulations [29] and can be expressed for $N_c = 3$ as

$$\frac{\sqrt{\sigma_s}}{g_M^2} = 0.553(1). \quad (1.105)$$

The relation between the MQCD gauge coupling g_M^2 and the EQCD gauge coupling g_E^2 , is known up to two-loop order [30] and reads

$$g_M^2 = g_E^2 \left[1 - \frac{1}{48} \frac{g_E^2 N_c}{\pi m_E} - \frac{17}{4608} \left(\frac{g_E^2 N_c}{\pi m_E} \right)^2 \right], \quad (1.106)$$

where we have neglected numerically insignificant contributions. For a discussion regarding higher order corrections to Eq. (1.106) see [31].

The next step would be to re-expand Eq. (1.101) in terms of the renormalised gauge coupling $g^2(\bar{\mu})$ and solve the RG equation. After these standard procedures, g_E^2 is a function of $\bar{\mu}/T$ and $\bar{\mu}/\Lambda_{\overline{\text{MS}}}$. Furthermore, the $\overline{\text{MS}}$ scheme scale parameter $\bar{\mu}$ can be fixed by the “principle of minimal sensitivity” [32, 33]. Considering this and Eq. (1.105), (1.106), the spatial string tension σ_s becomes a function of $T/\Lambda_{\overline{\text{MS}}}$.

In order to compare the three dimensional prediction of σ_s with 4d lattice data we still need a relation between “perturbative units” $\Lambda_{\overline{\text{MS}}}$ and the critical temperature T_c

$$\frac{T_c}{\Lambda_{\overline{\text{MS}}}} = 1.10, \dots, 1.35, \quad (1.107)$$

which takes into account the results obtained from three different approaches³ and their associated uncertainties.

³For more details see [31] and references therein.

2 Framework: Automated loop computations

2.1 One-loop evaluation by hand

This section consists of the one-loop computation without using CAS. It should give an impression of the complexity already for the one-loop correction. In order to simplify this task somewhat, we perform the whole computation in Feynman gauge i.e. with $\xi = 1$. At one-loop order there are 5 diagrams contributing to $\Pi_{\mu\nu}$ in background field gauge:



$$\begin{aligned}
&= -\frac{g^2}{24} \langle A_\mu^a(P) A_\nu^b(Q) \not\!\!\!\!\!\int_{R,S,T,U} A_\alpha^c(R) A_\beta^d(S) Q_\rho^e(T) Q_\sigma^f(U) \rangle_{0,c} \delta(R+S+T+U) \times \\
&\quad \times \left[f^{cex} f^{xdf} (\delta_{\alpha\beta} \delta_{\rho\sigma} - \delta_{\alpha\sigma} \delta_{\rho\beta} + \delta_{\alpha\rho} \delta_{\beta\sigma}) + f^{cdx} f^{xef} (\delta_{\alpha\rho} \delta_{\beta\sigma} - \delta_{\alpha\sigma} \delta_{\rho\beta}) + \right. \\
&\quad \left. + f^{cfx} f^{xed} (\delta_{\alpha\rho} \delta_{\beta\sigma} - \delta_{\alpha\beta} \delta_{\rho\sigma} + \delta_{\alpha\sigma} \delta_{\rho\beta}) \right] \\
&\stackrel{(*)}{=} -\frac{g^2}{12} \not\!\!\!\!\!\int_{R,S,T,U} \langle A_\mu^a(P) A_\alpha^c(R) \rangle_0 \langle A_\nu^b(Q) A_\beta^d(S) \rangle_0 \langle Q_\rho^e(T) Q_\sigma^f(U) \rangle_0 \delta(R+S+T+U) C_{\alpha\beta\rho\sigma}^{cdef} \\
&= -\frac{g^2}{12} \underbrace{\delta^{ac} \delta^{bd} \delta^{ef} \delta_{\mu\alpha} \delta_{\nu\beta} \delta_{\rho\sigma} C_{\alpha\beta\rho\sigma}^{cdef}}_{= 2dN_c \delta_{\mu\nu} \delta^{ab}} \not\!\!\!\!\!\int_{R,S,T,U} \frac{1}{P^2 Q^2 T^2} \delta(P+R) \delta(Q+S) \delta(T+U) \delta(R+\dots+U) \\
&= -\frac{g^2}{6} dN_c \delta^{ab} \delta_{\mu\nu} \not\!\!\!\!\!\int_{R,S,T,U} \frac{1}{P^2 Q^2 T^2} \delta(P+R) \delta(Q+S) \delta(T+U) \delta(R+S+T+U) \\
&= -\frac{g^2}{6} dN_c \delta^{ab} \delta_{\mu\nu} \frac{\delta(P+Q)}{(P^2)^2} \not\!\!\!\!\!\int_S \frac{1}{S^2}. \tag{2.1}
\end{aligned}$$

In (*) we introduced $C_{\alpha\beta\rho\sigma}^{cdef}$ and used its complete symmetry in interchanging Lorentz and color indices simultaneously.



$$\begin{aligned}
&= \frac{g^2}{2} \langle A_\mu^a(P) A_\nu^b(Q) \oint_{R,S,T,U} A_\alpha^c(R) A_\beta^d(S) \bar{c}^e(T) c^f(U) \rangle_{0,c} \delta(\dots) \left[f^{ecx} f^{xdf} + f^{edx} f^{xcf} \right] \delta_{\alpha\beta} \\
&\stackrel{(*)}{=} -g^2 \oint_{R,S,T,U} \langle A_\mu^a(P) A_\alpha^c(R) \rangle_0 \langle A_\nu^b(Q) A_\beta^d(S) \rangle_0 \langle c^f(U) \bar{c}^e(T) \rangle_0 \delta(R+S-T+U) \left[\dots \right] \delta_{\alpha\beta} \\
&= -g^2 \underbrace{\delta^{ac} \delta^{bd} \delta^{ef} \delta_{\mu\alpha} \delta_{\nu\beta} \delta_{\alpha\beta} \left[\dots \right]}_{=-2N_c \delta_{\mu\nu} \delta^{ab}} \oint_{R,S,T,U} \frac{1}{P^2 Q^2 T^2} \delta(P+R) \delta(Q+S) \delta(T-U) \delta(\dots) \\
&= 2g^2 N_c \delta^{ab} \delta_{\mu\nu} \oint_{R,S,T,U} \frac{1}{P^2 Q^2 T^2} \delta(P+R) \delta(Q+S) \delta(T-U) \delta(R+S-T+U) \\
&= 2g^2 N_c \delta^{ab} \delta_{\mu\nu} \frac{\delta(P+Q)}{(P^2)^2} \oint_S \frac{1}{S^2}, \tag{2.2}
\end{aligned}$$

where we used one more time the complete symmetry of $\left[\dots \right] \delta_{\alpha\beta}$ and Grassmann nature of the ghost fields.



$$\begin{aligned}
&= -\frac{g^2}{2} \langle A_\mu^a(P) A_\nu^b(Q) \oint_{R,S,T,U,V,X} \bar{c}^c(R) A_\alpha^d(S) c^e(T) \bar{c}^g(U) A_\beta^h(V) c^i(X) \rangle_{0,c} (R_\alpha + T_\alpha) (U_\beta + X_\beta) \times \\
&\quad \times f^{cde} f^{ghi} \delta(-R+S+T) \delta(-U+V+X) \\
&\stackrel{(*)}{=} -g^2 \oint_{R,S,T,U,V,X} \langle A_\mu^a(P) A_\alpha^d(S) \rangle_0 \langle A_\nu^b(Q) A_\beta^h(V) \rangle_0 \langle c^e(T) \bar{c}^g(U) \rangle_0 \langle c^i(X) \bar{c}^c(R) \rangle_0 (R_\alpha + T_\alpha) \times \\
&\quad \times (U_\beta + X_\beta) f^{cde} f^{ghi} \delta(-R+S+T) \delta(-U+V+X) \\
&= g^2 \underbrace{\delta^{ad} \delta^{bh} \delta^{eg} \delta^{ic} f^{cde} f^{ghi}}_{=-N_c \delta^{ab}} \oint_{R,S,T,U,V,X} \frac{\delta(P+S) \delta(Q+V) \delta(T-U) \delta(X-R)}{P^2 Q^2 T^2 X^2} (R_\mu + T_\mu) \times \\
&\quad \times (U_\nu + X_\nu) \delta(-R+S+T) \delta(-U+V+X).
\end{aligned}$$

Performing the momentum integrations over S,V,U and R and then X gives

$$= -g^2 N_c \delta^{ab} \frac{\delta(P+Q)}{(P^2)^2} \oint_S \frac{1}{S^2 (P-S)^2} (2S_\mu - P_\mu) (2S_\nu - P_\nu). \tag{2.3}$$

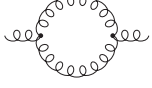
This is the first integral with a non-trivial tensor structure. It is convenient to write the 3-gluon vertex shown in Section 1.6 in short form as

$$D_{\alpha\beta\gamma}(R, S, T) \equiv \delta_{\alpha\gamma} (R_\beta - T_\beta - S_\beta) + \delta_{\gamma\beta} (T_\alpha - S_\alpha) + \delta_{\beta\alpha} (S_\gamma - R_\gamma + T_\gamma). \tag{2.4}$$

Changing Lorentz indices in addition to four-momentum e.g. $\beta \leftrightarrow \gamma, S \leftrightarrow T$ results in an overall minus sign

$$D_{\alpha\beta\gamma}(R, S, T) = -D_{\alpha\gamma\beta}(R, T, S). \quad (2.5)$$

The following gluon diagram and higher loop diagrams of this type, entirely composed of 3-gluon vertices, are the most complicated¹ ones appearing in this computation.



$$\begin{aligned} &= -\frac{g^2}{72} \langle A_\mu^a(P) A_\nu^b(Q) \oint_{R,S,T,U,V,X} A_\alpha^c(R) Q_\beta^d(S) Q_\gamma^e(T) A_\eta^g(U) Q_\rho^h(V) Q_\sigma^i(X) \rangle_{0,c} D_{\alpha\beta\gamma}(R, S, T) \times \\ &\quad \times D_{\eta\rho\sigma}(U, V, X) f^{cde} f^{ghi} \delta(R + S + T) \delta(U + V + X) \\ &= -\frac{g^2}{2} \oint_{R,S,T,U,V,X} \langle A_\mu^a(P) A_\alpha^c(R) \rangle_0 \langle A_\nu^b(Q) A_\eta^g(U) \rangle_0 \langle Q_\beta^d(S) Q_\rho^h(V) \rangle_0 \langle Q_\gamma^e(T) Q_\sigma^i(X) \rangle_0 \times \\ &\quad \times f^{cde} f^{ghi} \delta(R + S + T) \delta(U + V + X) D_{\alpha\beta\gamma}(R, S, T) D_{\eta\rho\sigma}(U, V, X) \\ &= -\frac{g^2}{2} \underbrace{\delta^{ac} \delta^{bg} \delta^{dh} \delta^{ei} f^{cde} f^{ghi}}_{=N_c \delta^{ab}} \oint_{R,S,T,U,V,X} \frac{1}{P^2 Q^2 S^2 T^2} \delta(P + R) \delta(Q + U) \delta(S + V) \delta(T + X) \times \\ &\quad \times \delta_{\mu\alpha} \delta_{\nu\eta} \delta_{\beta\rho} \delta_{\gamma\sigma} D_{\alpha\beta\gamma}(R, S, T) D_{\eta\rho\sigma}(U, V, X) \delta(R + S + T) \delta(U + V + X) \\ &= -\frac{g^2}{2} N_c \delta^{ab} \frac{\delta(P + Q)}{(P^2)^2} \oint_S \frac{1}{S^2 (P - S)^2} D_{\mu\beta\gamma}(-P, S, P - S) D_{\nu\beta\gamma}(P, -S, -P + S). \end{aligned}$$

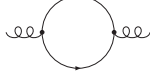
At this point we have to carry out the contractions of $D_{\mu\beta\gamma}(\dots) D_{\nu\beta\gamma}(\dots)$

$$\begin{aligned} &D_{\mu\beta\gamma}(-P, S, P - S) D_{\nu\beta\gamma}(P, -S, -P + S) = \\ &\quad [\delta_{\mu\gamma}(-P_\beta - (P - S)_\beta - S_\beta) + \delta_{\gamma\beta}((P - S)_\mu - S_\mu) + \delta_{\beta\mu}(S_\gamma + P_\gamma + (P - S)_\gamma)] \times \\ &\quad \times [\delta_{\nu\gamma}(-P_\beta - (S - P)_\beta + S_\beta) + \delta_{\gamma\beta}((S - P)_\nu + S_\nu) + \delta_{\beta\nu}(-S_\gamma - P_\gamma + (S - P)_\gamma)] \\ &= [-2\delta_{\mu\gamma}P_\beta + \delta_{\gamma\beta}(P_\mu - 2S_\mu) + 2\delta_{\beta\mu}P_\gamma] [2\delta_{\nu\gamma}P_\beta + \delta_{\gamma\beta}(2S_\nu - P_\nu) - 2\delta_{\beta\nu}P_\gamma] \\ &= -8\delta_{\mu\nu}P^2 + (8 - d)P_\mu P_\nu + 2d(S_\nu P_\mu - 2S_\mu S_\nu + S_\mu P_\nu), \end{aligned}$$

with $\delta_{\beta\beta} = d$. The final expression for the gluon diagram becomes

$$\begin{aligned} &= -\frac{g^2}{2} N_c \delta^{ab} \frac{\delta(P + Q)}{(P^2)^2} \oint_S \frac{1}{S^2 (P - S)^2} \left[-8\delta_{\mu\nu}P^2 + (8 - d)P_\mu P_\nu + \right. \\ &\quad \left. + 2d(S_\nu P_\mu - 2S_\mu S_\nu + S_\mu P_\nu) \right]. \end{aligned} \quad (2.6)$$

¹1-loop diagrams of this type consist of $\sim 2^{3l+1} 3^{2l}$ terms in presence of a general gauge parameter.



$$\begin{aligned}
&= -\frac{g^2}{2} \langle A_\mu^a(P) A_\nu^b(Q) \rangle \oint_{\{R,T,U,X\},S,V} \bar{\psi}_A(R) \gamma_\alpha A_\alpha^c(S) \psi_B(T) \bar{\psi}_C(U) \gamma_\beta A_\beta^d(V) \psi_D(X) \rangle_{0,c} T_{AB}^c T_{CD}^d \times \\
&\quad \times \delta(-R+S+T) \delta(-U+V+X) \\
&= g^2 \oint_{\{R,T,U,X\},S,V} \langle A_\mu^a(P) A_\alpha^c(S) \rangle_0 \langle A_\nu^b(Q) A_\beta^d(V) \rangle_0 \text{Tr} [\langle \psi_D(X) \bar{\psi}_A(R) \rangle_0 \gamma_\alpha \langle \psi_B(T) \bar{\psi}_C(U) \rangle_0 \gamma_\beta] \times \\
&\quad \times T_{AB}^c T_{CD}^d \delta(-R+S+T) \delta(-U+V+X) \\
&= -g^2 \underbrace{\delta^{ac} \delta^{bd} \delta_{BC} \delta_{DA} T_{AB}^c T_{CD}^d}_{=\text{Tr}[T^a T^b]=N_f/2} \oint_{\{R,T,U,X\},S,V} \frac{1}{P^2 Q^2 T^2 X^2} \underbrace{R_\sigma U_\rho \delta_{\mu\alpha} \delta_{\nu\beta} \text{Tr}[\gamma_\sigma \gamma_\alpha \gamma_\rho \gamma_\beta]}_{4[\delta_{\mu\nu} R \cdot U - R_\mu U_\nu - R_\nu Q_\mu]} \times \\
&\quad \times \delta(-R+S+T) \delta(-U+V+X) \delta(P+S) \delta(Q+V) \delta(T-U) \delta(X-R).
\end{aligned}$$

Curly brackets indicate fermionic Matsubara frequencies and integration over S, V, R, U, X gives the final result

$$= 2g^2 N_f \delta^{ab} \frac{\delta(P+Q)}{(P^2)^2} \oint_{\{S\}} \frac{1}{S^2 (P-S)^2} [\delta_{\mu\nu} (S^2 - P \cdot S) - 2S_\mu S_\nu + P_\mu S_\nu + P_\nu S_\mu].$$

In the next step we perform a Taylor expansion in the external momentum $P = (0, \mathbf{p})$ (which is taken purely spatial) and decouple all scalar products of P with loop momenta. In order to abbreviate the following expressions, we introduce a short-hand notation for the one-loop tadpole

$$\oint_P \frac{P_0^n}{(P^2)^m} \equiv I_b(m, n), \quad (2.7a)$$

$$\oint_{\{P\}} \frac{P_0^n}{(P^2)^m} \equiv I_f(m, n). \quad (2.7b)$$

There is a recursion relation² which allows us to reduce the appearing integrals with arbitrary value of m and n to lower ones $n' < n, m' < m$

$$I_b(m+1, n+2) = \frac{2m-d+1}{2m} I_b(m, n), \quad (2.8)$$

for $m \geq 1, n \geq 0$. Fortunately, at one-loop order all integrals are known explicitly

$$I_b(m, n) = \frac{2\pi^{3/2} T^4}{(2\pi T)^{2m-n}} \left(\frac{\mu^2}{\pi T^2} \right)^\epsilon \frac{\Gamma(m - \frac{3}{2} + \epsilon)}{\Gamma(m)} \zeta(2m - n - 3 + 2\epsilon), \quad (2.9)$$

²This can be shown via integration by parts (IBP) relations, see Section 2.4.

so that in principle, a reduction in terms of Eq. (2.8) is not needed. Furthermore, the fermionic one-loop tadpoles $I_f(m, n)$ are related³ to the corresponding bosonic ones via

$$I_f(m, n) = (2^{2m-n-d+1} - 1)I_b(m, n). \quad (2.10)$$

Adding all contributions and performing a Taylor expansion yields

$$\Pi_{\mu\nu,1} = N_c \left\{ (2-d) \oint_S \frac{\delta_{\mu\nu}}{S^2} + (2d-4) \oint_S \frac{S_\mu S_\nu}{(S^2)^2} \right\} + 2N_f \oint_{\{S\}} \frac{\delta_{\mu\nu} S^2 - 2S_\mu S_\nu}{(S^2)^2}, \quad (2.11)$$

$$\begin{aligned} \Pi'_{\mu\nu,1} = & -N_c \oint_S \left\{ (2d-4) \left(\frac{S_\nu P_\mu + S_\mu P_\nu}{(S^2)^3} (S \cdot P) + \frac{S_\mu S_\nu}{(S^2)^3} P^2 - 4 \frac{S_\mu S_\nu}{(S^2)^4} (S \cdot P)^2 \right) + \right. \\ & \left. + \left(5 - \frac{d}{2} \right) \frac{P_\mu P_\nu}{(S^2)^2} - 4 \frac{\delta_{\mu\nu}}{(S^2)^2} \right\} \\ & + 4N_f \oint_{\{S\}} \left\{ \frac{S_\nu P_\mu + S_\mu P_\nu}{(S^2)^3} (S \cdot P) - 4 \frac{S_\mu S_\nu}{(S^2)^4} (S \cdot P)^2 + \frac{S_\mu S_\nu}{(S^2)^3} P^2 + \frac{\delta_{\mu\nu}}{(S^2)^3} (S \cdot P)^2 - \right. \\ & \left. - \frac{\delta_{\mu\nu}}{2(S^2)^2} P^2 \right\}. \end{aligned} \quad (2.12)$$

As mentioned above, in order to express both Taylor coefficients in terms of one-loop tadpoles Eq. (2.7b) we have to extract the tensor structure out of the appearing tensor integrals in addition to decoupling the external momentum P :

$$\begin{aligned} \oint_S \frac{S_\mu S_\nu}{(S^2)^a} & \stackrel{(1.100b)}{=} \delta_{\mu 0} \delta_{\nu 0} \oint_S \frac{S_0 S_0}{(S^2)^a} + \delta_{\mu i} \delta_{\nu j} \oint_S \frac{S_i S_j}{(S^2)^a} \\ & = \delta_{\mu 0} \delta_{\nu 0} \oint_S \frac{S_0^2}{(S^2)^a} + \delta_{\mu i} \delta_{\nu j} \delta_{ij} \frac{1}{d-1} \oint_S \frac{\mathbf{S}^2}{(S^2)^a} \\ & = \delta_{\mu 0} \delta_{\nu 0} \oint_S \frac{S_0^2}{(S^2)^a} + \delta_{\mu i} \delta_{\nu i} \frac{1}{d-1} \oint_S \frac{S^2 - S_0^2}{(S^2)^a} \\ & = \delta_{\mu 0} \delta_{\nu 0} I_b(a, 2) + \frac{\delta_{\mu i} \delta_{\nu i}}{d-1} \left[I_b(a-1, 0) - I_b(a, 2) \right] \\ & = \left[\delta_{\mu 0} \delta_{\nu 0} \frac{2a-1-d}{2(a-1)} + \frac{\delta_{\mu i} \delta_{\nu i}}{d-1} \left\{ 1 - \frac{2a-1-d}{2(a-1)} \right\} \right] I_b(a-1, 0) \\ & = \frac{1}{2(a-1)} \left[\delta_{\mu 0} \delta_{\nu 0} (2a-1-d) + \delta_{\mu i} \delta_{\nu i} \right] I_b(a-1, 0) \end{aligned} \quad (2.13)$$

$$\oint_S \frac{S_\mu P_\nu}{(S^2)^a} (S \cdot P) = \dots = p_\mu p_\nu \frac{1}{d-1} \oint_S \frac{S^2 - S_0^2}{(S^2)^a} = \frac{p_\mu p_\nu}{d-1} \left[I_b(a-1, 0) - I_b(a, 2) \right] \quad (2.14)$$

³Can be seen by rescaling the spatial momentum by a factor of 2, see e.g. Eq. (3.5).

$$\oint_S \frac{1}{(S^2)^a} (S \cdot P)^2 = \dots = P^2 \frac{1}{d-1} \oint_S \frac{S^2 - S_0^2}{(S^2)^a} = \frac{P^2}{d-1} \left[I_b(a-1, 0) - I_b(a, 2) \right] \quad (2.15)$$

$$\begin{aligned} \oint_S \frac{S_\mu S_\nu}{(S^2)^a} (S \cdot P)^2 &= \delta_{\mu 0} \delta_{\nu 0} \oint_S \frac{S_0^2}{(S^2)^a} (S \cdot P)^2 + \delta_{\mu i} \delta_{\nu j} \oint_S \frac{S_i S_j}{(S^2)^a} (S \cdot P)^2 \\ &= \delta_{\mu 0} \delta_{\nu 0} \frac{P^2}{d-1} \oint_S \frac{S^2 - S_0^2}{(S^2)^a} S_0^2 + \delta_{\mu i} \delta_{\nu j} p_k p_l \oint_S \frac{S_i S_j S_k S_l}{(S^2)^a} \\ &= \delta_{\mu 0} \delta_{\nu 0} \frac{P^2}{d-1} \oint_S \frac{S^2 - S_0^2}{(S^2)^a} S_0^2 + \frac{P^2 \delta_{ij} + 2p_i p_j}{d^2 - 1} \oint_S \frac{S^4 - 2S_0^2 S^2 + S_0^4}{(S^2)^a} \\ &= \delta_{\mu 0} \delta_{\nu 0} \frac{P^2}{d-1} \left[I_b(a-1, 2) - I_b(a, 4) \right] + \\ &\quad + \frac{P^2 \delta_{ij} + 2p_i p_j}{d^2 - 1} \left[I_b(a-2, 0) - 2I_b(a-1, 2) + I_b(a, 4) \right]. \end{aligned} \quad (2.16)$$

Inserting Eq. (2.13) for $a = 2$ in Eq. (2.11) yields

$$\Pi_{\mu\nu,1} = \delta_{\mu 0} \delta_{\nu 0} (d-2) [N_c(2-d)I_b(1,0) + 2N_f I_f(1,0)], \quad (2.17)$$

and using Eqs. (2.12 - 2.16) and Eq. (2.8) gives

$$\begin{aligned} \Pi'_{\mu\nu,1} &= \delta_{\mu 0} \delta_{\nu 0} P^2 \left[\frac{N_f}{3} (2-d) I_f(2) + \frac{N_c}{6} (34-7d+d^2) I_b(2) \right] + \\ &\quad + \delta_{\mu i} \delta_{\nu j} (p_\mu p_\nu - \delta_{\mu\nu} P^2) \left[\frac{2N_f}{3} I_f(2) + \frac{N_c}{6} (d-26) I_b(2) \right]. \end{aligned} \quad (2.18)$$

Now we can easily read off the functions Π_E and Π_T according to Eq. (1.100b)

$$\Pi_{E1}(0) = (d-2) [N_c(2-d)I_b(1) + 2N_f I_f(1)], \quad (2.19a)$$

$$\Pi_{T1}(0) = 0, \quad (2.19b)$$

$$\Pi'_{E1}(0) = \frac{N_c}{6} (34-7d+d^2) I_b(2) + \frac{N_f}{3} (2-d) I_f(2), \quad (2.19c)$$

$$\Pi'_{T1}(0) = \frac{N_c}{6} (26-d) I_b(2) - \frac{2N_f}{3} I_f(2), \quad (2.19d)$$

where $I_{b,f}(i) \equiv I_{b,f}(i, 0)$. For $d \rightarrow d+1$ and multiplied by an overall minus sign this result agrees completely with the corresponding expressions for ξ^0 , given in [31]. Let us have a closer look on (2.19a). In $d = 4 - 2\epsilon$ the expansion for $I_b(1)$ and $I_f(1)$ up to $\mathcal{O}(1)$ reads

$$I_b(1) = \frac{T^2}{12} + \mathcal{O}(\epsilon), \quad I_f(1) = -\frac{T^2}{24} + \mathcal{O}(\epsilon), \quad (2.20)$$

and with Eq. (1.92) we find the well known *Debye screening mass*

$$m_E^2 = g^2 T^2 \left(\frac{N_f}{6} + \frac{N_c}{3} \right) + \mathcal{O}(g^4). \quad (2.21)$$

In Eqs. (2.13 - 2.16) we used several times a tensor decomposition which can be written in the most general case as

$$I_{i_1 \dots i_\alpha} \equiv \oint_S \frac{S_{i_1 \dots i_\alpha}}{(S^2)^a} = \frac{dd_{i_1 i_2 \dots i_{\alpha-1} i_\alpha}}{dd_{i_1 i_1 \dots i_\alpha i_\alpha}} \oint_S \frac{(S^2 - S_0^2)^{\alpha/2}}{(S^2)^a}, \quad (2.22)$$

where $dd_{i_1 \dots i_\alpha}$ stands for the total symmetric tensor build of metric tensors:

$$dd_{ij} = g_{ij}, \quad dd_{ijkl} = g_{ij}g_{kl} + g_{ik}g_{jl} + g_{il}g_{jk}, \quad \dots \quad (2.23)$$

2.2 Two-loop

To get a general idea of the complexity of the two-loop computation we show the corresponding diagrams in Fig. 2.1.

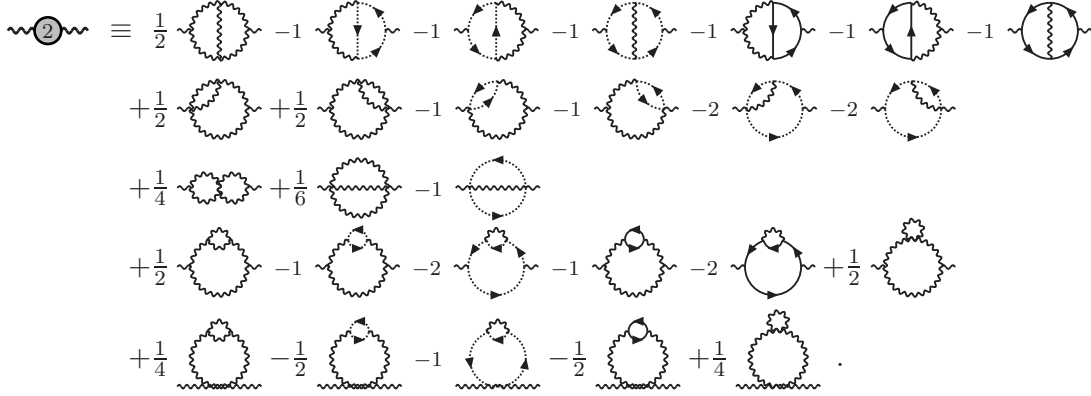


Figure 2.1: The two-loop self-energy diagrams in the background field gauge taken from [31]. Wavy (curly) lines represent gauge fields, dotted lines ghosts, and solid lines fermions.

It is not economical to evaluate every single diagram by hand like in the one-loop case shown in the previous section for two reasons. First, the evaluation of every single diagram shown in Fig. 2.1 is much more ‘expensive’ in terms of performing the tedious Lorentz- and colour contractions. Second, after the Taylor expansion, we are still faced with two-loop vacuum sum-integrals and unfortunately, neither a recursion relation as that in Eq. (2.8) nor an exact solution like in Eq. (2.9) is presently known.

In fact, we will use the one- and two-loop results given in [31] as a first serious cross-check of the methods introduced in the next sections. In addition, the one- and two-loop Taylor coefficients are required in order to check general gauge invariance for the three-loop corrections to m_E^2 and g_E^2 via Eq. (1.92) and (1.101) in which we are ultimately interested in.

2.3 Some preparations

Any perturbative expansion starts with generating the graphs. At 1-loop there are just 5 one-particle irreducible self-energy diagrams and it is easy to construct those directly from the Lagrangian in Eq. (1.75) with the corresponding combinatoric factors. But the number of diagrams increases rapidly at higher order and to avoid mistakes during Wick contractions we use a computer program called QGRAF⁴ which generates all diagrams for a given interaction and order. QGRAF requires three input files; the model

```

1 % QCD in background field gauge
2 % particle content
3 %   qu quark
4 %   uq antiquark
5 %   gl gluon
6 %   gh ghost
7 %   hg antighost
8 %   ge background gauge field
9
10 % propagators
11
12 [qu, uq, -]
13 [gl, gl, +]
14 [ge, ge, +, external]
15 [gh, hg, -]
16
17 % 3vertices
18
19 [gl, qu, uq]
20 [ge, qu, uq]
21 [gl, gl, gl]
22 [ge, gl, gl]
23 [gl, gh, hg]
24 [ge, gh, hg]
25
26 [ge, ge, ge]
27 [ge, ge, gl]
28
29 % 4vertices
30
31 [gl, gl, gl, gl]
32 [ge, gl, gl, gl]
33 [ge, ge, gl, gl]
34 [ge, gl, gh, hg]
35 [ge, ge, gh, hg]
36
37 [ge, ge, ge, gl]
38 [ge, ge, ge, ge]
```

Listing 2.1: bg QCD model file for QGRAF: (% are comment-lines)

file where the interactions and propagators are specified; a style file which controls the form of the output; and a file which contains parameters like the desired order and type of diagram (number of external legs, 1PI, ...).

Loop order	# of diagrams
1	5
2	31
3	447
4	8999
5	222864
⋮	...

Table 2.1: Total number of 2-point 1PI diagrams at a given loop order

In this framework it turns out that not the number of graphs is the limiting factor (as it would be for a evaluation by hand) rather than the complexity of a few graphs appearing in this computation. In order to later manipulate the QGRAF output we use

⁴See [34] and [35] for the implemented algorithm.

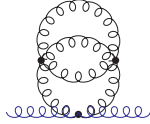
```

1  +tag(1)*(+1/12)*
2  ext(ge(-1,kq),ge(-2,-kq1))*
3  prop(gl(1,-k1),gl(2,k1))*
4  prop(gl(3,k1),gl(4,-k1))*
5  prop(gl(5,k2+k3-k1),gl(6,k1-k2-k3))*
6  prop(gl(7,-k2),gl(8,k2))*
7  prop(gl(9,-k3),gl(10,k3))*
8  vtx(ge(-1,kq),ge(-2,-kq1),gl(1,-k1),gl(3,k1))*
9  vtx(gl(2,k1),gl(5,k2+k3-k1),gl(7,-k2),gl(9,-k3))*
10 vtx(gl(4,-k1),gl(6,k1-k2-k3),gl(8,k2),gl(10,k3))

```

Listing 2.2: QGRAF output at 3-loop for diagram 1/447

an output style which can be directly interpreted by FORM [36]. Let us have a closer look at Listing 2.2. The first line specifies the diagram and contains the combinatoric factor. Then **ext(...)** holds the information about the external particles including its momentum. Furthermore, lines 3 - 7 specify propagators **prop(...)** and the last three lines determine the vertices via **vtx(...)**. Considering this we can easily draw the corresponding diagram:



A brief overview of the most important steps in the automation process is as follows:

1. Generating graphs: **self.A.frm** [37]
2. Mapping QGRAF's momenta to our convention: **self.B.frm** [37]
3. **self.C.frm** [37]:
 - a) Feynman rules, color sums, Lorentz contractions and gamma traces
 - b) Taylor expansion in external momentum
 - c) Decoupling of external momentum
4. Reducing integrals to some master integrals by using Laporta algorithm
5. Solving the remaining master integrals by hand

In order to express the appearing integrals in a unique representation we have to map QGRAF's momenta⁵ to ours shown in Fig. 2.2. For example we consider Listing 2.2. The momenta emphasised are not part of our convention. Performing the momentum shift $k_2 \rightarrow k_2 - k_3$ on Listing 2.2 gives the desired momenta. However, in general there is external momentum flowing within the loops and therefore we are not able to express the integrals in our convention from the very beginning. This means, at that point, we

⁵Which are in fact not unique.

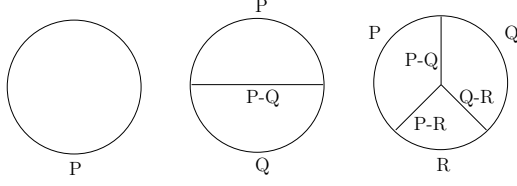


Figure 2.2: Vacuum diagram momenta convention up to 3-loop level

just ‘prepare’ the occuring propagators for a unique representation. In the end (3.b) we Taylor expand the propagators and can identify the momentum flow with specific list entries according to our vacuum convention in Fig. 2.2. The momenta mapping is implemented in **self.B.frm** and the most important statement is shown below and reads in our example

```
1 id fshift(k2,-k3+k2) = replace_(k2,-k3+k2);
```

which replaces all occurrences of $k2$ by $k2 - k3$. In contrast to the 1-loop evaluation of Section 2.1 we start with projecting out the relevant quantities of $\Pi_{\mu\nu}$ to avoid tensor-like integrals such in (2.12) by

$$\begin{aligned}\Pi_G &\equiv \delta_{\mu\nu} \Pi_{\mu\nu}, \\ \Pi_E &= \delta_{\mu 0} \delta_{\nu 0} \Pi_{\mu\nu}, \\ \Pi_L &= \frac{p_\mu p_\nu}{P^2} \Pi_{\mu\nu}.\end{aligned}\tag{2.24}$$

Then with Eq. (1.100b) it follows

$$\left(\delta_{\mu\nu} - \frac{p_\mu p_\nu}{P^2} - \delta_{\mu 0} \delta_{\nu 0}\right) \Pi_{\mu\nu} = \Pi_{00} + \Pi_{ii} - \frac{p_i p_j}{P^2} \Pi_{ij} - \Pi_{00} = (d-2) \Pi_T,\tag{2.25}$$

and finally with (2.24) we obtain

$$\begin{aligned}\Pi_T &= \frac{1}{d-2} \left(\delta_{\mu\nu} - \frac{p_\mu p_\nu}{P^2} - \delta_{\mu 0} \delta_{\nu 0}\right) \Pi_{\mu\nu} \\ &= \frac{1}{d-2} \left(\Pi_G - \Pi_L - \Pi_E\right).\end{aligned}\tag{2.26}$$

In FORM this is done by the following statements

```
1 id once ext(ge?(m1?,kq),ge?(m2?,-kq))=
2 ( sProjg*d_(m1,m2)
3 +sProjL*kq(m1)*kq(m2)*G(kq,0)
4 +sProjE*ku(m1)*ku(m2))*G(kq,0);
```

where $G(P,0) = 1/P^2$ and m_i are Lorentz indices with dimension d . In addition, we also perform color projections for the external background field:

$$A_{\mu\nu}^{ab} = \delta^{ab} \frac{1}{d_A} A_{\mu\nu}^{cc},\tag{2.27}$$

where $A_{\mu\nu}^{ab}$ denotes a 2-point function, for example $\Pi_{\mu\nu}^{ab}$ and $d_A \equiv \delta^{aa} = N_c^2 - 1$. From here on we follow the standard procedure outlined in Section 2.1, i.e. inserting vertex and propagator structures, performing color sums and gamma traces. Finally we Taylor expand propagators with external momentum P up to a given order using the recursion

$$\frac{1}{(P-S)^2} = \frac{1}{S^2} + \frac{2S \cdot P - P^2}{S^2} \frac{1}{(P-S)^2}, \quad (2.28)$$

and decouple all scalar products with external momentum and loop momenta according to Eq. (2.22). After these manipulations all appearing integrals up to 3-loop can be written in the following notation:

$$I_{a;c1;\alpha} \equiv \oint_{P_{c1}} \frac{P_0^\alpha}{(P^2)^a}, \quad (2.29a)$$

$$I_{a,b,c;c1,c2;\alpha,\beta} \equiv \oint_{P_{c1}, Q_{c2}} \frac{P_0^\alpha Q_0^\beta}{(P^2)^a (Q^2)^b ((P-Q)^2)^c}, \quad (2.29b)$$

$$I_{a,b,c,d,e,f;c1,c2,c3;\alpha,\beta,\gamma} \equiv \oint_{P_{c1}, Q_{c2}, R_{c3}} \frac{P_0^\alpha Q_0^\beta R_0^\gamma}{(P^2)^a (Q^2)^b (R^2)^c ((P-Q)^2)^d ((P-R)^2)^e ((Q-R)^2)^f}, \quad (2.29c)$$

where $P_{c1=0}$ refers to bosonic Matsubara frequencies and $P_{c1=1}$ to the fermionic ones. The 1-loop tadpole in Eq. (2.29a) for $c1 = 0, 1$ is equivalent to Eq. (2.7a) and (2.7b), respectively. Naively, we would expect two indicies for every propagator, the corresponding power and fermion information. However, the latter property for the remaining three lines in Eq. (2.29c) is given by

$$\begin{aligned} c4 &= (c1 + c2) \pmod{2}, \\ c5 &= (c1 + c3) \pmod{2}, \\ c6 &= (c2 + c3) \pmod{2}. \end{aligned} \quad (2.30)$$

In Fig. 2.3 all non-trivial topologies are displayed. For their representations see Tables

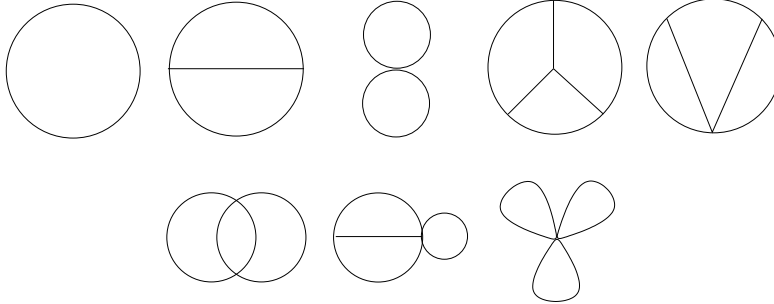


Figure 2.3: Non-trivial topologies at one, two and three-loop order

2.2 and 2.3. Since some topologies can be represented by more than one choice of momenta, we have emphasised (in red) our choice of a unique representative.

a	b	c	d	e	f	Typ
1	1	1	1	1	1	Mercedes
1	1	1	1	1	0	Spectacles
1	1	1	1	0	1	Spectacles
1	1	1	0	1	1	Spectacles
1	1	0	1	1	1	Spectacles
1	0	1	1	1	1	Spectacles
0	1	1	1	1	1	Spectacles
1	1	0	0	1	1	Basketball
1	0	1	1	0	1	Basketball
0	1	1	1	1	0	Basketball

Table 2.2: 3-loop topologies and representations in list notation cf. Eq. (2.29c): 1 stands for positive integers and 0 for negative/zero integers.

a	b	c	d	e	f	Typ	a	b	c	d	e	f	Typ
0	0	1	1	1	1	2loop×1loop	0	1	0	1	0	1	(1loop) ³
0	1	0	1	1	1	2loop×1loop	0	1	0	1	1	0	(1loop) ³
0	1	1	0	1	1	2loop×1loop	0	1	1	0	1	0	(1loop) ³
0	1	1	1	0	1	2loop×1loop	0	1	1	1	0	0	(1loop) ³
1	0	0	1	1	1	2loop×1loop	1	0	0	0	1	1	(1loop) ³
1	0	1	0	1	1	2loop×1loop	1	0	0	1	0	1	(1loop) ³
1	0	1	1	1	0	2loop×1loop	1	0	0	1	1	0	(1loop) ³
1	1	0	1	0	1	2loop×1loop	1	0	1	0	0	1	(1loop) ³
1	1	0	1	1	0	2loop×1loop	1	0	1	1	0	0	(1loop) ³
1	1	1	0	0	1	2loop×1loop	1	1	0	0	1	0	(1loop) ³
1	1	1	0	1	0	2loop×1loop	1	1	0	0	0	1	(1loop) ³
1	1	1	1	0	0	2loop×1loop	1	1	1	0	0	0	(1loop) ³
0	0	1	0	1	1	(1loop) ³	1	1	0	1	0	0	2l×SumI.=0
0	0	1	1	0	1	(1loop) ³	1	0	1	0	1	0	2l×SumI.=0
0	0	1	1	1	0	(1loop) ³	0	1	1	0	0	1	2l×SumI.=0
0	1	0	0	1	1	(1loop) ³	0	0	0	1	1	1	2l×SumI.=0

Table 2.3: Factorized topologies appearing in the 3-loop computation with 3 or 4 positive lines cf. Eq. (2.29c). Everything else i.e. with more than 3 negative lines vanishes in dimensional regularisation.

2.4 Integration by parts relations and shifts

As mentioned above, in order to reduce the large amount of integrals to a small set of so called master integrals⁶, we need relations among them. There are two different kinds of relations we use in the following: first the integration by parts (IBP) relations and second relations obtained by using momentum shifts. A generic Feynman integral in d dimensions reads

$$F(p_1, \dots, p_n) \equiv \int_{k_1, \dots, k_n} d^d k_1 \dots d^d k_n \prod_i \frac{(p \cdot k)_i^{b_i}}{(q_i^2 + m_i^2)^{a_i}}, \quad (2.31)$$

where $(p \cdot k)_i^{b_i}$ are irreducible scalar products of loop momenta k_j and external momenta p_k to the power b_i . The integration by parts relations [5] are generated by the fact that

$$\int_{k_1, \dots, k_n} d^d k_1 \dots d^d k_n \frac{\partial}{\partial k_j^\mu} \left(k_l^\mu \prod_i \frac{(p \cdot k)_i^{b_i}}{(q_i^2 + m_i^2)^{a_i}} \right) = 0, \quad (2.32)$$

for $j, l = 1, \dots, n$. Applying this to the 1-loop case in Eq. (2.29a), we obtain

$$\begin{aligned} 0 &= \oint_{P_{c1}} \frac{\partial}{\partial p^i} \left(p^i \frac{P_0^n}{(P^2)^m} \right) \\ &= \oint_{P_{c1}} \left\{ (d-1) \frac{P_0^n}{(P^2)^m} - 2m \mathbf{p}^2 \frac{P_0^n}{(P^2)^{m+1}} \right\} \\ &= \oint_{P_{c1}} \left\{ (d-1-2m) \frac{P_0^n}{(P^2)^m} + 2m \frac{P_0^{n+2}}{(P^2)^{m+1}} \right\} \\ &= (d-1-2m) I_{c1}(m, n) + 2m I_{c1}(m+1, n+2), \end{aligned} \quad (2.33)$$

which is precisely the recursion relation Eq. (2.8) used in the previous section.

Already at 2-loop we are faced with the problem of how to apply the IBP relations in a systematic way because there is no obvious recursion relation as in the case of Eq. (2.33):

$$\begin{aligned} 0 &= (-1 + d - c - 2a) I_{\mathbf{a}, b, c; c1, c2; \alpha, \beta} \\ &\quad - 2c I_{\mathbf{a}, b, c+1; c1, c2; \alpha+1, \beta+1} \\ &\quad + 2c I_{\mathbf{a}, b, c+1; c1, c2; \alpha+2, \beta} \\ &\quad + c I_{\mathbf{a}, b-1, c+1; c1, c2; \alpha, \beta} \\ &\quad + 2a I_{\mathbf{a}+1, b, c; c1, c2; \alpha+2, \beta} \\ &\quad - c I_{\mathbf{a}-1, b, c+1; c1, c2; \alpha, \beta} \end{aligned} \quad (2.34)$$

⁶IBP relations produce an under-determined system of linear equations with unknowns called master integrals.

In Eq. (2.34) we emphasised a possible way to use this relation to reduce the power of the first propagator for $a \geq 1$ (by bringing the second-last term to the left hand side (lhs)). But in the end we just ‘replaced’ a given 2-loop integral by many other 2-loop integrals in addition to some $(1\text{loop})^2$ integrals, cf. the last line of Eq. (2.34). The same holds for the other IBP relations and simple linear combinations thereof. A solution to the problem is given by the Laporta algorithm introduced in Section 2.5.

Further relations can be obtained by shifting integration variables. As an example we consider the 3-loop case

$$\begin{aligned}
I_{a,b,c,d,e,f;c1,c2,c3;\alpha,\beta,\gamma} &= \oint_{P_{c1}, Q_{c2}, R_{c3}} \frac{P_0^\alpha Q_0^\beta R_0^\gamma}{(P^2)^a (Q^2)^b (R^2)^c ((P-Q)^2)^d ((P-R)^2)^e ((Q-R)^2)^f} \\
Q \rightarrow P-Q &:= \oint_{P_{c1}, Q_{c2}, R_{c3}} \frac{P_0^\alpha (P_0-Q_0)^\beta R_0^\gamma}{(P^2)^a ((P-Q)^2)^b (R^2)^c (Q^2)^d ((P-R)^2)^e ((P-Q-R)^2)^f} \\
R \rightarrow P-R &:= \oint_{P_{c1}, Q_{c2}, R_{c3}} \frac{P_0^\alpha (P_0-Q_0)^\beta (P_0-R_0)^\gamma}{(P^2)^a ((P-Q)^2)^b ((P-R)^2)^c (Q^2)^d (R^2)^e ((R-Q)^2)^f} \\
&= \sum_{n=0}^{\beta} \sum_{m=0}^{\gamma} \binom{\beta}{n} \binom{\gamma}{m} (-1)^{\beta-n} (-1)^{\gamma-m} \times \\
&\quad \times \oint_{P_{c1}, Q_{c4}, R_{c5}} \frac{P_0^{\alpha+n+m} Q_0^{\beta-n} R_0^{\gamma-m}}{(P^2)^a (Q^2)^d (R^2)^e ((P-Q)^2)^b ((P-R)^2)^c ((Q-R)^2)^f} \\
&= \sum_{n=0}^{\beta} \sum_{m=0}^{\gamma} \binom{\beta}{n} \binom{\gamma}{m} (-1)^{\beta-n} (-1)^{\gamma-m} I_{a,d,e,b,c,f;c1,c4,c5;\alpha+n+m,\beta-n,\gamma-m},
\end{aligned} \tag{2.35}$$

where c_4 and c_5 are determined by Eq. (2.30). Symmetries implied by momentum shifts are equivalent to interchanging lines within the corresponding diagrams.

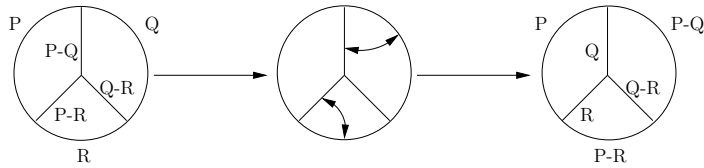


Figure 2.4: Symmetry of the Mercedes diagram implied by the momentum shifts used in Eq. (2.35), cf. Lst. A.1.

In the following we solely focus on the 3-loop case because all methods required for the one- and two loop computation are contained⁷ in the complete 3-loop computation. As

⁷More precisely: in the $2\text{loop} \times 1\text{loop}$ sector.

a next step we have to consider the different fermion signatures appearing. As it turns out, only a few signatures are needed in the following because the others can be shifted to the former ones.

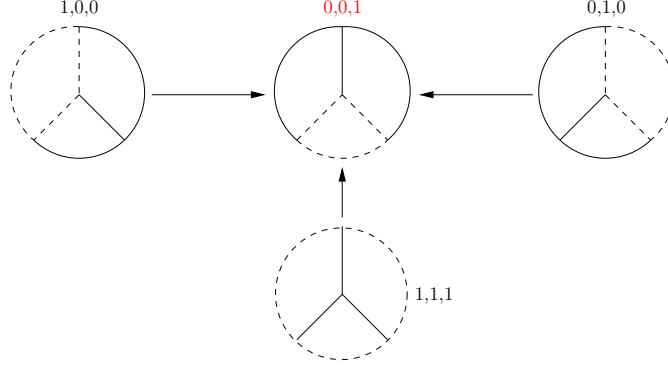


Figure 2.5: Fermion shifts for the Mercedes topology; dotted lines stands for fermions, cf. Lst. A.2.

Our fermion signature convention for non-trivial topologies is shown in Table 2.4. In

Topo+FermSig.	#SYM	#IBP
$I_{1,1,1,1,1,1,1;0,0,0;\dots}$	23	9
$I_{1,1,1,1,1,1,1;0,0,1;\dots}$	5	9
$I_{1,1,1,1,1,1,1;0,1,1;\dots}$	7	9
$I_{1,1,1,1,1,1,0;0,0,0;\dots}$	7	9
$I_{1,1,1,1,1,1,0;0,0,1;\dots}$	3	9
$I_{1,1,1,1,1,1,0;0,1,1;\dots}$	7	9
$I_{1,1,1,1,1,1,0;1,0,0;\dots}$	1	9
$I_{1,1,0,0,1,1,1;0,0,0;\dots}$	23	9
$I_{1,1,0,0,1,1,1;0,0,1;\dots}$	3	9
$I_{1,1,0,0,1,1,1;1,1,0;\dots}$	23	9

Table 2.4: Total number of symmetries and IBP relations for non-trivial topologies and our convention for the fermion signature.

order to avoid mistakes during the implementation of IBP relations, symmetries, shifts and fermion shifts we have automated the process of generating these relations completely.

It is important to understand the difference between shifts, fermion shifts, symmetries and IBP relations. All of them, except for the IBP relations, are generated by the same momentum shifts like in Eq. (2.35). Shifts respect the topology but not necessarily the fermion signature in contrary to symmetries, whereas fermion shifts respect the particular representative (cf. Table 2.4) in addition to the fermion signature.

2.5 Reduction: Laporta algorithm and decompositions

We already encountered the problem of how to apply the IBP relations and symmetries in a systematic way. For this purpose we implement an algorithm based on Laporta's ideas outlined in [8]. The basic concept is shown in Fig. 2.6. There are two new 'components'

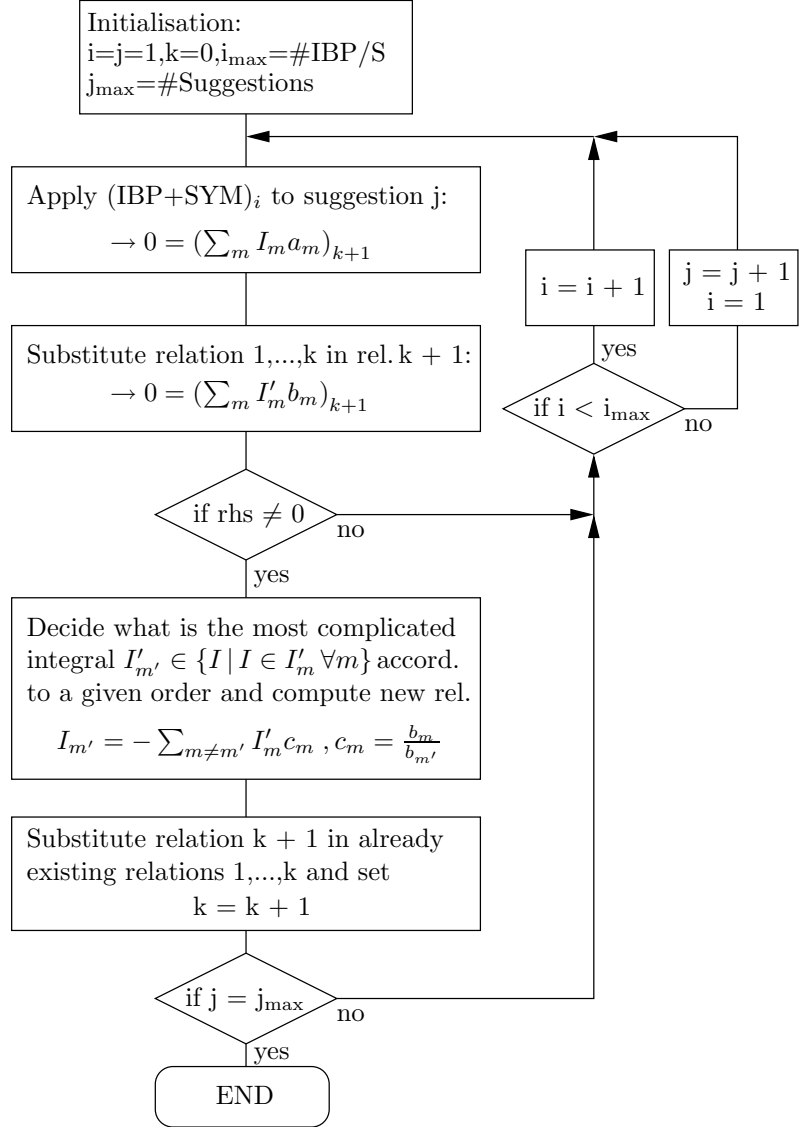


Figure 2.6: Schematic Laporta algorithm

which are indispensable for the Laporta algorithm: A unique directive in order to decide what is the most complicated integral out of a set of integrals; and a list of so-called 'suggestions' which specifies, roughly speaking, the search area⁸. For our purposes, a

⁸At 3-loop we have 6 propagators + 3 irr. scalar products → discrete 9-dimensional search space.

convenient choice⁹ for choosing the most complicated integral looks as follows ($f_1 = a, \dots, f_6 = f, q_1 = \alpha, \dots, q_3 = \gamma$):

1. Count positive lines: $\sum_i \theta(f_i)$ and choose the highest, if equal go to 2,
2. Compute abs. sum of powers of props.: $\sum_i |f_i|$, choose highest, if equal go to 3,
3. Count zero lines: $\sum_i \delta(f_i)$, choose lowest, if equal go to 4,
4. Comp. sum of pow. of irr. scalar products: $\sum_i q_i$, choose highest, if equal go to 5,
5. Choose integral with highest power on propagator 6,5,4,3,2,1, if equal go to 6,
6. Pick integral with highest power of irreducible scalar product 3,2,1,

where f_i, q_i refers to the power of propagators and irreducible scalar products, respectively. The above rules can be divided into two categories: Rules 1 to 4 classify the integral according to its complexity and rules 5 and 6 guarantee uniqueness.

We then move to consider the question how to generate ‘suggestions’. For this task it is necessary to find out what are the most difficult integrals needed for the computation. We find the following integrals for Π_3 and Π'_3 (in which we are ultimately interested in) as the most difficult ones (according to above ordering):

$$I_{3,3,0,-5,2,2;0,0,0;0,0,0} \quad (2.36)$$

$$I_{3,3,-1,-2,1,1;0,0,1;0,0,0}$$

$$I_{4,4,0,-6,2,2;0,0,0;0,0,0} \quad (2.37)$$

$$I_{4,4,-1,-3,1,1;0,0,1;0,0,0} \cdot$$

The observation is, for both Taylor coefficients, that the bosonic integrals are more difficult than the fermionic ones. This is simply due to the difference between boson and fermion propagators Eqs. (1.78a), (1.78c) respectively. In Feynman gauge we would get the same depth¹⁰. Back to the initial problem, Eqs. (2.36) and (2.37) tell us how deep the reduction needs to run. It gives us an upper bound for suggestions and hence for the total number of suggestions.

In addition to the number of suggestions also the order in which they are processed is important. We follow Laporta’s initial proposal and order the suggestions *inverse* to the above order for extraction. This means that the simplest integrals (according to above ordering) are processed first and integrals like in Eq. (2.36) or (2.37) last.

$$\begin{aligned} &I_{2,1,0,0,1,1;0,0,0;0,0,0} \\ &I_{1,2,0,0,1,1;0,0,0;0,0,0} \\ &I_{1,1,0,0,2,1;0,0,0;0,0,0} \\ &I_{1,1,0,0,1,2;0,0,0;0,0,0} \\ &\vdots \end{aligned} \quad (2.38)$$

⁹In the literature also called ‘lexicographic’ order.

¹⁰The depth measures the deviation from base-integrals: $I_{2,1,0,0,1,1;\dots}$ for Π_3 and $I_{3,1,0,0,1,1;\dots}$ for Π'_3 .

Furthermore, we truncate the maximum number of suggestions by discarding integrals with more than $\sum_i q_i = 6$ which leaves us with a few ten thousand¹¹ suggestions per topology and fermion signature (cf. Table 2.4). In Fig. 2.7 we outlined the reduction

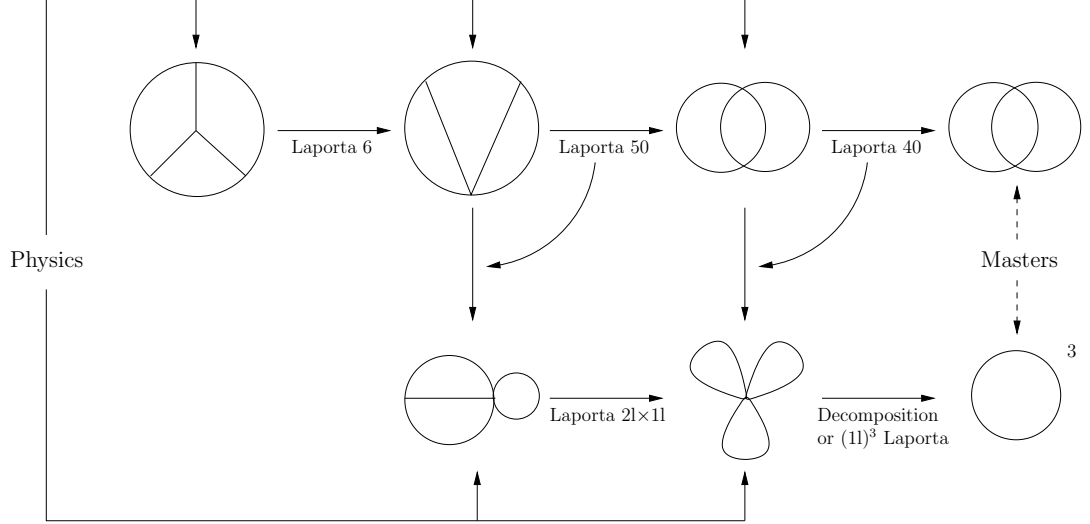


Figure 2.7: 3-loop reduction via Laporta algorithm and decompositions

process and two important things should be noted. Firstly we parallelise the reduction in such a way that each topology and fermion signature runs independently, indicated by Laporta 6, 40, 50, 21 \times 11 and (11)³. This is done by restricting the lhs's in Fig. 2.6 (during extraction) to their particular topology. Secondly, the above-mentioned decomposition is just a consequence of Eq. (2.22)

$$\begin{aligned}
I_{1,1,1,0,0,0;c1,c2,c3;\dots} &\rightarrow \oint_{P_{c1}, Q_{c2}, R_{c3}} \frac{P_0^{\dots} Q_0^{\dots} R_0^{\dots} (\mathbf{P} \cdot \mathbf{Q})^a (\mathbf{P} \cdot \mathbf{R})^b (\mathbf{Q} \cdot \mathbf{R})^c}{(P^2)^{\dots} (Q^2)^{\dots} (R^2)^{\dots}} \quad (2.39) \\
&= \oint_{P_{c1}, Q_{c2}} \frac{P_0^{\dots} Q_0^{\dots} (\mathbf{P} \cdot \mathbf{Q})^a}{(P^2)^{\dots} (Q^2)^{\dots}} \oint_{R_{c3}} \frac{R_0^{\dots} (\mathbf{P} \cdot \mathbf{R})^b (\mathbf{Q} \cdot \mathbf{R})^c}{(R^2)^{\dots}} \\
&\rightarrow \oint_{P_{c1}, Q_{c2}} \frac{P_0^{\dots} Q_0^{\dots} (\mathbf{P} \cdot \mathbf{Q})^a (\mathbf{P} \cdot \mathbf{Q})^{a'} + (\mathbf{P}^2)^{b'} (\mathbf{Q}^2)^{c'}}{(P^2)^{\dots} (Q^2)^{\dots}} \frac{dd_{i_1, i_1, \dots, i_{(b+c)/2}, i_{(b+c)/2}}}{dd_{i_1, i_1, \dots, i_{(b+c)/2}, i_{(b+c)/2}}} \oint_{R_{c3}} \frac{R_0^{\dots} (\mathbf{R}^2)^{\frac{b}{2}} (\mathbf{R}^2)^{\frac{c}{2}}}{(R^2)^{\dots}} \\
&\rightarrow \left\{ \oint_{P_{c1}, Q_{c2}} \frac{P_0^{\dots} Q_0^{\dots} (\mathbf{P}^2 \mathbf{Q}^2)^{\frac{a+a'}{2}}}{(P^2)^{\dots} (Q^2)^{\dots}} + \oint_{P_{c1}, Q_{c2}} \frac{P_0^{\dots} Q_0^{\dots} (\mathbf{P}^2)^{\frac{a}{2}+b'} (\mathbf{Q}^2)^{\frac{a}{2}+c'}}{(P^2)^{\dots} (Q^2)^{\dots}} \right\} \times
\end{aligned}$$

¹¹ Instead of a few hundred thousand suggestions which is far beyond what our implementation can handle in a realistic period (~ 1 -2 months runtime).

$$\times \left[dd_{i_1, i_1, \dots, i_{(b+c)/2}, i_{(b+c)/2}} \cdot dd_{j_1, j_1, \dots, j_{(a+a')/2}, j_{(a+a')/2}} \right]^{-1} \oint_{R_{c3}} \frac{R_0^{\dots} (\mathbf{R}^2)^{\frac{b+c}{2}}}{(R^2)^{\dots}},$$

where we have omitted prefactors and irrelevant integrals indicated by arrows. The last expression in Eq. (2.39) equals a sum of products of three 1-loop tadpoles times a rational function in d . It is also possible to derive an analogue decomposition for the 2loop \times 1loop sector but without any practical advantage over the Laporta approach because we are still faced with 2-loop diagrams.

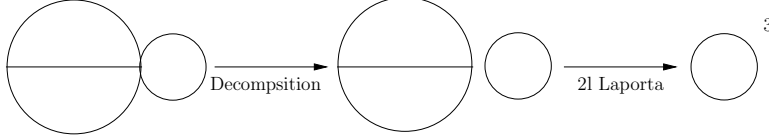


Figure 2.8: 2loop \times 1loop decomposition with 2-loop Laporta

$$\begin{aligned} I_{1,1,1,1,0,0;c1,c2,c3;\dots} &\rightarrow \oint_{P_{c1}, Q_{c2}, R_{c3}} \frac{P_0^{\dots} Q_0^{\dots} R_0^{\dots} (\mathbf{P} \cdot \mathbf{R})^b (\mathbf{Q} \cdot \mathbf{R})^c}{(P^2)^{\dots} (Q^2)^{\dots} (R^2)^{\dots} ((P-Q)^2)^{\dots}} \\ &= \oint_{P_{c1}, Q_{c2}} \frac{P_0^{\dots} Q_0^{\dots}}{(P^2)^{\dots} (Q^2)^{\dots} ((P-Q)^2)^{\dots}} \oint_{R_{c3}} \frac{R_0^{\dots} (\mathbf{P} \cdot \mathbf{R})^b (\mathbf{Q} \cdot \mathbf{R})^c}{(R^2)^{\dots}} \\ &\rightarrow \oint_{P_{c1}, Q_{c2}} \frac{P_0^{\dots} Q_0^{\dots}}{(P^2)^{\dots} (Q^2)^{\dots} ((P-Q)^2)^{\dots}} \frac{(\mathbf{P} \cdot \mathbf{Q})^{a'} + (\mathbf{P}^2)^{b'} (\mathbf{Q}^2)^{c'}}{dd_{i_1, i_1, \dots, i_{(b+c)/2}, i_{(b+c)/2}}} \oint_{R_{c3}} \frac{R_0^{\dots} (\mathbf{R}^2)^{\frac{b+c}{2}}}{(R^2)^{\dots}} \\ &\rightarrow \left\{ \oint_{P_{c1}, Q_{c2}} \frac{P_0^{\dots} Q_0^{\dots} (\mathbf{P} \cdot \mathbf{Q})^{a'}}{(P^2)^{\dots} (Q^2)^{\dots} ((P-Q)^2)^{\dots}} + \oint_{P_{c1}, Q_{c2}} \frac{P_0^{\dots} Q_0^{\dots} (\mathbf{P}^2)^{\frac{a}{2}+b'} (\mathbf{Q}^2)^{c'}}{(P^2)^{\dots} (Q^2)^{\dots}} \right\} \times \\ &\times \left[dd_{i_1, i_1, \dots, i_{(b+c)/2}, i_{(b+c)/2}} \right]^{-1} \oint_{R_{c3}} \frac{R_0^{\dots} (\mathbf{R}^2)^{\frac{b+c}{2}}}{(R^2)^{\dots}}. \end{aligned} \quad (2.40)$$

The first integral in Eq. (2.40) corresponds (after re-expressing the scalar product in terms of inverse propagators) to some generic 2-loop integrals in addition to (1-loop)³ integrals. As an example, we consider the bosonic Mercedes diagram. A complete reduction according to Fig. 2.7 looks as follows

$$\begin{aligned} I_{1,1,1,1,1,1;0,0,0;2,0,0} &= \frac{208 - 87d + 9d^2}{-600 + 390d - 84d^2 + 6d^3} I_{3,1,0,0,1,1;0,0,0;2,0,0} \\ &\quad + \frac{8}{60 - 27d + 3d^2} I_{2,1,0,0,1,1;0,0,0;0,0,0}, \end{aligned} \quad (2.41)$$

and the ϵ expansion for both masters can be found in Chapter 3. We end up this section with a flow chart which shows all manipulations needed in order to reduce the **self.C**

output (cf. Sec. 2.3) to master integrals. In Fig. 2.9, we show schematically how the different reduction steps discussed above work together in order to substantially reduce the number of integrals to be computed for Π_3 .

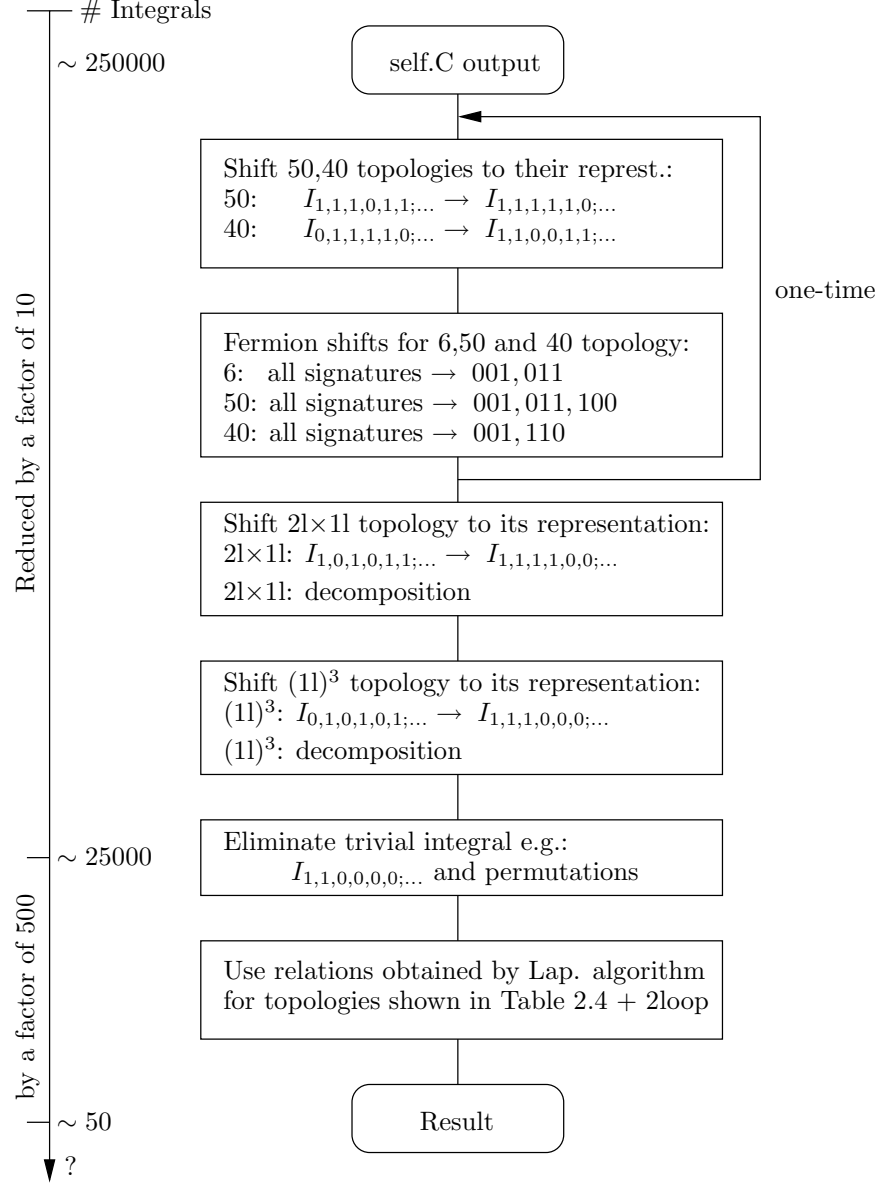


Figure 2.9: Overview of 3-loop reduction from **self.C** output to masters: The iteration is needed in cases like $I_{1,1,1,1,1,0;0,1,0;...} \rightarrow I_{1,1,1,1,1,0;0,0,1;...} + I_{0,1,1,1,1,0;0,0,1;...} + \dots \rightarrow I_{1,1,0,0,1,1;1,0,0;...} + \dots \rightarrow I_{1,1,0,0,1,1;0,0,1;...} + \dots$

2.6 Implementation of the Laporta algorithm

In this section we describe the concrete implementation of Laporta's method outlined in Section 2.5. In principle, the implementation of Fig. 2.6 looks rather simple. However, there are still problems we should pay attention to. In particular, during the extraction

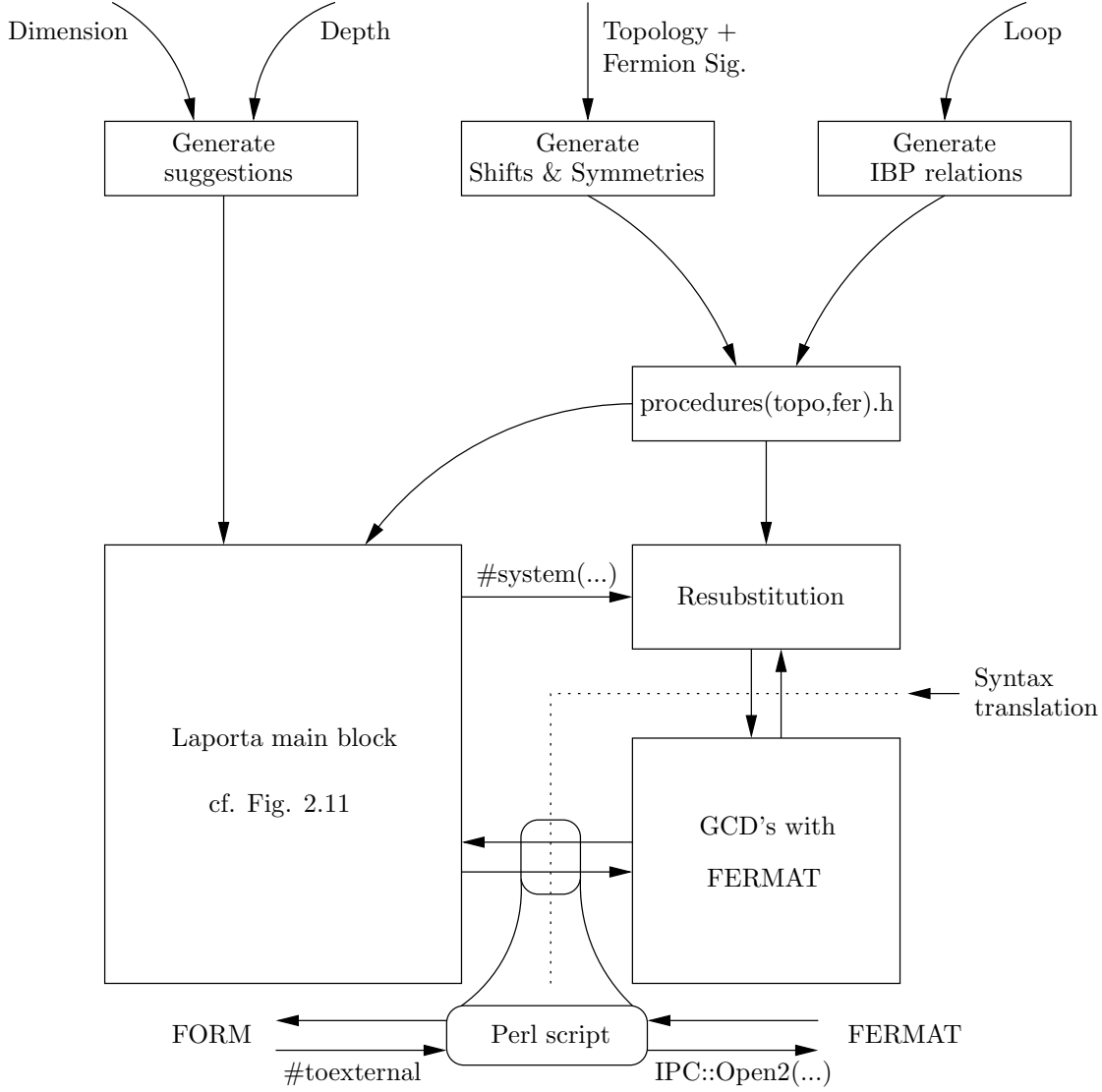


Figure 2.10: Laporta implementation in FORM with external program FERMAT.

and generation of new relations we are faced with the problem how to compute the coefficients

$$c_m = \frac{b_m}{b_{m'}} \quad \forall m, \quad (2.42)$$

where b_m stands for polynomials in one or more variables. In other words, the computa-

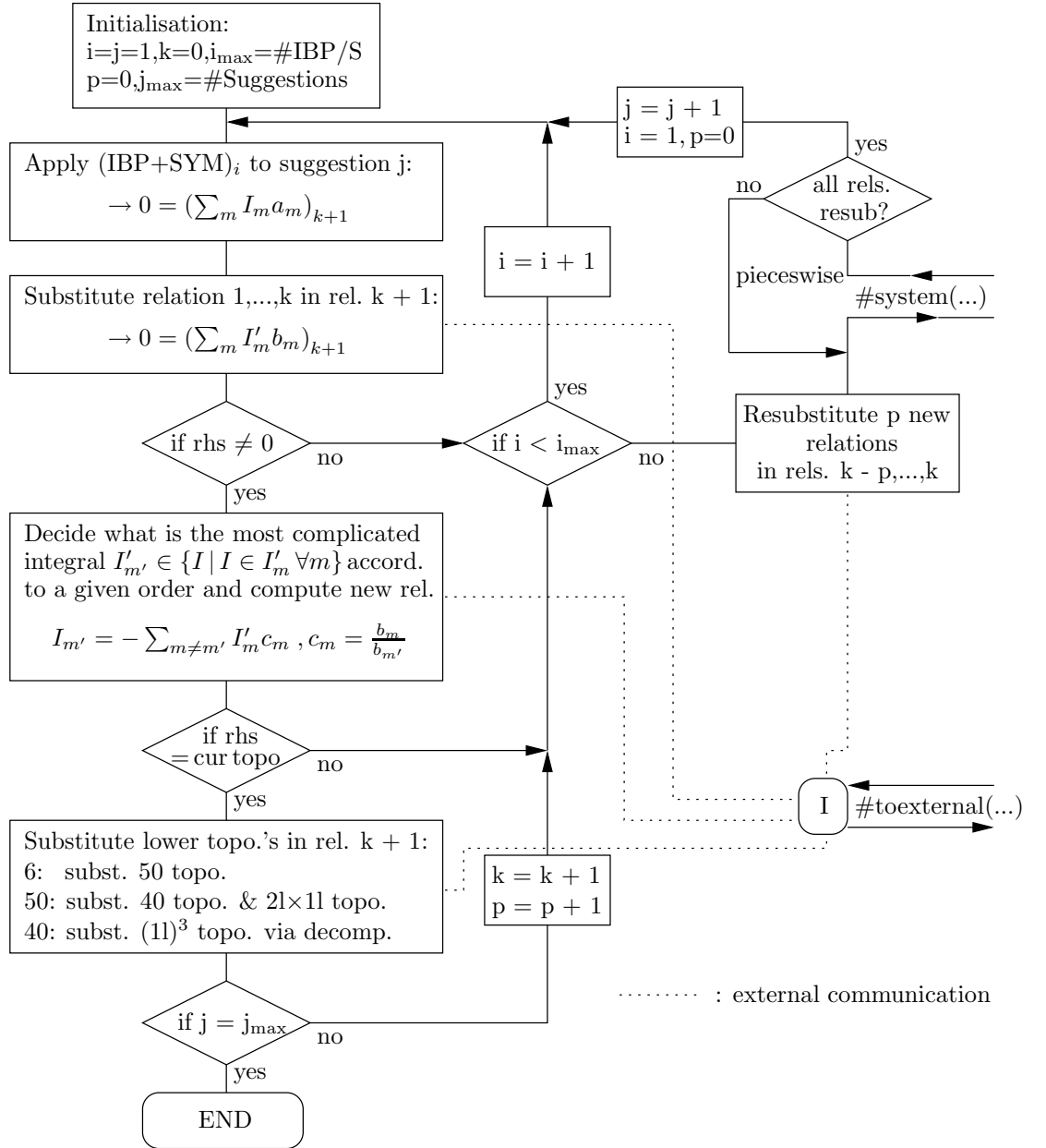


Figure 2.11: Laporta main block

tion of coefficients c_m corresponds to determining the greatest common divisor (GCD) of two polynomials in one or more variables. Unfortunately, the current version of FORM is not capable to compute polynomial GCD's in a reliable way so that we revert to external software. In the following we use the external program FERMAT [38] for all polynomial algebra during the reduction process. In addition, as indicated in Fig. 2.10, a script is needed for syntax translation [39] between FORM and FERMAT.

Let us have a closer look at Fig. 2.11: A comparison with Fig. 2.6 reveals slight differences. In principle, a straightforward implementation of Fig. 2.6 works quite well, at least for the two-loop computation. However, if we try to apply the 'naive' approach at three-loop we run into a dead end for two reasons. The first problem occurs simply due to the required 'depth' (cf. sec. 2.5) which results in systems with $\sim 10^3 - 10^5$ relations¹² and eventually the question of how to handle such a huge amount of relations in an efficient way. The second problem is, as always, to optimise the implementation as far as possible to reach an acceptable run-time behaviour. To this end, we

1. restrict lhs's to current topology \rightarrow reduces number of irrelevant relations,
2. use relations obtained from other topologies \rightarrow minimises size of rhs's,
3. suppress simplification of 'simple' coefficients \rightarrow reduces external communication.

Without going into great detail, everything together results in a speed-up factor of ~ 25 depending on topology and fermion signature. In Fig. 2.11 we also indicated the way how to perform the re-substitution safely¹³. In addition, this approach allows to parallelise the time-consuming re-substitutions (cf. sec. A.4) on multi-core systems and we observe a good scaling behaviour on two- and four-core machines.

In order to estimate the complexity, we make the following assumptions: average number of new relations per suggestion $\equiv N_r$, number of relations after j processed suggestions $\equiv N_j \approx N_r \cdot j$, then the average time for suggestion $j + 1$ becomes

$$t_j \approx N_r \sum_{i=1}^{N_j} T_i \approx N_r T \sum_{i=1}^{N_j} 1 \approx N_r^2 T j \quad (2.43)$$

where we made the naive assumption $T_i \approx T$. The behaviour in Eq. (2.43) agrees roughly with Figs. A.3 and A.4 (green curve) in Appendix A.4. In general, it is rather difficult to predict the concrete run-time behaviour for a given topology and fermion signature. But it turns out, at least for our implementation, that large rhs's are the biggest problem and affect the run-time behaviour significantly. This is the main reason for using lower topologies during the reduction. Moreover, the symmetries introduced in Sec. 2.4 play also an essential role in minimising the rhs's. For instance, the purely bosonic spectacles topology runs about three times faster than the mixed-spectacles one (fermion sig. 001).

¹²A factor of 10 to 1000 more compared to the two-loop computation.

¹³In terms of avoiding memory overflows.

3 Evaluation of master integrals

As we have seen in Sec. 2.5 all non-trivial masters are basketball-type integrals. We start with a brief review of already known basketball sum-integrals. For convenience we define, in the notation of Eq. (2.29c),

$$\begin{aligned} S_1^{\text{bb}} &\equiv I_{1,1,0,0,1,1;0,0,0;0,0,0}, \\ S_1^{\text{bf}} &\equiv I_{1,1,0,0,1,1;0,0,1;0,0,0}, \\ S_1^{\text{ff}} &\equiv I_{1,1,0,0,1,1;1,1,0;0,0,0}. \end{aligned} \quad (3.1)$$

The simplest basketball sum-integral evaluated by Arnold and Zhai [40] in $3-2\epsilon$ spatial dimensions reads

$$S_1^{\text{bb}} = \frac{1}{(4\pi)^2} \left(\frac{T^2}{12} \right)^2 \left[\frac{6}{\epsilon} + 36 \ln \frac{\bar{\mu}}{4\pi T} - 12 \frac{\zeta'(-3)}{\zeta(-3)} + 48 \frac{\zeta'(-1)}{\zeta(-1)} + \frac{182}{5} \right] + \mathcal{O}(\epsilon), \quad (3.2)$$

and the corresponding fermionic basketball diagram evaluates to [41]:

$$S_1^{\text{ff}} = \frac{1}{(4\pi)^2} \left(\frac{T^2}{12} \right)^2 \left[\frac{3}{2\epsilon} + 9 \ln \frac{\bar{\mu}}{4\pi T} - 3 \frac{\zeta'(-3)}{\zeta(-3)} + 12 \frac{\zeta'(-1)}{\zeta(-1)} + \frac{173}{20} - \frac{63}{5} \ln 2 \right] + \mathcal{O}(\epsilon). \quad (3.3)$$

Fortunately, the mixed basketball S_1^{bf} is just a linear combination of Eq. (3.2) and (3.3) and is given by

$$S_1^{\text{bf}} = \frac{1}{6} (2^{6\epsilon-1} - 1) S_1^{\text{bb}} - \frac{1}{6} S_1^{\text{ff}}, \quad (3.4)$$

and can be seen by rescaling spatial momenta by a factor of 2:

$$\begin{aligned} S_1^{\text{bb}} &= \oint_{P,Q,R} \frac{1}{P^2 Q^2 (P-R)^2 (Q-R)^2} = \oint_{P,Q,K,R} \frac{\delta(P+Q+K+R)}{P^2 Q^2 K^2 R^2} \\ &= \mu^{-2\epsilon} \frac{1}{T} \oint_{P,Q,K,R} \frac{\delta_{p_0+q_0+k_0+r_0} (2\pi)^{3-2\epsilon} \delta^{3-2\epsilon}(\mathbf{p} + \mathbf{q} + \mathbf{k} + \mathbf{r})}{P^2 Q^2 K^2 R^2} \\ &= \mu^{-2\epsilon} \frac{1}{T} 2^{4-8\epsilon} \oint_{P,Q,K,R} \frac{\delta_{p_0+q_0+k_0+r_0} (2\pi)^{3-2\epsilon} \delta^{3-2\epsilon}(2\mathbf{p} + 2\mathbf{q} + 2\mathbf{k} + 2\mathbf{r})}{[(\pi T n)^2 + \mathbf{p}^2] Q^2 K^2 R^2} \\ &= \mu^{-2\epsilon} \frac{1}{T} 2^{1-6\epsilon} \oint_{P+\{P\}} \dots \oint_{R+\{R\}} \frac{\delta_{p_0+q_0+k_0+r_0} (2\pi)^{3-2\epsilon} \delta^{3-2\epsilon}(\mathbf{p} + \mathbf{q} + \mathbf{k} + \mathbf{r})}{P^2 Q^2 K^2 R^2} \end{aligned}$$

$$\begin{aligned}
&= 2^{1-6\epsilon} \oint_{P+\{P\}} \cdots \oint_{R+\{R\}} \frac{1}{P^2 Q^2 R^2} \left[\underbrace{\frac{1}{(p_0 + q_0 + r_0)^2 + (\dots)^2}}_{\text{even}} + \underbrace{\frac{1}{(p_0 + q_0 + r_0)^2 + (\dots)^2}}_{\text{odd}} \right] \\
&= 2^{1-6\epsilon} \left[S_1^{\text{bb}} + 6 S_1^{\text{bf}} + S_1^{\text{ff}} \right], \tag{3.5}
\end{aligned}$$

where we have used fermion shifts and symmetries of S_1^{bb} , S_1^{bf} and S_1^{ff} . A similar identity can be obtained for

$$\begin{aligned}
S_2^{\text{bb}} &\equiv I_{2,1,0,0,1,1;0,0,0;0,0,0}, \\
S_2^{\text{bf}} &\equiv I_{2,1,0,0,1,1;0,0,1;0,0,0}, \\
S_2^{\text{ff}} &\equiv I_{2,1,0,0,1,1;1,1,0;0,0,0}, \\
S_{2,1}^{\text{bf}} &\equiv I_{1,1,0,0,1,2;0,0,1;0,0,0},
\end{aligned} \tag{3.6}$$

and reads

$$S_2^{\text{bb}} = 2^{-1-6\epsilon} \left[S_2^{\text{bb}} + 3 S_2^{\text{bf}} + 3 S_{2,1}^{\text{bf}} + S_2^{\text{ff}} \right]. \tag{3.7}$$

The integrals shown in (3.6) are needed for the computation of Π_3 . S_2^{bb} is already known [42] and can be written as

$$\begin{aligned}
S_2^{\text{bb}} &= \frac{T^2}{8(4\pi)^2} \left\{ \frac{1}{\epsilon^2} + \frac{1}{\epsilon} \left[3 \ln \frac{\mu^2}{4\pi T^2} + \frac{17}{6} + \gamma_E + 2 \frac{\zeta'(-1)}{\zeta(-1)} \right] + \frac{9}{2} \left(\ln \frac{\mu^2}{4\pi T^2} \right)^2 + \right. \\
&\quad + \left(\frac{17}{2} + 3\gamma_E + 6 \frac{\zeta'(-1)}{\zeta(-1)} \right) \ln \frac{\mu^2}{4\pi T^2} + \frac{131}{12} + \frac{31\pi^2}{36} + 8 \ln 2\pi - \frac{9}{2} \gamma_E - \\
&\quad \left. - \frac{15}{2} \gamma_E^2 + (5 + 2\gamma_E) \frac{\zeta'(-1)}{\zeta(-1)} + 2 \frac{\zeta''(-1)}{\zeta(-1)} - 16\gamma_1 + 0.388594531408(4) \right\} + \mathcal{O}(\epsilon) \tag{3.8}
\end{aligned}$$

where γ_1 refers to the first Stieltjes constant, defined through the series $\zeta(s) = 1/(s-1) + \sum_{n=0}^{\infty} \gamma_n (-1)^n (s-1)^n / n!$.

3.1 Bosonic basketball S_3^{bb}

As a first example we demonstrate the feasibility of adapting the techniques used for the basketball diagrams S_1^{bb} and S_2^{bb} in order to determine the new master integral

$$S_3^{\text{bb}} \equiv I_{3,1,0,0,1,1;0,0,0;0,0,0}, \tag{3.9}$$

which appears as a master in the computation of Π'_3 . Let us start with noting that, by a momentum shift, the integral (3.9) can be written as

$$S_3^{\text{bb}} = \oint_P \Pi(P) \bar{\Pi}(P), \tag{3.10}$$

with

$$\Pi(P) \equiv \oint_Q \frac{1}{Q^2(Q-P)^2}, \quad (3.11)$$

$$\bar{\Pi}(P) \equiv \oint_Q \frac{1}{Q^6(Q-P)^2}. \quad (3.12)$$

First of all, we review some properties regarding the UV behaviour of (3.11). We split (3.11) into its zero-temperature and finite-temperature part

$$\Pi(P) = \Pi^{(0)}(P) + \Pi^{(T)}(P), \quad (3.13)$$

and note that the leading UV behaviour of (3.11) is given by its zero-temperature limit

$$\Pi^{(0)}(P) = \mu^{2\epsilon} \int \frac{d^{3-2\epsilon}Q}{(2\pi)^{3-2\epsilon}} \frac{1}{Q^2(P-Q)^2} \equiv \frac{\beta}{(P^2)^\epsilon} = \frac{\mu^{2\epsilon}}{(4\pi)^{2-\epsilon}} \frac{\Gamma(\epsilon)\Gamma^2(1-\epsilon)}{\Gamma(2-2\epsilon)} \frac{1}{(P^2)^\epsilon}, \quad (3.14)$$

where the last equality sign can be seen through Feynman parametrisation. For the finite-temperature part we first evaluate the sum via the usual contour integral trick

$$\Pi^{(T)}(P) = \mu^{2\epsilon} \int \frac{d^{3-2\epsilon}q}{(2\pi)^{3-2\epsilon}} \int_{-\infty+iO^+}^{+\infty-iO^+} \frac{dp}{2\pi} [f(p) + f(-p)] n(ip), \quad (3.15)$$

where $n(ip) \equiv [\exp(i\beta p) - 1]^{-1}$ refers to the bosonic distribution function and

$$f(p') = \frac{1}{[p'^2 + \mathbf{q}^2][(p_0 + p')^2 + (\mathbf{p} + \mathbf{q})^2]}. \quad (3.16)$$

Computing the residues of (3.15) results in

$$\Pi^{(T)}(P) = -\mu^{2\epsilon} \int \frac{d^{3-2\epsilon}q}{(2\pi)^{3-2\epsilon}} \frac{n(q)}{q} \left[\frac{1}{(q-ip_0)^2 - |\mathbf{q} + \mathbf{p}|^2} + \frac{1}{(q+ip_0)^2 - |\mathbf{q} - \mathbf{p}|^2} \right], \quad (3.17)$$

and Taylor expanding the denominators for $P \gg T$ yields

$$\Pi^{(T)}(P) = -\mu^{2\epsilon} \int \frac{d^{3-2\epsilon}q}{(2\pi)^{3-2\epsilon}} \frac{n(q)}{q} \left[\frac{2}{P^2} + \frac{8(ip_0q + \mathbf{p} \cdot \mathbf{q})^2}{P^6} \right] + \mathcal{O}(T^6/P^6), \quad (3.18)$$

which is justified by the fact that only $q \lesssim T$ contribute. Then our final result becomes

$$\Pi(P) = \Pi^{(0)}(P) + \frac{2}{P^2} I_b(1) + \Delta\Pi(P), \quad (3.19)$$

where $\Delta\Pi(P)$ behaves in the UV as $1/P^4$. In addition, let us for convenience, define a third function

$$\tilde{\Pi}(P) \equiv \oint_Q \frac{\Pi^{(0)}(Q)}{(Q-P)^2}, \quad (3.20)$$

for which an analogous examination gives

$$\tilde{\Pi}(P) = \tilde{\Pi}^{(0)}(P) + \Pi^{(0)}(P)I_b(1) + \Delta\tilde{\Pi}(P), \quad (3.21)$$

with

$$\tilde{\Pi}^{(0)}(P) \equiv \tilde{\beta}(P^2)^{1-2\epsilon} = \frac{\mu^{2\epsilon}}{(4\pi)^{2-\epsilon}} \frac{\Gamma(1-\epsilon)\Gamma(2-2\epsilon)\Gamma(-1+2\epsilon)}{\Gamma(\epsilon)\Gamma(3-3\epsilon)} \beta(P^2)^{1-2\epsilon}. \quad (3.22)$$

All following computations are performed in configuration space and therefore we need Fourier-representations for propagators and for the functions introduced above. Defining the inverse Fourier transformation

$$\mathcal{F}(q_0, r; \alpha) \equiv \int \frac{d^3\mathbf{q}}{(2\pi)^3} \frac{e^{-i\mathbf{q}\cdot\mathbf{r}}}{(q^2 + q_0^2)^\alpha} = \frac{2^{-1/2-\alpha}\pi^{-3/2}}{\Gamma(\alpha)} \left(\frac{|q_0|}{r}\right)^{3/2-\alpha} K_{3/2-\alpha}(|q_0|r), \quad (3.23)$$

and using Eqs. (3.19), (3.21) we obtain

$$\begin{aligned} \frac{1}{(Q-P)^2} &= \int d^3r e^{i(\mathbf{q}-\mathbf{p})\cdot\mathbf{r}} \mathcal{F}(q_0 - r_0, r; 1) \\ &= \frac{1}{4\pi} \int d^3r e^{i(\mathbf{q}-\mathbf{p})\cdot\mathbf{r}} e^{-|q_0-p_0|r} \frac{1}{r}, \end{aligned} \quad (3.24)$$

$$\frac{1}{P^6} = \frac{1}{2^3 4\pi} \int d^3r e^{i\mathbf{p}\cdot\mathbf{r}} e^{-|p_0|r} \left(1 + \frac{1}{|p_0|r}\right) \frac{r}{|p_0|^2}, \quad (3.25)$$

$$\frac{1}{P^8} = \frac{1}{2^4 4\pi} \int d^3r e^{i\mathbf{p}\cdot\mathbf{r}} e^{-|p_0|r} \left(\frac{1}{3} + \frac{1}{|p_0|r} + \frac{1}{(|p_0|r)^2}\right) \frac{r^2}{|p_0|^3}, \quad (3.26)$$

$$\Delta\Pi(P) = \frac{T}{(4\pi)^2} \int d^3r \frac{1}{r^2} e^{i\mathbf{p}\cdot\mathbf{r}} e^{-|p_0|r} \left(\coth \bar{r} - \frac{1}{\bar{r}} - \frac{\bar{r}}{3}\right), \quad (3.27)$$

$$\begin{aligned} \Delta\tilde{\Pi}(P) &= \frac{T}{(4\pi)^4} \int d^3r \frac{1}{r^4} e^{i\mathbf{p}\cdot\mathbf{r}} e^{-|p_0|r} \left\{ \bar{r} \text{csch}^2 \bar{r} + (2 + |\bar{p}_0|\bar{r})(|\bar{p}_0| + \coth \bar{r}) - \right. \\ &\quad \left. - \frac{1}{\bar{r}}(3 + 3|\bar{p}_0|\bar{r} + \bar{p}_0^2 \bar{r}^2) - \frac{\bar{r}}{3}(1 + |\bar{p}_0|\bar{r}) \right\}, \end{aligned} \quad (3.28)$$

where we have introduced the dimensionless variables

$$\bar{r} \equiv 2\pi T r, \quad \bar{p}_0 \equiv p_0/2\pi T, \quad (3.29)$$

and noted that $\Delta\Pi(P), \Delta\tilde{\Pi}(P)$ behaves as $1/P^4$ and $1/P^2$ at large P , respectively. Finally, we consider Eq. (3.12) and start with separating the Matsubara zero-mode

$$\bar{\bar{\Pi}}(P) = \not\int_Q' \frac{1}{Q^6(Q-P)^2} + T\mu^{2\epsilon} \int \frac{d^{3-2\epsilon}q}{(2\pi)^{3-2\epsilon}} \frac{1}{q^6 [(\mathbf{q}-\mathbf{p})^2 + p_0^2]} \equiv \bar{\bar{\Pi}}_r(P) + \bar{\bar{\Pi}}_0(P), \quad (3.30)$$

where the prime indicates the leaving out of the Matsubara zero-mode. $\bar{\bar{\Pi}}_r(P)$ is both UV and IR convergent and hence we perform the momentum integration in three dimensions

$$\bar{\bar{\Pi}}_r(P) = \frac{T}{2^3(4\pi)^2} \int d^3r e^{i\mathbf{p}\cdot\mathbf{r}} \sum_{q_0 \neq 0} \frac{1}{|q_0|^2} \left(1 + \frac{1}{|q_0|r}\right) e^{-(|q_0|+|q_0-p_0|)r}, \quad (3.31)$$

in which we used Eq. (3.24) and (3.25). The zero-mode contribution $\bar{\bar{\Pi}}_0(P)$ is UV but not IR convergent

$$\bar{\bar{\Pi}}_0(P) = T\mu^{2\epsilon} \int \frac{d^{3-2\epsilon}q}{(2\pi)^{3-2\epsilon}} \left\{ \frac{1}{q^6 [(\mathbf{q} - \mathbf{p})^2 + p_0^2]} - \left[\frac{1}{q^6 P^2} + \frac{1}{3} \frac{P^2 - 4p_0^2}{q^4 (P^2)^3} \right] \right\}$$

where the last two terms vanish in dimensional regularisation but render the expression IR convergent and allow for a momentum integration in three dimensions

$$\begin{aligned} &= -\frac{T}{(2\pi)^2} \int_0^\infty dq \frac{1}{q^2} \left\{ \frac{2}{q^2 P^2} + \frac{2}{3} \frac{P^2 - 4p_0^2}{(P^2)^3} + \frac{1}{2pq^3} \ln \left[\frac{(p-q)^2 + p_0^2}{(p+q)^2 + p_0^2} \right] \right\} \\ &= -\frac{T}{4\pi} \left[\frac{2|p_0|^3}{(P^2)^4} - \frac{|p_0|}{(P^2)^3} \right], \end{aligned} \quad (3.32)$$

such that using the expressions in Eq. (3.25) and (3.26) finally yields

$$\bar{\bar{\Pi}}_0(P) = -\frac{T}{24(4\pi)^2} \int d^3r r^2 e^{i\mathbf{p}\cdot\mathbf{r}} e^{-|p_0|r}. \quad (3.33)$$

We now proceed in complete analogy with the appendix of [42] and begin the calculation by dividing Eq. (3.10) into two categories of terms, contributions that are potentially divergent $S_3^{\text{bb},\dots,\text{b}}$ but simple enough to allow an analytic evaluation, and contributions which are perhaps complicated but both UV and IR convergent $S_3^{\text{bb},\dots,\text{a}}$. First we write

$$\begin{aligned} S_3^{\text{bb}} &= \not\!\!\!\int_P \Delta\Pi(P) \bar{\bar{\Pi}}_r(P) + \not\!\!\!\int_P \Delta\Pi(P) \bar{\bar{\Pi}}_0(P) + 2I_b(1) \not\!\!\!\int_P \frac{\Pi(P)}{P^6} + \not\!\!\!\int_P \frac{\tilde{\Pi}(P)}{P^6} \\ &\equiv S_3^{\text{bb,I}} + S_3^{\text{bb,II}} + S_3^{\text{bb,III}} + S_3^{\text{bb,IV}}, \end{aligned} \quad (3.34)$$

where we have used Eq. (3.19) for the split-up procedure. We repeat the procedure in $S_3^{\text{bb,IV}}$ by using Eq. (3.21) and take into account that integrals without scales¹ vanish in dimensional regularisation. Thereby

$$S_3^{\text{bb,I}} = \not\!\!\!\int_P \Delta\Pi(P) \bar{\bar{\Pi}}_r(P) \quad (3.35)$$

$$\begin{aligned} S_3^{\text{bb,II}} &= \not\!\!\!\int_P' \Delta\Pi(P) \bar{\bar{\Pi}}_0(P) + T\mu^{2\epsilon} \int \frac{d^{3-2\epsilon}p}{(2\pi)^{3-2\epsilon}} \Pi(p_0=0, p) \bar{\bar{\Pi}}_0(p_0=0, p) \\ &\equiv S_3^{\text{bb,II,a}} + S_3^{\text{bb,II,b}} \end{aligned} \quad (3.36)$$

$$\begin{aligned} S_3^{\text{bb,III}} &= 2I_b(1) \left\{ \not\!\!\!\int_P' \frac{\Pi^{(T)}(P)}{P^6} + T\mu^{2\epsilon} \int \frac{d^{3-2\epsilon}p}{(2\pi)^{3-2\epsilon}} \frac{\Pi(p_0=0, p)}{\mathbf{p}^6} + \not\!\!\!\int_P \frac{\Pi^{(0)}(P)}{P^6} \right\} \\ &\equiv S_3^{\text{bb,III,a}} + S_3^{\text{bb,III,b}} + S_3^{\text{bb,III,c}} \end{aligned} \quad (3.37)$$

¹ $\Delta\Pi \rightarrow \Pi - \Pi^{(0)} - 2I_b(1)/P^2$ in $S_3^{\text{bb,II,b}}$, $\Pi^{(T)} \rightarrow \Pi - \Pi^{(0)}$ in $S_3^{\text{bb,III,b}}$ and $\Delta\tilde{\Pi} \rightarrow \tilde{\Pi} - \tilde{\Pi}^{(0)} - I_b(1)\Pi^{(0)}$ in $S_3^{\text{bb,IV,b}}$

$$\begin{aligned}
S_3^{\text{bb,IV}} &= \not\int'_P \frac{\Delta \tilde{\Pi}(P)}{P^6} + T\mu^{2\epsilon} \int \frac{d^{3-2\epsilon}p}{(2\pi)^{3-2\epsilon}} \frac{\tilde{\Pi}(p_0=0, p)}{\mathbf{p}^6} + I_b(1)\beta \not\int_P \frac{1}{(P^2)^{3+\epsilon}} + \not\int_P \frac{\tilde{\Pi}^{(0)}(P)}{P^6} \\
&\equiv S_3^{\text{bb,IV,a}} + S_3^{\text{bb,IV,b}} + S_3^{\text{bb,IV,c}} + S_3^{\text{bb,IV,d}}
\end{aligned} \tag{3.38}$$

Let us start evaluating the integrals which are both UV and IR convergent i.e. $S_3^{\text{bb},\dots,\text{a}}$:

$$\begin{aligned}
S_3^{\text{bb,I}} &= \frac{T^3}{8(4\pi)^4} \int d^3r \frac{1}{r^2} \left(\coth \bar{r} - \frac{1}{\bar{r}} - \frac{\bar{r}}{3} \right) \sum_{p_0} \sum_{q_0 \neq 0} \left(\frac{1}{|q_0|^2} + \frac{1}{|q_0|^3 r} \right) e^{-(|p_0|+|q_0|+|q_0+p_0|)r} \\
&= \frac{2}{(4\pi)^6} \int_0^\infty dr \left(\coth r - \frac{1}{r} - \frac{r}{3} \right) \left(\text{Li}_2(e^{-2r}) \left(\coth r + \frac{1}{r} \right) + \text{Li}_3(e^{-2r}) \frac{\coth r}{r} - \right. \\
&\quad \left. - \ln(1 - e^{-2r}) \right) \\
&\approx -\frac{2}{(4\pi)^6} \times 0.0256487(1),
\end{aligned} \tag{3.39}$$

where the last integration was performed numerically with MATHEMATICA [43] and

$$\begin{aligned}
&\sum_{p_0} \sum_{q_0 \neq 0} \left(\frac{1}{|q_0|^2} + \frac{1}{|q_0|^3 r} \right) e^{-(|p_0|+|q_0|+|q_0+p_0|)r} \\
&= \sum_{q_0 \neq 0} \left(\frac{1}{|q_0|^2} + \frac{1}{|q_0|^3 r} \right) \left(|\bar{q}_0| + \coth \bar{r} \right) e^{-2|q_0|r} \\
&= \frac{2}{(2\pi T)^2} \sum_{n=1}^\infty \left[\frac{1}{n} + \frac{1}{n^2} \left(\coth \bar{r} + \frac{1}{\bar{r}} \right) + \frac{1}{n^3} \frac{\coth \bar{r}}{\bar{r}} \right] e^{-2n\bar{r}},
\end{aligned} \tag{3.40}$$

where we first carried out the p_0 sum

$$\begin{aligned}
&e^{-|q_0|r} \sum_{p_0} e^{-(|p_0|+|q_0+p_0|)r} = e^{-|q_0|r} \sum_{n=-\infty}^\infty e^{-(|n|+|n+|m||)\bar{r}} \\
&= e^{-|q_0|r} \left[\sum_{n=-\infty}^{-|m|-1} e^{n\bar{r}} e^{(n+|m|)\bar{r}} + \sum_{n=-|m|}^0 e^{n\bar{r}} e^{-(n+|m|)\bar{r}} + \sum_{n=1}^\infty e^{-n\bar{r}} e^{-(n+|m|)\bar{r}} \right] \\
&= e^{-2|q_0|r} \left[|\bar{q}_0| + \coth \bar{r} \right].
\end{aligned} \tag{3.41}$$

Using Eq. (3.36) in addition to Eq. (3.27) and (3.33) yields

$$\begin{aligned}
S_3^{\text{bb,II,a}} &= -\frac{T^3}{24(4\pi)^4} \int d^3r \left(\coth \bar{r} - \frac{1}{\bar{r}} - \frac{\bar{r}}{3} \right) \sum_{p_0 \neq 0} e^{-2|p_0|r} \\
&= -\frac{2}{3(4\pi)^6} \int_0^\infty dr r^2 \left(\coth r - \frac{1}{r} - \frac{r}{3} \right) \frac{1}{e^{2r} - 1} \\
&= -\frac{2}{3(4\pi)^6} \frac{1}{720} (30\pi^2 - \pi^4 - 180\zeta(3)).
\end{aligned} \tag{3.42}$$

For $S_3^{\text{bb,III,a}}$ the Fourier-representation of $\Pi^{(T)}$ is needed and can be obtained through Eq. (3.13) by subtracting the zero-temperature limit

$$\begin{aligned} S_3^{\text{bb,III,a}} &= I_b(1) \frac{T^2}{4(4\pi)^3} \int d^3r \frac{1}{r^2} \left(\coth r - \frac{1}{r} \right) \sum_{p_0 \neq 0} \left(1 + \frac{1}{|p_0|r} \right) \frac{r}{|p_0|^2} e^{-2|p_0|r} \\ &= \frac{2}{3(4\pi)^6} \int_0^\infty dr \left(\coth r - \frac{1}{r} \right) \left(r \text{Li}_2(e^{-2r}) + \text{Li}_3(e^{-2r}) \right) \\ &\approx \frac{2}{3(4\pi)^6} \times 0.15565346169869(1), \end{aligned} \quad (3.43)$$

where we have used Eq. (2.20) and (3.37). Finally, with Eq. (3.25), (3.28) and (3.38) we get

$$\begin{aligned} S_3^{\text{bb,IV,a}} &= \frac{T^2}{8(4\pi)^5} \int d^3r \frac{1}{r^3} \sum_{p_0 \neq 0} \left\{ \bar{r} \text{csch}^2 \bar{r} + (2 + |\bar{p}_0| \bar{r})(|\bar{p}_0| + \coth \bar{r}) - \right. \\ &\quad \left. - \frac{1}{\bar{r}}(3 + 3|\bar{p}_0| \bar{r} + \bar{p}_0^2 \bar{r}^2) - \frac{\bar{r}}{3}(1 + |\bar{p}_0| \bar{r}) \right\} \left(\frac{1}{|p_0|^2} + \frac{1}{|p_0|^3 r} \right) e^{-2|p_0|r} \\ &= \frac{1}{(4\pi)^6} \int_0^\infty dr \frac{1}{r} \sum_{n=1}^\infty \left\{ r \text{csch}^2 r + (2 + nr)(n + \coth r) - \right. \\ &\quad \left. - \frac{1}{r}(3 + 3nr + n^2 r^2) - \frac{r}{3}(1 + nr) \right\} \left(\frac{1}{n^2} + \frac{1}{n^3 r} \right) e^{-2nr} \\ &\approx -\frac{1}{(4\pi)^6} \times 0.0036161(1). \end{aligned} \quad (3.44)$$

For purposes of clarity we left out the lengthy expression which appears when performing the sum. At this point it is resonable to begin the computation of zero-mode contributions $S_3^{\text{bb},\dots,\text{b}}$ by recalling two formulas for Feynman parametrisation [28]

$$\frac{1}{A_1^{m_1} \dots A_n^{m_n}} = \int_0^1 dx_1 \dots dx_n \delta\left(\sum x_i - 1\right) \frac{\prod x_i^{m_i-1}}{[\sum x_i A_i]^{\sum m_i}} \frac{\Gamma(m_1 + \dots + m_n)}{\Gamma(m_1) \dots \Gamma(m_n)}, \quad (3.45)$$

where $m_1, \dots, m_n \in \mathbb{R}$ and

$$\int \frac{d^d l}{(2\pi)^d} \frac{1}{(l^2 + \Delta)^n} = \frac{1}{(4\pi)^{d/2}} \frac{\Gamma(n - d/2)}{\Gamma(n)} \left(\frac{1}{\Delta} \right)^{n-d/2}. \quad (3.46)$$

Applying Eq. (3.45) to $\bar{\Pi}_0(p_0 = 0, \mathbf{p})$ in Eq. (3.30) gives

$$\begin{aligned} \bar{\Pi}_0(p_0 = 0, \mathbf{p}) &= T\mu^{2\epsilon} \int \frac{d^{3-2\epsilon} q}{(2\pi)^{3-2\epsilon}} \int_0^1 dx dy \delta(x + y - 1) \frac{3x^2}{[x\mathbf{q}^2 + y(\mathbf{q} - \mathbf{p})^2]^4} \\ &= \frac{T\mu^{2\epsilon}}{(4\pi)^{3/2-\epsilon}} \frac{\Gamma(\frac{5}{2} + \epsilon)}{2} \int_0^1 dx \frac{x^2}{(x - x^2)^{5/2+\epsilon}} \frac{1}{(p^2)^{5/2+\epsilon}} \\ &= \frac{T\mu^{2\epsilon}}{2(4\pi)^{3/2-\epsilon}} \frac{\Gamma(\frac{5}{2} + \epsilon) \Gamma(\frac{1}{2} - \epsilon) \Gamma(-\frac{3}{2} - \epsilon)}{\Gamma(-1 + 2\epsilon)} \frac{1}{(p^2)^{5/2+\epsilon}}, \end{aligned} \quad (3.47)$$

where $\mathbf{l} \equiv \mathbf{q} - \mathbf{p} + x\mathbf{p}$, $\Delta \equiv x\mathbf{p}^2 - x^2\mathbf{p}^2$. An analogous reasoning for Eq. (3.11) and (3.20) produces

$$\Pi(p_0 = 0, \mathbf{p}) = T\mu^{2\epsilon} \frac{\Gamma(\frac{1}{2} + \epsilon)}{(4\pi)^{3/2-\epsilon}} \sum_{q_0} \int_0^1 dx \frac{1}{[x(1-x)p^2 + q_0^2]^{1/2+\epsilon}}, \quad (3.48)$$

$$\tilde{\Pi}(p_0 = 0, \mathbf{p}) = \frac{\beta T\mu^{2\epsilon}}{(4\pi)^{3/2-\epsilon}} \frac{\Gamma(-\frac{1}{2} + 2\epsilon)}{\Gamma(\epsilon)} \sum_{q_0} \int_0^1 dx \frac{(1-x)^{-1+\epsilon}}{[x(1-x)p^2 + q_0^2]^{-1/2+2\epsilon}}. \quad (3.49)$$

$$\begin{aligned} S_3^{\text{bb,II,b}} &= \frac{T^3\mu^{6\epsilon}}{2(4\pi)^{3-2\epsilon}} \frac{\Gamma(\frac{5}{2} + \epsilon)\Gamma(\frac{1}{2} + \epsilon)\Gamma(\frac{1}{2} - \epsilon)\Gamma(-\frac{3}{2} - \epsilon)}{\Gamma(-1 + 2\epsilon)} \sum_{q_0} \int_0^1 dx \int \frac{d^{3-2\epsilon}p}{(2\pi)^{3-2\epsilon}} \times \\ &\times \frac{1}{(p^2)^{5/2+\epsilon} [x(1-x)p^2 + q_0^2]^{1/2+\epsilon}} \\ &= \frac{T^3\mu^{6\epsilon}}{2(4\pi)^{3-2\epsilon}} \frac{\Gamma(\frac{5}{2} + \epsilon)\Gamma(\frac{1}{2} + \epsilon)\Gamma(\frac{1}{2} - \epsilon)\Gamma(-\frac{3}{2} - \epsilon)}{\Gamma(-1 + 2\epsilon)} \frac{2\pi^{3/2-\epsilon}}{\Gamma(\frac{3}{2} - \epsilon)(2\pi)^{3-2\epsilon}} \times \\ &\times \left\{ \sum_{q_0} (q_0^2)^{-3/2-3\epsilon} \right\} \left\{ \int_0^1 [x(1-x)]^{1+2\epsilon} \right\} \left\{ \int_0^\infty \frac{p^{-3-4\epsilon}}{(p^2+1)^{1/2+\epsilon}} \right\} \\ &= \frac{T^3\mu^{6\epsilon}}{2(4\pi)^{3-2\epsilon}} \frac{\Gamma(\frac{5}{2} + \epsilon)\Gamma(\frac{1}{2} + \epsilon)\Gamma(\frac{1}{2} - \epsilon)\Gamma(-\frac{3}{2} - \epsilon)}{\Gamma(-1 + 2\epsilon)} \frac{2\pi^{3/2-\epsilon}}{\Gamma(\frac{3}{2} - \epsilon)(2\pi)^{3-2\epsilon}} \times \\ &\times 2(2\pi T)^{-3-6\epsilon} \zeta(3+6\epsilon) \frac{\Gamma^2(2+2\epsilon)}{\Gamma(4+4\epsilon)} \frac{\Gamma(-1-2\epsilon)\Gamma(\frac{3}{2}+3\epsilon)}{2\Gamma(\frac{1}{2}+\epsilon)} \\ &= -\frac{\zeta(3)}{6(4\pi)^6} + \mathcal{O}(\epsilon), \end{aligned} \quad (3.50)$$

where we made use of $d^d p = 2\pi^{d/2}\Gamma^{-1}(\frac{d}{2}) |\mathbf{p}|^{d-1} d|\mathbf{p}|$ and rescaled the momentum integration by $q_0/(x(1-x))^{1/2}$. Similarly,

$$\begin{aligned} S_3^{\text{bb,III,b}} &= 2I_b(1)T^2\mu^{4\epsilon} \frac{\Gamma(\frac{1}{2} + \epsilon)}{(4\pi)^{3/2-\epsilon}} \sum_{q_0} \int_0^1 dx \int \frac{d^{3-2\epsilon}p}{(2\pi)^{3-2\epsilon}} \frac{1}{p^6 [x(1-x)p^2 + q_0^2]^{1/2+\epsilon}} \\ &= 2I_b(1)T^2\mu^{4\epsilon} \frac{\Gamma(\frac{1}{2} + \epsilon)}{(4\pi)^{3/2-\epsilon}} \frac{2\pi^{3/2-\epsilon}}{\Gamma(\frac{3}{2} - \epsilon)(2\pi)^{3-2\epsilon}} \left\{ \sum_{q_0} (q_0^2)^{-2-2\epsilon} \right\} \times \\ &\times \left\{ \int_0^1 dx [x(1-x)]^{3/2+\epsilon} \right\} \left\{ \int_0^\infty \frac{p^{-4-2\epsilon}}{(p^2+1)^{1/2+\epsilon}} \right\} \\ &= 2I_b(1)T^2\mu^{4\epsilon} \frac{\Gamma(\frac{1}{2} + \epsilon)}{(4\pi)^{3/2-\epsilon}} \frac{2\pi^{3/2-\epsilon}}{\Gamma(\frac{3}{2} - \epsilon)(2\pi)^{3-2\epsilon}} (2\pi T)^{-4-4\epsilon} 2\zeta(4+4\epsilon) \times \\ &\times \frac{\Gamma^2(\frac{5}{2} + \epsilon)}{\Gamma(5+2\epsilon)} \frac{\Gamma(-\frac{3}{2} - \epsilon)\Gamma(2+2\epsilon)}{2\Gamma(\frac{1}{2} + \epsilon)} \\ &= \frac{1}{6(4\pi)^6} \frac{\pi^4}{180} + \mathcal{O}(\epsilon). \end{aligned} \quad (3.51)$$

The last remaining zero-mode contribution becomes

$$\begin{aligned}
S_3^{\text{bb,IV,b}} &= \frac{\beta T^2 \mu^{4\epsilon}}{(4\pi)^{3/2-\epsilon}} \frac{\Gamma(-\frac{1}{2} + 2\epsilon)}{\Gamma(\epsilon)} \sum_{q_0} \int_0^1 dx \int \frac{d^{3-2\epsilon} p}{(2\pi)^{3-2\epsilon}} \frac{(1-x)^{-1+\epsilon}}{p^6 [x(1-x)p^2 + q_0^2]^{-1/2+2\epsilon}} \\
&= \frac{\beta T^2 \mu^{4\epsilon}}{(4\pi)^{3/2-\epsilon}} \frac{\Gamma(-\frac{1}{2} + 2\epsilon)}{\Gamma(\epsilon)} \frac{2\pi^{3/2-\epsilon}}{\Gamma(\frac{3}{2} - \epsilon)(2\pi)^{3-2\epsilon}} \left\{ \sum_{q_0} (q_0^2)^{-1-3\epsilon} \right\} \times \\
&\times \left\{ \int_0^1 dx x^{3/2+\epsilon} (1-x)^{1/2+2\epsilon} \right\} \left\{ \int_0^\infty \frac{p^{-4-2\epsilon}}{(p^2 + 1)^{-1/2+2\epsilon}} \right\} \\
&= \frac{\beta T^2 \mu^{4\epsilon}}{(4\pi)^{3/2-\epsilon}} \frac{\Gamma(-\frac{1}{2} + 2\epsilon)}{\Gamma(\epsilon)} \frac{2\pi^{3/2-\epsilon}}{\Gamma(\frac{3}{2} - \epsilon)(2\pi)^{3-2\epsilon}} (2\pi T)^{-2+6\epsilon} 2\zeta(2+6\epsilon) \times \\
&\times \frac{\Gamma(\frac{5}{2} + \epsilon) \Gamma(\frac{3}{2} + 2\epsilon) \Gamma(-\frac{3}{2} - \epsilon) \Gamma(1+3\epsilon)}{\Gamma(4+3\epsilon) 2\Gamma(-\frac{1}{2} + 2\epsilon)} \\
&= \frac{1}{6(4\pi)^6} \frac{\pi^2}{3} + \mathcal{O}(\epsilon). \tag{3.52}
\end{aligned}$$

We end up with expanding the tadpole contributions $S_3^{\text{bb,III,c}}$, $S_3^{\text{bb,IV,c}}$ and $S_3^{\text{bb,IV,d}}$ according to Eq. (2.9),

$$\begin{aligned}
S_3^{\text{bb,III,c}} + S_3^{\text{bb,IV,c}} + S_3^{\text{bb,IV,d}} &= 2I_b(1) \oint_P \frac{\Pi^{(0)}(P)}{P^6} + I_b(1)\beta \oint_P \frac{1}{(P^2)^{3+\epsilon}} + \oint_P \frac{\tilde{\Pi}^{(0)}(P)}{P^6} \\
&= \frac{1}{12(4\pi)^6} \left\{ -\frac{1}{\epsilon^2} + \frac{1}{\epsilon} \left[6\zeta(3) - \frac{9}{2} - 3\gamma_E - 3\ln\left(\frac{\mu^2}{4\pi T^2}\right) \right] \right\} + \\
&+ \frac{9}{2} \left(\ln \frac{\mu^2}{4\pi T^2} \right)^2 + \left(\frac{27}{2} + 9\gamma_E - 18\zeta(3) \right) \ln \frac{\mu^2}{4\pi T^2} + \frac{79}{4} + \\
&+ \frac{7\pi^2}{4} + \frac{27\gamma_E}{2} (1 - \gamma_E) + \left(18\gamma_E - 39 - 12 \frac{\zeta'(-1)}{\zeta(-1)} \right) \zeta(3) - \\
&- 24\zeta'(3) - 36\gamma_1 \Big\} + \mathcal{O}(\epsilon), \tag{3.53}
\end{aligned}$$

and collecting all parts to obtain the final result for the sum-integral S_3^{bb} :

$$\begin{aligned}
S_3^{\text{bb}} &= \frac{1}{12(4\pi)^6} \left\{ -\frac{1}{\epsilon^2} + \frac{1}{\epsilon} \left[6\zeta(3) - \frac{9}{2} - 3\gamma_E - 3\ln\left(\frac{\mu^2}{4\pi T^2}\right) \right] \right\} + \frac{9}{2} \left(\ln \frac{\mu^2}{4\pi T^2} \right)^2 + \\
&+ \left(\frac{27}{2} + 9\gamma_E - 18\zeta(3) \right) \ln \frac{\mu^2}{4\pi T^2} + \frac{79}{4} + \frac{25\pi^2}{12} + \frac{\pi^4}{45} + \frac{27\gamma_E}{2} (1 - \gamma_E) + \\
&+ \left(18\gamma_E - 39 - 12 \frac{\zeta'(-1)}{\zeta(-1)} \right) \zeta(3) - 24\zeta'(3) - 36\gamma_1 + 0.586266(1) \Big\} + \mathcal{O}(\epsilon). \tag{3.54}
\end{aligned}$$

In general, we need the ϵ expansion of master integrals up to $\mathcal{O}(\epsilon)$ because most of the corresponding coefficients contain poles in three dimensions, cf. Eqs. (A.2a - A.2f).

3.2 Bosonic basketball $S_{3,1}^{\text{bb}}$

As a further example we consider the basketball-like sum-integral

$$S_{3,1}^{\text{bb}} \equiv I_{3,1,0,0,1,1;0,0,0;2,0,0}, \quad (3.55)$$

with an irreducible scalar product. It turns out that due to its similarity to S_3^{bb} , we can use some intermediate results obtained during the S_3^{bb} computation. Let us start by noting that

$$S_{3,1}^{\text{bb}} = \oint_P \Pi(P) \bar{\bar{\Pi}}(P), \quad (3.56)$$

with

$$\bar{\bar{\Pi}}(P) \equiv \oint_Q \frac{Q_0^2}{Q^6(P-Q)^2}, \quad (3.57)$$

and $\Pi(P)$ from Eq. (3.11). From here on, we just repeat the procedure applied to the sum-integral S_3^{bb} , i.e. separating Eq. (3.55) into possibly divergent contributions but simple enough for an analytic evaluation and perhaps complicated contributions but both UV and IR convergent:

$$\begin{aligned} S_{3,1}^{\text{bb}} &= \oint_P \Delta \Pi(P) \bar{\bar{\Pi}}_r(P) + \oint_P \frac{\tilde{\Pi}(P) P_0^2}{P^6} + 2 I_b(1) \oint_P \frac{\Pi(P) P_0^2}{P^6} \\ &= S_{3,1}^{\text{bb,I}} + \underbrace{S_{3,1}^{\text{bb,II}}}_{=0} + S_{3,1}^{\text{bb,III}} + S_{3,1}^{\text{bb,IV}}, \end{aligned} \quad (3.58)$$

where we have taken into account that the zero-mode contribution vanishes identically cf. Eq. (3.36). The x -space representation of $\bar{\bar{\Pi}}_r(P)$ can be obtained immediately from Eq. (3.31) by multiplying from the right with Q_0^2 :

$$\bar{\bar{\Pi}}_r(P) = \frac{T}{2^3(4\pi)^2} \int d^3r e^{i\mathbf{p}\cdot\mathbf{r}} \sum_{q_0 \neq 0} \left(1 + \frac{1}{|q_0|r} \right) e^{-(|q_0|+|q_0-p_0|)r}. \quad (3.59)$$

Taking once more into account that integrals without scales vanish in dimensional regularisation (cf. Eq. (3.35 - 3.38)) gives

$$S_{3,1}^{\text{bb,I}} = \oint_P \Delta \Pi(P) \bar{\bar{\Pi}}_r(P) \quad (3.60)$$

$$\begin{aligned} S_{3,1}^{\text{bb,III}} &= 2 I_b(1) \oint_P \frac{\Pi^{(T)}(P) P_0^2}{P^6} + 2 I_b(1) \oint_P \frac{\Pi^{(0)}(P) P_0^2}{P^6} \\ &\equiv S_{3,1}^{\text{bb,III,a}} + S_{3,1}^{\text{bb,III,b}} \end{aligned} \quad (3.61)$$

$$\begin{aligned} S_{3,1}^{\text{bb,IV}} &= \oint_P \frac{\Delta \tilde{\Pi}(P) P_0^2}{P^6} + I_b(1) \beta \oint_P \frac{P_0^2}{(P^2)^{3+\epsilon}} + \oint_P \frac{\tilde{\Pi}^{(0)}(P) P_0^2}{P^6} \\ &\equiv S_{3,1}^{\text{bb,IV,a}} + S_{3,1}^{\text{bb,IV,b}} + S_{3,1}^{\text{bb,IV,c}} \end{aligned} \quad (3.62)$$

As before, we start by evaluating contributions which are both UV and IR finite. Plugging Eq. (3.27) and (3.59) in Eq. (3.60) results in

$$\begin{aligned}
S_{3,1}^{\text{bb,I}} &= \frac{T^3}{8(4\pi)^4} \int d^3r \frac{1}{r^2} \left(\coth \bar{r} - \frac{1}{\bar{r}} - \frac{\bar{r}}{3} \right) \sum_{p_0} \sum_{q_0 \neq 0} \left(1 + \frac{1}{|q_0| r} \right) e^{-(|p_0| + |q_0| + |q_0 + p_0|)r} \\
&= \frac{T^2}{2(4\pi)^4} \int_0^\infty dr \left(\coth r - \frac{1}{r} - \frac{r}{3} \right) \left(\frac{\text{csch}^2 r}{4} + \left(\frac{\coth r}{2} - \frac{1}{2} \right) \left(\coth r + \frac{1}{r} \right) - \right. \\
&\quad \left. - \frac{\coth r}{r} \ln(1 - e^{-2r}) \right) \\
&\approx -\frac{T^2}{2(4\pi)^4} \times 0.029779679922(1), \tag{3.63}
\end{aligned}$$

where we rescaled the integration variable by $1/2\pi T$ and used

$$\begin{aligned}
&\sum_{p_0} \sum_{q_0 \neq 0} \left(1 + \frac{1}{|q_0| r} \right) e^{-(|p_0| + |q_0| + |q_0 + p_0|)r} \\
&\stackrel{(3.41)}{=} \sum_{q_0 \neq 0} \left(1 + \frac{1}{|q_0| r} \right) \left(|\bar{q}_0| + \coth \bar{r} \right) e^{-2|q_0|r} \\
&= 2 \sum_{n=1}^\infty \left[n + \coth \bar{r} + \frac{1}{\bar{r}} + \frac{1}{n} \frac{\coth \bar{r}}{\bar{r}} \right] e^{-2n\bar{r}} \\
&= 2 \left[\frac{\text{csch}^2 \bar{r}}{4} + \left(\frac{\coth \bar{r}}{2} - \frac{1}{2} \right) \left(\coth \bar{r} + \frac{1}{\bar{r}} \right) - \frac{\coth \bar{r}}{\bar{r}} \ln(1 - e^{-2\bar{r}}) \right]. \tag{3.64}
\end{aligned}$$

Using the Fourier representation of $\Pi^{(T)}$ as in Eq. (3.43) gives

$$\begin{aligned}
S_{3,1}^{\text{bb,III,a}} &= I_b(1) \frac{T^2}{16(4\pi)^2} \int d^3r \frac{1}{r^2} \left(\coth r - \frac{1}{r} \right) \sum_{p_0 \neq 0} \left(1 + \frac{1}{|p_0| r} \right) r e^{-2|p_0|r} \\
&= \frac{T^2}{6(4\pi)^4} \int_0^\infty dr \left(\coth r - \frac{1}{r} \right) \left(\frac{r \coth r}{2} - \frac{r}{2} - \ln(1 - e^{-2\bar{r}}) \right) \\
&\approx \frac{T^2}{6(4\pi)^4} \times 0.1825395997(1). \tag{3.65}
\end{aligned}$$

The last remaining non-trivial contribution can be obtained via Eq. (3.62), (3.25) and (3.28) and reads

$$\begin{aligned}
S_{3,1}^{\text{bb,IV,a}} &= \frac{T^2}{8(4\pi)^5} \int d^3r \frac{1}{r^3} \sum_{p_0 \neq 0} \left\{ \bar{r} \text{csch}^2 \bar{r} + (2 + |\bar{p}_0| \bar{r})(|\bar{p}_0| + \coth \bar{r}) - \right. \\
&\quad \left. - \frac{1}{\bar{r}}(3 + 3|\bar{p}_0| \bar{r} + \bar{p}_0^2 \bar{r}^2) - \frac{\bar{r}}{3}(1 + |\bar{p}_0| \bar{r}) \right\} \left(1 + \frac{1}{|p_0| r} \right) e^{-2|p_0|r} \\
&= \frac{T^2}{4(4\pi)^4} \int_0^\infty dr \frac{1}{r} \sum_{n=1}^\infty \left\{ r \text{csch}^2 r + (2 + nr)(n + \coth r) - \right.
\end{aligned}$$

$$\begin{aligned}
& -\frac{1}{r}(3+3nr+n^2r^2)-\frac{r}{3}(1+nr)\left\{\left(1+\frac{1}{nr}\right)e^{-2nr}\right. \\
& \approx -\frac{T^2}{2(4\pi)^4}\times 0.00201064(1).
\end{aligned} \tag{3.66}$$

Expanding the tadpole contributions $S_{3,1}^{\text{bb,III,c}}$, $S_{3,1}^{\text{bb,IV,c}}$ and $S_{3,1}^{\text{bb,IV,d}}$ according to Eq. (2.9) yields

$$\begin{aligned}
S_{3,1}^{\text{bb,III,b}} + S_{3,1}^{\text{bb,IV,b}} + S_{3,1}^{\text{bb,IV,c}} &= 2I_b(1)\oint_P \frac{\Pi^{(0)}(P)P_0^2}{P^6} + I_b(1)\beta\oint_P \frac{P_0^2}{(P^2)^{3+\epsilon}} + \oint_P \frac{\tilde{\Pi}^{(0)}(P)P_0^2}{P^6} \\
&= \frac{T^2}{32(4\pi)^4}\left\{\frac{1}{\epsilon^2} + \frac{1}{\epsilon}\left[\frac{41}{6} + \gamma_E + 3\ln\left(\frac{\mu^2}{4\pi T^2}\right) + 2\frac{\zeta'(-1)}{\zeta(-1)}\right] + \right. \\
&\quad + \frac{9}{2}\left(\ln\frac{\mu^2}{4\pi T^2}\right)^2 + \left(\frac{41}{2} + 3\gamma_E + 6\frac{\zeta'(-1)}{\zeta(-1)}\right)\ln\frac{\mu^2}{4\pi T^2} + \\
&\quad + \frac{231}{12} + \frac{13\pi^2}{13} + \frac{\gamma_E}{6}(33 - 45\gamma_E) + \frac{\zeta'(-1)}{\zeta(-1)}(2\gamma_E + 15) + \\
&\quad \left. + 2\frac{\zeta''(-1)}{\zeta(-1)} - 16\gamma_1\right\} + \mathcal{O}(\epsilon).
\end{aligned} \tag{3.67}$$

Summing up all contributions results in

$$\begin{aligned}
S_{3,1}^{\text{bb}} &= \frac{T^2}{32(4\pi)^4}\left\{\frac{1}{\epsilon^2} + \frac{1}{\epsilon}\left[\frac{41}{6} + \gamma_E + 3\ln\left(\frac{\mu^2}{4\pi T^2}\right) + 2\frac{\zeta'(-1)}{\zeta(-1)}\right] + \frac{9}{2}\left(\ln\frac{\mu^2}{4\pi T^2}\right)^2 + \right. \\
&\quad + \left(\frac{41}{2} + 3\gamma_E + 6\frac{\zeta'(-1)}{\zeta(-1)}\right)\ln\frac{\mu^2}{4\pi T^2} + \frac{231}{12} + \frac{13\pi^2}{12} + \frac{\gamma_E}{6}(33 - 45\gamma_E) + \\
&\quad \left. + \frac{\zeta'(-1)}{\zeta(-1)}(2\gamma_E + 15) + 2\frac{\zeta''(-1)}{\zeta(-1)} - 16\gamma_1 + 0.4648994(1)\right\} + \mathcal{O}(\epsilon).
\end{aligned} \tag{3.68}$$

3.3 Mixed basketball $S_{2,1}^{\text{bf}}$

We have already encountered two different categories of master integrals appearing in this computation (cf. Chapter 4). We close this chapter by computing the last remaining ‘prototype’, $S_{2,1}^{\text{bf}}$ defined in Eq. (3.6). With the following definition

$$\bar{\Pi}_f(P) \equiv \oint_{\{Q\}} \frac{1}{Q^4(Q-P)^2}, \tag{3.69}$$

we can write $S_{2,1}^{\text{bf}}$ as

$$S_{2,1}^{\text{bf}} = \oint_P \Pi(P)\bar{\Pi}_f(P). \tag{3.70}$$

It should be noted that the computation for $S_{2,1}^{\text{bf}}$ is very similar to S_2^{bb} given in [42], except the fact that we replaced the ‘inner’ bosonic Matsubara sum by the corresponding

fermionic one. As a consequence, due to the absence of zero-modes, the separation of Eq. (3.70) simplifies to

$$\begin{aligned} S_{2,1}^{\text{bf}} &= \oint_P \Delta \Pi(P) \bar{\Pi}_f(P) + 2 I_b(1) \oint_{\{P\}} \frac{\Pi(P)}{P^4} + \oint_{\{P\}} \frac{\tilde{\Pi}(P)}{P^4} \\ &= S_{2,1}^{\text{bf,I}} + S_{2,1}^{\text{bf,III}} + S_{2,1}^{\text{bf,IV}}, \end{aligned} \quad (3.71)$$

where we have interchanged the order of integrations and made use of Eq. (3.19) and (3.20). As in section 3.2, with Eq. (3.13) and (3.21) we get

$$S_{2,1}^{\text{bf,I}} = \oint_P \Delta \Pi(P) \bar{\Pi}_f(P), \quad (3.72)$$

$$\begin{aligned} S_{2,1}^{\text{bf,III}} &= 2 I_b(1) \oint_{\{P\}} \frac{\Pi^{(T)}(P)}{P^4} + 2 I_b(1) \oint_{\{P\}} \frac{\Pi^{(0)}(P)}{P^4} \\ &\equiv S_{2,1}^{\text{bf,III,a}} + S_{2,1}^{\text{bf,III,b}}, \end{aligned} \quad (3.73)$$

$$\begin{aligned} S_{2,1}^{\text{bf,IV}} &= \oint_{\{P\}} \frac{\Delta \tilde{\Pi}(P)}{P^4} + I_b(1) \beta \oint_{\{P\}} \frac{1}{(P^2)^{2+\epsilon}} + \oint_{\{P\}} \frac{\tilde{\Pi}^{(0)}(P)}{P^4} \\ &\equiv S_{2,1}^{\text{bf,IV,a}} + S_{2,1}^{\text{bf,IV,b}} + S_{2,1}^{\text{bf,IV,c}}. \end{aligned} \quad (3.74)$$

Expressing Eq. (3.69) in Fourier representation yields

$$\bar{\Pi}_f(P) = \frac{T}{2(4\pi)^2} \int d^3 r \frac{1}{r} \sum_{q_{0,f}} \frac{1}{|q_0|} e^{-(|q_0|+|q_0-p_0|)r}, \quad (3.75)$$

where $q_{0,f}$ refers to fermionic Matsubara frequencies. Let us start with evaluating $S_{2,1}^{\text{bf,I}}$

$$\begin{aligned} S_{2,1}^{\text{bf,I}} &= \frac{T^3}{2(4\pi)^4} \int d^3 r \frac{1}{r^3} \left(\coth \bar{r} - \frac{1}{\bar{r}} - \frac{\bar{r}}{3} \right) \sum_{p_{0,b}} \sum_{q_{0,f}} \frac{1}{|q_0|} e^{-(|p_0|+|q_0|+|q_0-p_0|)r} \\ &= \frac{T^2}{(4\pi)^4} \int_0^\infty dr \frac{1}{r} \left(\coth r - \frac{1}{r} - \frac{r}{3} \right) \left[4 \operatorname{arccoth} e^r \coth r + \operatorname{csch} r \right] \\ &\approx -\frac{T^2}{(4\pi)^4} \times 0.185119(1), \end{aligned} \quad (3.76)$$

where the mixed bosonic/fermionic sum is given by

$$\begin{aligned} \sum_{p_{0,b}} \sum_{q_{0,f}} \frac{1}{|q_0|} e^{-(|p_0|+|q_0|+|q_0-p_0|)r} &= \sum_{q_{0,f}} \frac{e^{-|q_0|r}}{|q_0|} \sum_{p_{0,b}} e^{-(|p_0|+|q_0-p_0|)r} \\ &= \sum_{q_{0,f}} \frac{e^{-2|q_0|r}}{|q_0|} \left(|\bar{q}_0| + \coth \bar{r} \right) \\ &= \frac{1}{2\pi T} \left[\sum_{n=1}^\infty e^{-2(\frac{1}{2}+n)\bar{r}} \left(1 + \frac{\coth \bar{r}}{\frac{1}{2}+n} \right) + \sum_{n=-\infty}^{-1} e^{2(\frac{1}{2}+n)\bar{r}} \left(1 - \frac{\coth \bar{r}}{\frac{1}{2}+n} \right) + \right. \end{aligned}$$

$$\begin{aligned}
& + e^{-\bar{r}} (1 + 2 \coth \bar{r}) \Big] \\
& = \frac{1}{2\pi T} \left[4 \operatorname{arccoth} e^r \coth r + \operatorname{csch} r \right].
\end{aligned} \tag{3.77}$$

In Eq. (3.77) we interchanged the order of summations and used Eq. (3.41) for the usual bosonic sum. Expressing $1/P^4$ and $\Pi^{(T)}(P)$ in Fourier representation via Eqs. (3.23),(3.13) and using Eq. (3.73) yields

$$\begin{aligned}
S_{2,1}^{\text{bf,III,a}} &= I_b(1) \frac{T^2}{(4\pi)^3} \int d^3 r \frac{1}{r^2} \left(\coth \bar{r} - \frac{1}{\bar{r}} \right) \sum_{p_{0,\text{f}}} \frac{e^{-2|p_0|r}}{|p_0|} \\
&= \frac{4}{3} \frac{T^2}{(4\pi)^4} \int_0^\infty dr \left(\coth r - \frac{1}{r} \right) \operatorname{arccoth} e^r \\
&\approx \frac{4}{3} \frac{T^2}{(4\pi)^4} \times 0.287113(1).
\end{aligned} \tag{3.78}$$

We obtain $S_{2,1}^{\text{bf,IV,a}}$ by repeating the calculation above but with Eq. (3.28) instead of $\Pi^{(T)}(P)$

$$\begin{aligned}
S_{2,1}^{\text{bf,IV,a}} &= \frac{T^2}{2(4\pi)^5} \int d^3 r \frac{1}{r^4} \sum_{p_{0,\text{f}}} \frac{1}{|p_0|} \left\{ \bar{r} \operatorname{csch}^2 \bar{r} + (2 + |\bar{p}_0| \bar{r})(|\bar{p}_0| + \coth \bar{r}) - \right. \\
&\quad \left. - \frac{1}{\bar{r}} (3 + 3|\bar{p}_0| \bar{r} + \bar{p}_0^2 \bar{r}^2) - \frac{\bar{r}}{3} (1 + |\bar{p}_0| \bar{r}) \right\} e^{-2|p_0|r} \\
&= \frac{T^2}{2(4\pi)^4} \int_0^\infty dr \frac{1}{r^2} \left[4 \operatorname{arccoth} e^r \left(r \operatorname{csch}^2 r + 2 \coth r - \frac{3}{r} - \frac{r}{3} \right) + \right. \\
&\quad \left. + \operatorname{csch} r \left(r \coth r - 1 - \frac{r^2}{3} \right) \right] \\
&\approx -\frac{T^2}{(4\pi)^4} \times 0.00652384(1).
\end{aligned} \tag{3.79}$$

The fermionic tadpoles can be expressed in terms of the corresponding bosonic ones via Eq. (2.10) and then easily expanded in ϵ according to Eq. (2.9):

$$\begin{aligned}
S_{2,1}^{\text{bf,III,b}} + S_{2,1}^{\text{bf,IV,b}} + S_{2,1}^{\text{bf,IV,c}} &= 3 I_b(1) \beta (2^{4\epsilon+1} - 1) \not\int_P \frac{1}{(P^2)^{2+\epsilon}} + \tilde{\beta} (2^{6\epsilon-1} - 1) \not\int_P \frac{1}{(P^2)^{1+2\epsilon}} \\
&= \frac{T^2}{8(4\pi)^4} \left\{ \frac{1}{\epsilon^2} + \frac{1}{\epsilon} \left[3 \ln \frac{\mu^2}{4\pi T^2} + \frac{37}{12} + \gamma_E + 4 \ln 4 + 2 \frac{\zeta'(-1)}{\zeta(-1)} \right] \right. \\
&\quad \left. + \epsilon^0 \operatorname{fct}(\ln \mu, \ln T) \right\} + \mathcal{O}(\epsilon),
\end{aligned} \tag{3.80}$$

where we leave out the lengthy expression indicated by $\text{fct}(\ln \mu, \ln T)$. The result for $S_{2,1}^{\text{bf}}$ reads

$$S_{2,1}^{\text{bf}} = \frac{T^2}{8(4\pi)^4} \left\{ \frac{1}{\epsilon^2} + \frac{1}{\epsilon} \left[3 \ln \frac{\mu^2}{4\pi T^2} + \frac{37}{12} + \gamma_E + 4 \ln 4 + 2 \frac{\zeta'(-1)}{\zeta(-1)} \right] + \right. \\ \left. + \epsilon^0 \text{fct}(\ln \mu, \ln T) + 1.529395(1) \right\} + \mathcal{O}(\epsilon). \quad (3.81)$$

We conclude with a few remarks. In order to complete the calculation of the remaining masters shown in Eq. (3.6) we have to compute either the fermion basketball sum-integral S_2^{ff} or the other mixed basketball sum-integral S_2^{bf} . The first one can be obtained just by replacing the bosonic $\Pi(P)$ in Eq. (3.70) by the corresponding fermionic version

$$\Pi_f(P) \equiv \not\!\!\!\!\!\int_{\{Q\}} \frac{1}{Q^2(P-Q)^2}, \quad (3.82)$$

and the latter one simply by carrying out the S_2^{bb} computation given in [42] with an ‘outer’ fermionic sum instead of a bosonic sum. The same holds for

$$\begin{aligned} S_3^{\text{bb}} &\equiv I_{3,1,0,0,1,1;0,0,0;0,0,0}, \\ S_3^{\text{bf}} &\equiv I_{3,1,0,0,1,1;0,0,1;0,0,0}, \\ S_3^{\text{ff}} &\equiv I_{3,1,0,0,1,1;1,1,0;0,0,0}, \\ S_{3,1}^{\text{bf}} &\equiv I_{1,1,0,0,1,3;0,0,1;0,0,0}, \end{aligned} \quad (3.83)$$

with

$$S_3^{\text{bb}} = 2^{-3-6\epsilon} \left[S_3^{\text{bb}} + 3 S_3^{\text{bf}} + 3 S_{3,1}^{\text{bf}} + S_3^{\text{ff}} \right], \quad (3.84)$$

which are needed for the Π'_3 computation. Another important class of master integrals are those with irreducible scalar products and only one propagator with power more than one

$$\begin{aligned} S_i^{\text{bb}} &\equiv I_{i,1,0,0,1,1;0,0,0;\dots}, \\ S_i^{\text{bf}} &\equiv I_{i,1,0,0,1,1;0,0,1;\dots}, \\ S_i^{\text{ff}} &\equiv I_{i,1,0,0,1,1;1,1,0;\dots}, \\ S_{i,1}^{\text{bf}} &\equiv I_{1,1,0,0,1,i;0,0,1;\dots}, \end{aligned} \quad (3.85)$$

where the dots stands for permutations of irreducible scalar products, e.g.

$$\begin{aligned} \Pi_3 : i = 3 &\Rightarrow 2, 0, 0 \mid 0, 2, 0 \mid 0, 0, 2 \mid \dots, \\ \Pi'_3 : i = 4 &\Rightarrow 2, 0, 0 \mid 0, 2, 0 \mid 0, 0, 2 \mid \dots \end{aligned} \quad (3.86)$$

All basketball-like sum-integrals of this type can be evaluated exactly parallel to the above ones. The remaining master integrals (i.e. with dots on two different lines) can be obtained by deriving analogous representations for new functions $\Pi'(P)$ and $\tilde{\Pi}'(P)$ as in Eqs. (3.19),(3.21) and then proceeding as in the examples above.

4 Results and discussion

This chapter is primarily concerned with discussing the three-loop results obtained by the methods introduced in Chapter 2. However, before we focus on the three-loop results, we would like to point out that all one- and two-loop results given in [31] have been confirmed by our computation. Our results can be found in Appendix A.1.

4.1 Π_{E3} and Π'_{T3} reduction

The Taylor coefficient Π_{E3} is needed in order to compute the $\mathcal{O}(g^6)$ correction to m_E^2 . As indicated in Chapter 2, we perform the whole reduction in d dimensions with a general gauge parameter ξ . We observed that the longitudinal part vanishes identically

$$\Pi_{L3} = 0, \quad (4.1)$$

and verified the gauge parameter independence of Eq. (1.92) up to $\mathcal{O}(g^6)$. The corresponding expression reads (with $C_A = N_c, C_F = (N_c^2 - 1)/(2N_c), T_F = N_f/2$)

$$\begin{aligned} \Pi_{E3} = & C_A^3 [\alpha_1 I_{2,1,0,0,1,1;0,0,0;0,0,0} + \alpha_2 I_{2,2,0,0,1,1;0,0,0;0,0,2} + \alpha_3 I_{3,1,0,0,1,1;0,0,0;0,2,0} \\ & + \alpha_4 I_{3,1,0,0,1,1;0,0,0;2,0,0} + \alpha_5 I_{4,1,0,0,1,1;0,0,0;1,3,0} + \alpha_6 I_{5,1,0,0,1,1;0,0,0;6,0,0}] \\ & + T_F C_A C_F [\alpha_7 I_{1,1,0,0,2,1;0,0,1;0,0,0} + \alpha_8 I_{1,1,0,0,2,2;0,0,1;2,0,0} + \alpha_9 I_{2,1,0,0,1,1;0,0,1;0,0,0} + \\ & \alpha_{10} I_{2,1,0,0,1,1;1,1,0;0,0,0} + \alpha_{11} I_{2,1,0,0,2,1;0,0,1;0,2,0} + \alpha_{12} I_{2,1,0,0,2,1;0,0,1;2,0,0} + \\ & \alpha_{13} I_{2,2,0,0,1,1;0,0,1;1,1,0} + \alpha_{14} I_{2,2,0,0,1,1;0,0,1;2,0,0} + \alpha_{15} I_{3,1,0,0,1,1;0,0,1;0,2,0} + \\ & \alpha_{16} I_{3,1,0,0,1,1;0,0,1;1,1,0} + \alpha_{17} I_{3,1,0,0,1,1;0,0,1;2,0,0} + \alpha_{18} I_{3,1,0,0,1,1;1,1,0;2,0,0} + \\ & \alpha_{19} I_{3,1,0,0,2,1;0,0,1;1,3,0} + \alpha_{20} I_{3,2,0,0,1,1;0,0,1;0,4,0} + \alpha_{21} I_{4,1,0,0,1,1;0,0,1;1,3,0} + \\ & \alpha_{22} I_{4,1,0,0,1,1;0,0,1;2,2,0} + \alpha_{23} I_{4,1,0,0,1,1;0,0,1;4,0,0} + \alpha_{24} I_{4,2,0,0,1,1;0,0,1;6,0,0} + \\ & \alpha_{25} I_{5,1,0,0,1,1;0,0,1;3,3,0}] \\ & + T_F^2 C_F^2 [\alpha_{26} I_{1,1,0,0,2,1;0,0,1;0,0,0} + \alpha_{27} I_{1,1,0,0,2,2;0,0,1;2,0,0} + \alpha_{28} I_{1,1,0,0,3,1;0,0,1;1,1,0} + \\ & \alpha_{29} I_{2,1,0,0,1,1;0,0,1;0,0,0} + \alpha_{30} I_{2,1,0,0,1,1;1,1,0;0,0,0} + \alpha_{31} I_{2,1,0,0,2,1;0,0,1;0,2,0} + \\ & \alpha_{32} I_{2,1,0,0,2,1;0,0,1;2,0,0} + \alpha_{33} I_{2,2,0,0,1,1;0,0,1;1,1,0} + \alpha_{34} I_{2,2,0,0,1,1;0,0,1;2,0,0} + \\ & \alpha_{35} I_{3,1,0,0,1,1;0,0,1;0,2,0} + \alpha_{36} I_{3,1,0,0,1,1;0,0,1;1,1,0} + \alpha_{37} I_{3,1,0,0,1,1;0,0,1;2,0,0} + \\ & \alpha_{38} I_{3,1,0,0,1,1;1,1,0;2,0,0} + \alpha_{39} I_{3,1,0,0,2,1;0,0,1;1,3,0} + \alpha_{40} I_{3,2,0,0,1,1;0,0,1;0,4,0} + \\ & \alpha_{41} I_{4,1,0,0,1,1;0,0,1;1,3,0} + \alpha_{42} I_{4,1,0,0,1,1;0,0,1;2,2,0} + \alpha_{43} I_{4,1,0,0,1,1;0,0,1;4,0,0} + \\ & \alpha_{44} I_{4,2,0,0,1,1;0,0,1;6,0,0} + \alpha_{45} I_{5,1,0,0,1,1;0,0,1;3,3,0} + \alpha_{46} I_{5,1,0,0,1,1;0,0,1;5,1,0}] \\ & + T_F^2 C_A [\alpha_{47} I_{2,1,0,0,1,1;1,1,0;0,0,0} + \alpha_{48} I_{2,2,0,0,1,1;1,1,0;0,0,2} + \alpha_{49} I_{3,1,0,0,1,1;1,1,0;0,2,0} + \\ & \alpha_{50} I_{3,1,0,0,1,1;1,1,0;2,0,0} + \alpha_{51} I_{4,1,0,0,1,1;1,1,0;1,3,0} + \alpha_{52} I_{5,1,0,0,1,1;1,1,0;6,0,0}] \end{aligned}$$

$$\begin{aligned}
& +T_F^2 C_F [\alpha_{53} I_{2,1,0,0,1,1;1,1,0;0,0,0} + \alpha_{54} \textcolor{red}{I}_{2,2,0,0,1,1;1,1,0;0,0,2} + \alpha_{55} \textcolor{red}{I}_{3,1,0,0,1,1;1,1,0;0,2,0} + \\
& \quad \alpha_{56} I_{3,1,0,0,1,1;1,1,0;2,0,0} + \alpha_{57} \textcolor{red}{I}_{5,1,0,0,1,1;1,1,0;6,0,0}] \\
& +T_F C_A^2 [\alpha_{58} I_{1,1,0,0,2,1;0,0,1;0,0,0} + \alpha_{59} I_{1,1,0,0,2,2;0,0,1;2,0,0} + \alpha_{60} I_{1,1,0,0,3,1;0,0,1;1,1,0} + \\
& \quad \alpha_{61} \textcolor{red}{I}_{1,1,0,0,3,1;0,0,1;2,0,0} + \alpha_{62} \textcolor{red}{I}_{1,1,0,0,4,1;0,0,1;3,1,0} + \alpha_{63} \textcolor{red}{I}_{1,1,0,0,4,1;0,0,1;4,0,0} + \\
& \quad \alpha_{64} I_{2,1,0,0,1,1;0,0,1;0,0,0} + \alpha_{65} I_{2,1,0,0,1,1;1,1,0;0,0,0} + \alpha_{66} I_{2,1,0,0,2,1;0,0,1;0,2,0} + \\
& \quad \alpha_{67} I_{2,1,0,0,2,1;0,0,1;2,0,0} + \alpha_{68} \textcolor{red}{I}_{2,1,0,0,3,1;0,0,1;0,4,0} + \alpha_{69} \textcolor{red}{I}_{2,1,0,0,3,1;0,0,1;3,1,0} + \\
& \quad \alpha_{70} \textcolor{red}{I}_{2,1,0,0,3,1;0,0,1;4,0,0} + \alpha_{71} \textcolor{red}{I}_{2,2,0,0,1,1;0,0,1;0,0,2} + \alpha_{72} I_{2,2,0,0,1,1;0,0,1;1,1,0} + \\
& \quad \alpha_{73} I_{2,2,0,0,1,1;0,0,1;2,0,0} + \alpha_{74} \textcolor{red}{I}_{3,1,0,0,1,1;0,0,1;0,0,2} + \alpha_{75} I_{3,1,0,0,1,1;0,0,1;0,2,0} + \\
& \quad \alpha_{76} I_{3,1,0,0,1,1;0,0,1;1,1,0} + \alpha_{77} I_{3,1,0,0,1,1;0,0,1;2,0,0} + \alpha_{78} I_{3,1,0,0,1,1;1,1,0;2,0,0} + \\
& \quad \alpha_{79} \textcolor{red}{I}_{3,1,0,0,2,1;0,0,1;0,4,0} + \alpha_{80} I_{3,1,0,0,2,1;0,0,1;1,3,0} + \alpha_{81} I_{3,2,0,0,1,1;0,0,1;0,4,0} + \\
& \quad \alpha_{82} \textcolor{red}{I}_{4,1,0,0,1,1;0,0,1;0,2,2} + \alpha_{83} \textcolor{red}{I}_{4,1,0,0,1,1;0,0,1;0,4,0} + \alpha_{84} \textcolor{red}{I}_{4,1,0,0,1,1;0,0,1;1,1,2} + \\
& \quad \alpha_{85} I_{4,1,0,0,1,1;0,0,1;1,3,0} + \alpha_{86} I_{4,1,0,0,1,1;0,0,1;2,2,0} + \alpha_{87} I_{4,1,0,0,1,1;0,0,1;4,0,0} + \\
& \quad \alpha_{88} I_{4,2,0,0,1,1;0,0,1;6,0,0} + \alpha_{89} \textcolor{red}{I}_{5,1,0,0,1,1;0,0,1;2,4,0} + \alpha_{90} I_{5,1,0,0,1,1;0,0,1;3,3,0} + \\
& \quad \alpha_{91} \textcolor{red}{I}_{5,1,0,0,1,1;0,0,1;4,0,2} + \alpha_{92} I_{5,1,0,0,1,1;0,0,1;5,1,0} + \alpha_{93} \textcolor{red}{I}_{5,1,0,0,1,1;0,0,1;6,0,0}] \\
& + (1\text{loop})^3 [\xi^0 + \xi^1 + \xi^2] , \tag{4.2}
\end{aligned}$$

where we leave out trivial contributions indicated by $(1\text{loop})^3$ and introduced a shorthand for the rational functions appearing by $\alpha_1, \dots, \alpha_{93}(d)$. The above expression leaves us with 46 (6 bosonic + 40 fermionic) basketball-like sum-integrals emphasised in red. This number depends significantly on the basis we choose. Expressing certain combinations of integrals shown above in terms of others could reduce the number of masters to ~ 25 but with the disadvantage of introducing spectacles-type integrals and basketball-type integrals with non-vanishing ‘central’ lines. The last line of Eq. (4.2) indicates symbolically that the gauge dependence is restricted to 1-loop structures as it should be in order to cancel against the one- and two-loop contributions given in Appendix A.1 via Eq. (1.92). Finally, the transverse part vanishes identically

$$\Pi_{T3} = 0. \tag{4.3}$$

Unfortunately, due to its complexity (cf. Eq. (2.37)), we are forced to perform the reduction of Π'_{T3} in Feynman gauge. As before, we observed

$$\Pi'_{L3} = 0 \tag{4.4}$$

and the relevant transverse part reads

$$\begin{aligned}
\Pi'_{T3} = & C_A^3 [\beta_1 \textcolor{red}{I}_{2,2,0,0,1,1;0,0,0;0,0,0} + \beta_2 \textcolor{red}{I}_{3,1,0,0,1,1;0,0,0;0,0,0} + \beta_3 \textcolor{red}{I}_{3,2,0,0,1,1;0,0,0;0,0,2} + \\
& \beta_4 \textcolor{red}{I}_{4,1,0,0,1,1;0,0,0;0,2,0} + \beta_5 \textcolor{red}{I}_{4,1,1,1,1,0;0,0,0;0,2,2} + \beta_6 \textcolor{red}{I}_{5,1,0,0,1,1;0,0,0;2,2,0} + \\
& \beta_7 \textcolor{red}{I}_{5,1,0,0,1,1;0,0,0;4,0,0}] \\
& +T_F C_A C_F [\beta_8 \textcolor{red}{I}_{1,1,0,0,2,2;0,0,1;0,0,0} + \beta_9 \textcolor{red}{I}_{1,1,0,0,3,1;0,0,1;0,0,0} + \beta_{10} \textcolor{red}{I}_{1,1,0,0,3,2;0,0,1;2,0,0} + \\
& \beta_{11} \textcolor{red}{I}_{1,1,0,0,4,1;0,0,1;2,0,0} + \beta_{12} \textcolor{red}{I}_{2,1,0,0,2,1;0,0,1;0,0,0} + \beta_{13} \textcolor{red}{I}_{2,1,0,0,3,1;0,0,1;0,2,0} + \\
& \beta_{14} \textcolor{red}{I}_{2,1,0,0,3,1;0,0,1;2,0,0} + \beta_{15} \textcolor{red}{I}_{2,2,0,0,1,1;0,0,1;0,0,0} + \beta_{16} \textcolor{red}{I}_{2,2,0,0,1,1;1,1,0;0,0,0} +
\end{aligned}$$

$$\begin{aligned}
& \beta_{17} I_{3,1,0,0,1,1,0,0,1,0,0,0} + \beta_{18} I_{3,1,0,0,1,1,1,1,0,0,0,0} + \beta_{19} I_{3,1,0,0,2,1,0,0,1,0,2,0} + \\
& \beta_{20} I_{3,1,0,0,2,1,0,0,1,1,1,0} + \beta_{21} I_{3,1,0,0,3,1,0,0,1,4,0,0} + \beta_{22} I_{3,2,0,0,1,1,0,0,1,0,2,0} + \\
& \beta_{23} I_{3,2,0,0,1,1,0,0,1,1,1,0} + \beta_{24} I_{4,1,0,0,1,1,0,0,1,0,2,0} + \beta_{25} I_{4,1,0,0,1,1,0,0,1,1,1,0} + \\
& \beta_{26} I_{4,1,0,0,1,1,0,0,1,2,0,0} + \beta_{27} I_{4,2,0,0,1,1,0,0,1,4,0,0} + \beta_{28} I_{5,1,0,0,1,1,0,0,1,2,2,0} + \\
& \beta_{29} I_{5,1,0,0,1,1,0,0,1,3,1,0} + \beta_{30} I_{5,1,0,0,1,1,0,0,1,4,0,0} + \beta_{31} I_{5,1,0,0,1,1,1,1,0,4,0,0} + \\
& \beta_{32} I_{6,1,0,0,1,1,0,0,1,4,2,0} + \beta_{33} I_{6,1,0,0,1,1,0,0,1,6,0,0} \\
& + T_F C_F^2 [\beta_{34} I_{1,1,0,0,2,2,0,0,1,0,0,0} + \beta_{35} I_{1,1,0,0,3,1,0,0,1,0,0,0} + \beta_{36} I_{2,1,0,0,2,1,0,0,1,0,0,0} + \\
& \beta_{37} I_{2,1,0,0,3,1,0,0,1,2,0,0} + \beta_{38} I_{2,2,0,0,1,1,0,0,1,0,0,0} + \beta_{39} I_{2,2,0,0,1,1,1,1,0,0,0,0} + \\
& \beta_{40} I_{3,1,0,0,1,1,0,0,1,0,0,0} + \beta_{41} I_{3,1,0,0,1,1,1,1,0,0,0,0} + \beta_{42} I_{3,1,0,0,2,1,0,0,1,1,1,0} + \\
& \beta_{43} I_{3,2,0,0,1,1,0,0,1,0,2,0} + \beta_{44} I_{3,2,0,0,1,1,0,0,1,1,1,0} + \beta_{45} I_{4,1,0,0,1,1,0,0,1,1,1,0} + \\
& \beta_{46} I_{4,1,0,0,1,1,0,0,1,2,0,0} + \beta_{47} I_{4,2,0,0,1,1,0,0,1,4,0,0} + \beta_{48} I_{5,1,0,0,1,1,0,0,1,3,1,0} + \\
& \beta_{49} I_{5,1,0,0,1,1,0,0,1,4,0,0} + \beta_{50} I_{5,1,0,0,1,1,1,1,0,4,0,0} + \beta_{51} I_{6,1,0,0,1,1,0,0,1,6,0,0}] \\
& + T_F^2 C_A [\beta_{52} I_{2,2,0,0,1,1,1,1,0,0,0,0} + \beta_{53} I_{3,1,0,0,1,1,1,1,0,0,0,0} + \beta_{54} I_{3,2,0,0,1,1,1,1,0,0,0,2} + \\
& \beta_{55} I_{4,1,0,0,1,1,1,1,0,0,2,0} + \beta_{56} I_{4,1,1,1,1,0,0,1,1,0,2,2} + \beta_{57} I_{5,1,0,0,1,1,1,1,0,2,2,0} + \\
& \beta_{58} I_{5,1,0,0,1,1,1,1,0,4,0,0}] \\
& + T_F^2 C_F [\beta_{59} I_{2,2,0,0,1,1,1,1,0,0,0,0} + \beta_{60} I_{3,1,0,0,1,1,1,1,0,0,0,0} + \beta_{61} I_{3,2,0,0,1,1,1,1,0,0,0,2} + \\
& \beta_{62} I_{4,1,0,0,1,1,1,1,0,0,2,0} + \beta_{63} I_{5,1,0,0,1,1,1,1,0,2,2,0} + \beta_{64} I_{5,1,0,0,1,1,1,1,0,4,0,0}] \\
& + T_F C_A^2 [\beta_{65} I_{1,1,0,0,2,2,0,0,1,0,0,0} + \beta_{66} I_{1,1,0,0,3,1,0,0,1,0,0,0} + \beta_{67} I_{1,1,0,0,3,2,0,0,1,2,0,0} + \\
& \beta_{68} I_{1,1,0,0,4,1,0,0,1,2,0,0} + \beta_{69} I_{2,1,0,0,2,1,0,0,1,0,0,0} + \beta_{70} I_{2,1,0,0,3,1,0,0,1,0,2,0} + \\
& \beta_{71} I_{2,1,0,0,3,1,0,0,1,2,0,0} + \beta_{72} I_{2,2,0,0,1,1,0,0,1,0,0,0} + \beta_{73} I_{2,2,0,0,1,1,1,1,0,0,0,0} + \\
& \beta_{74} I_{3,1,0,0,1,1,0,0,1,0,0,0} + \beta_{75} I_{3,1,0,0,1,1,1,1,0,0,0,0} + \beta_{76} I_{3,1,0,0,2,1,0,0,1,0,2,0} + \\
& \beta_{77} I_{3,1,0,0,2,1,0,0,1,1,1,0} + \beta_{78} I_{3,1,0,0,3,1,0,0,1,4,0,0} + \beta_{79} I_{3,2,0,0,1,1,0,0,1,0,0,2} + \\
& \beta_{80} I_{3,2,0,0,1,1,0,0,1,0,2,0} + \beta_{81} I_{3,2,0,0,1,1,0,0,1,1,1,0} + \beta_{82} I_{4,1,0,0,1,1,0,0,1,0,0,2} + \\
& \beta_{83} I_{4,1,0,0,1,1,0,0,1,0,2,0} + \beta_{84} I_{4,1,0,0,1,1,0,0,1,1,1,0} + \beta_{85} I_{4,1,0,0,1,1,0,0,1,2,0,0} + \\
& \beta_{86} I_{4,1,1,1,1,0,0,0,1,0,2,2} + \beta_{87} I_{4,2,0,0,1,1,0,0,1,4,0,0} + \beta_{88} I_{5,1,0,0,1,1,0,0,1,2,0,2} + \\
& \beta_{89} I_{5,1,0,0,1,1,0,0,1,2,2,0} + \beta_{90} I_{5,1,0,0,1,1,0,0,1,3,1,0} + \beta_{91} I_{5,1,0,0,1,1,0,0,1,4,0,0} + \\
& \beta_{92} I_{5,1,0,0,1,1,1,1,0,4,0,0} + \beta_{93} I_{6,1,0,0,1,1,0,0,1,4,2,0} + \beta_{94} I_{6,1,0,0,1,1,0,0,1,6,0,0}] \\
& + (\text{1loop})^3 \xi^0, \tag{4.5}
\end{aligned}$$

where we emphasised (7 bosonic and 34 fermionic) master integrals in red. It should be noted that the occurrence of spectacles-type integrals above can be seen as an indication of an incomplete reduction. The last term in Eq. (4.5) stands symbolically for trivial (1loop)³ contributions and due to the Feynman gauge, of course, proportional to ξ^0 . However, also with a general gauge parameter, all gauge dependent contributions should vanish because there is no contribution via Eq. (1.101).

The last remaining coefficient Π'_{E3} is comparable in terms of the appearing master integrals to the above one for Π'_{T3} . We leave out its explicit expression because it is not needed for the three-loop corrections to m_E^2 or g_E^2 .

4.2 Conclusions and Outlook

We have successfully shown the feasibility of calculating the next-to-next-to-leading order (NNLO) contributions for both matching coefficients m_E^2 and g_E^2 . The reduction by means of Laporta's method leaves us with approximately 40 to a large extent unknown basketball-like sum-integrals per coefficient. However, as demonstrated in Chapter 3, the computation of those is solely a question of man-power. We strongly believe that a semi-automatic application of Arnold & Zhai's method would be the most promising approach to deal with the remaining master integrals.

On the other hand, there are still problems we should pay attention to. The first task would be to check general gauge independence of Π'_{T3} i.e. the cancellation of all gauge dependent contributions to Π'_{T3} and, of course, $\Pi'_{L3} = 0$. Currently, the limiting factor is the pure bosonic basketball-type reduction. Furthermore, it would also be interesting to see if the still remaining spectacles-type integrals can be expressed through simpler ones, which we strongly believe to be the case.

In conclusion it should be stressed that future calculations in finite temperature QCD (e.g. $\mathcal{O}(g^6)$ pressure) depend on more sophisticated reduction methods and especially a systematic approach to dealing with hundreds of multi-loop master sum-integrals. Moreover, we believe that this thesis has shown that, while the combinatoric- and algebraic part seems to be under algorithmic control, the second part, i.e. the reduction, requires new methods, for which the computation outlined here can serve as an ideal — but already non-trivial — playground in order to develop the necessary tools.

A Appendix

A.1 Taylor coefficients

The one-loop coefficients up to second derivative read

$$\Pi_{T1}(0) = 0, \quad (\text{A.1a})$$

$$\Pi_{E1}(0) = (d-2) \left[C_A(d-2)I_b(1) - 2N_f I_f(1) \right], \quad (\text{A.1b})$$

$$\Pi'_{T1}(0) = \frac{2N_f}{3} I_f(2) + \frac{C_A}{6} (d-26) I_b(2), \quad (\text{A.1c})$$

$$\Pi'_{E1}(0) = \frac{N_f}{3} (d-2) I_f(2) - C_A \left[\frac{34-7d+d^2}{6} + (4-d)\xi \right] I_b(2), \quad (\text{A.1d})$$

$$\Pi''_{T1}(0) = \frac{C_A}{3} \left[\frac{21}{5} - \frac{1}{10}d + 2\xi - \frac{1}{4}\xi^2 \right] I_b(3) - \frac{4N_f}{15} I_f(3), \quad (\text{A.1e})$$

$$\Pi''_{E1}(0) = \frac{C_A}{3} \left[\frac{27}{5} - \frac{9}{10}d + \frac{1}{10}d^2 + \xi(d-4) + \frac{\xi^2}{4}(d-7) \right] I_b(3) + \frac{N_f}{15} (2-d) I_f(3), \quad (\text{A.1f})$$

while the two-loop coefficients up to first derivative are given by

$$\Pi_{T2}(0) = 0, \quad (\text{A.1g})$$

$$\begin{aligned} \Pi_{E2}(0) = (d-2)(d-4) \Big\{ (1+\xi) \left[2I_f(1) - (d-2)C_A I_b(1) \right] C_A I_b(2) + \\ + 2N_f C_F \left[I_b(1) - I_f(1) \right] I_f(2) \Big\}, \end{aligned} \quad (\text{A.1h})$$

$$\begin{aligned} \Pi'_{T2}(0) = \frac{(d-4)(d-5)}{(d-8)(d-6)(d-3)(d-1)} \Big\{ (36-58d+8d^2) C_A^2 I_b^2(2) - \\ - 4 \left[4C_F + (8-8d+d^2)C_A \right] N_f I_b(2) I_f(2) - \left[\left(\frac{d^3}{2} - \frac{15d^2}{2} + 33d - 32 \right) C_A - \right. \\ \left. - (68-68d+15d^2-d^3)C_F \right] N_f I_f^2(2) \Big\} \\ + \frac{(d-2)}{3(8+(d-9)d)} \Big\{ (176-33d+d^2) \left[(2-d)C_A I_b(1) + 2N_f I_f(1) \right] C_A I_b(3) - \\ - 4(d-7)(d-2)C_F N_f \left[I_b(1) - I_f(1) \right] I_f(3) \Big\}, \end{aligned} \quad (\text{A.1i})$$

$$\begin{aligned}
\Pi'_{E2}(0) = & \frac{(d-4)}{(d-8)(d-6)(d-3)(d-1)} \left\{ \left[-276 + 484d - 216d^2 + \frac{77}{2}d^3 - \frac{5}{2}d^4 \right] N_c^2 I_b^2(2) \right. \\
& + \left[(80 - 126d + 67d^2 - 14d^3 + d^4) C_A + (80 - 56d + 8d^2) C_F \right] N_f I_b(2) I_f(2) \\
& + (d-2) \left[(16 + 17d - 10d^2 + d^3) C_A + (18 + 19d - 10d^2 + d^3) C_F \right] N_f I_f^2(2) \left. \right\} \\
& + \frac{(d-4)}{24(d-3)} \left[(-324 + 184d - 40d^2 + 4d^3) \xi + (96 - 57d + 9d^2) \xi^2 \right] C_A^2 I_b^2(2) \\
& - \frac{1}{3} (8 - 6d + d^2) \xi C_A N_f I_b(2) I_f(2) + \frac{(d-2)}{3(8-9d+d^2)} \left\{ (20 - 38d + 13d^2 - d^3) \times \right. \\
& \times C_F N_f \left[I_f(1) - I_b(1) \right] I_f(3) + \left[(-256 + 142d - 32d^2 + 2d^3) + (-16 + 34d \right. \\
& \left. - 20d^2 + 2d^3) \xi + (-56 + 71d - 16d^2 + d^3) \xi^2 \right] \left[\frac{C_A}{2} I_b(1) - N_f I_f(1) \right] C_A I_b(3) \left. \right\}, \tag{A.1j}
\end{aligned}$$

where $\xi_{\text{here}} = 1 - \xi_{\text{standard}}$. As an example we give the coefficients for the bosonic contribution to Π_{E3} :

$$\begin{aligned}
\alpha_1 = & 156d^3 - 3530d^2 + \frac{97081d}{4} + \frac{1775}{8(d-7)} + \frac{120}{d-6} - \frac{20115}{16(d-5)} + \frac{666}{d-4} - \\
& - \frac{5927087}{528(d-3)} - \frac{9016}{99(3d-20)} - \frac{3377681}{72}, \tag{A.2a}
\end{aligned}$$

$$\begin{aligned}
\alpha_2 = & 72d^2 - \frac{4839d}{4} - \frac{3525}{16(d-7)} + \frac{128}{d-6} - \frac{9600}{d-4} + \frac{1503803}{176(d-3)} - \frac{1120}{11(3d-20)} + \frac{11713}{2}, \tag{A.2b}
\end{aligned}$$

$$\alpha_3 = -66d^2 + \frac{4511d}{4} - \frac{6225}{16(d-7)} + \frac{688}{d-6} - \frac{455977}{176(d-3)} + \frac{4480}{11(3d-20)} - 4459, \tag{A.2c}$$

$$\begin{aligned}
\alpha_4 = & 970d^2 - \frac{223195d}{12} + \frac{5025}{16(d-7)} - \frac{1136}{3(d-6)} - \frac{76744}{d-4} + \frac{16092929}{176(d-3)} - \frac{21280}{99(3d-20)} + \\
& + \frac{1554067}{18}, \tag{A.2d}
\end{aligned}$$

$$\alpha_5 = -\frac{567}{11(d-3)} + \frac{26880}{11(3d-20)} - 12 - \frac{675}{d-7}, \tag{A.2e}$$

$$\alpha_6 = \frac{237056}{d-4} - \frac{147456}{d-3} - 24576 + \frac{17408}{d-6}. \tag{A.2f}$$

A.2 Vertices of QCD in background field gauge

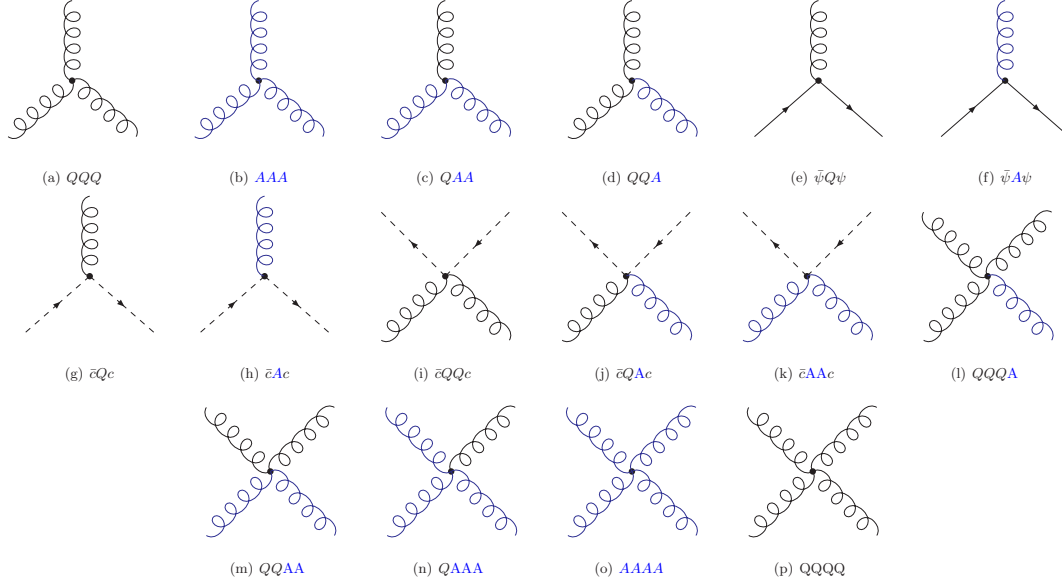


Figure A.1: Vertices of QCD in the background field gauge (A = background field, Q = fluctuating field, c, \bar{c} = ghost field)

A.3 Selected three-loop self-energy diagrams

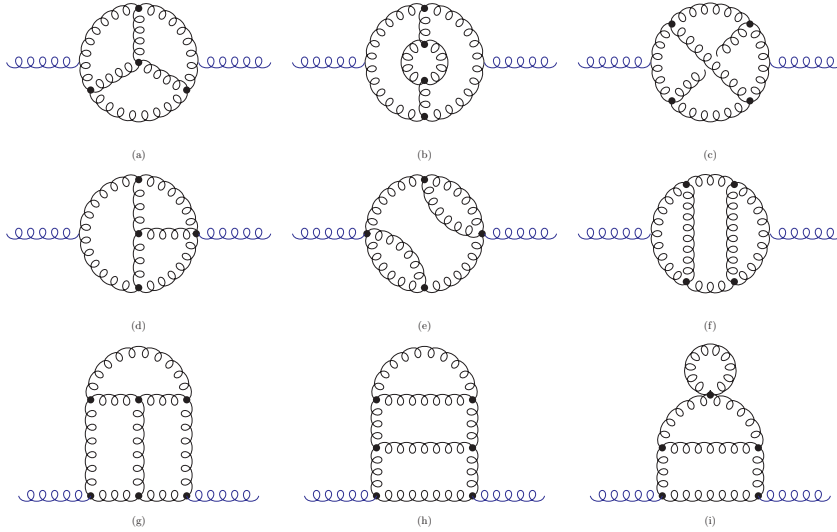


Figure A.2: Selected three-loop self-energy diagrams in background field gauge. The diagrams entirely composed of 3-gluon vertices contain 1 – 2.5 million terms.

A.4 Computation details

We perform the reduction on a linux cluster with 16 dual-core Intel Xeon 3.00GHz processors each with 4 GB RAM and use FORM 3.2(May 21 2008), FERMAT 3.9.8c.

Topology	Dimension	Suggestions	Run-time
Mercedes	Π_3	96	8 mins
Mercedes	Π'_3	300	3 hrs
Spectacles	Π_3	5500	1-3 weeks
Spectacles	Π'_3	13000+	2+ months
Basketball	Π_3	15500	1 month
Basketball	Π'_3	15500+	2+ months

Table A.1: Computing time for different topologies and Taylor coefficients.

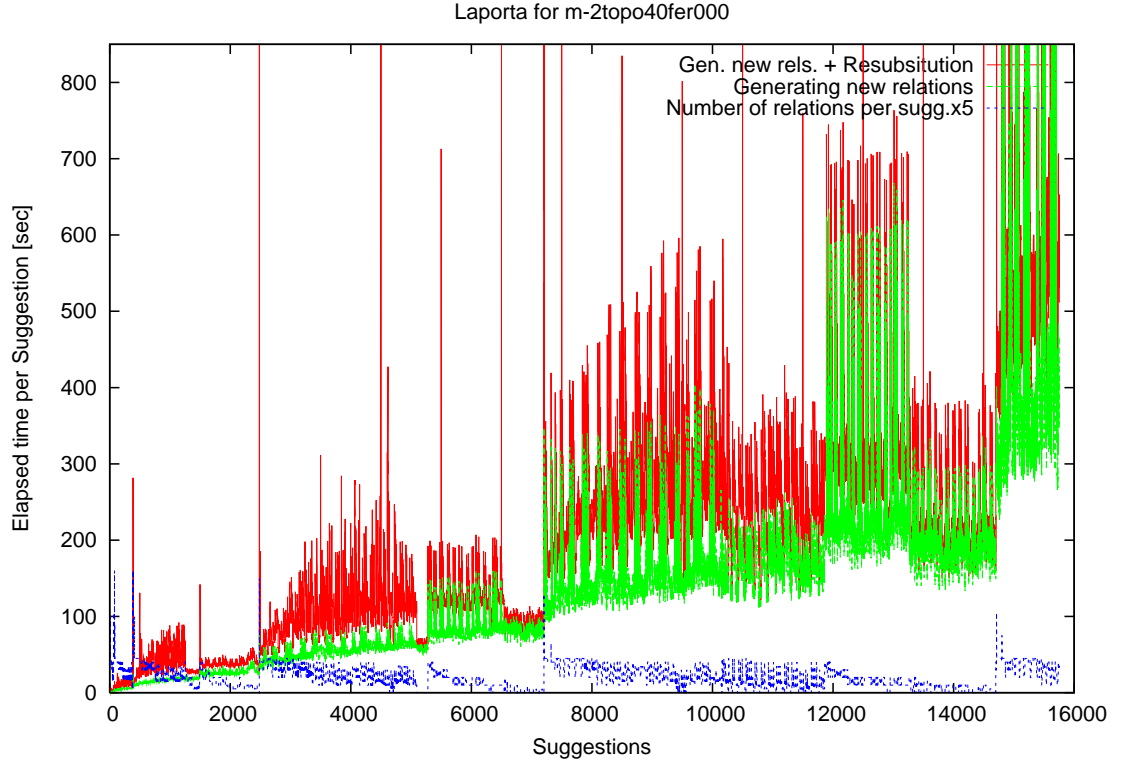


Figure A.3: Run-time behaviour for purely bosonic Basketball topology: The red curve shows the overall CPU-time needed to process the i -th suggestion and possible re-substitutions. The green curve displays only the CPU-time to process the i -th suggestion and the blue curve stands for the number ($\times 5$) of new relations which are found during the i -th suggestion.

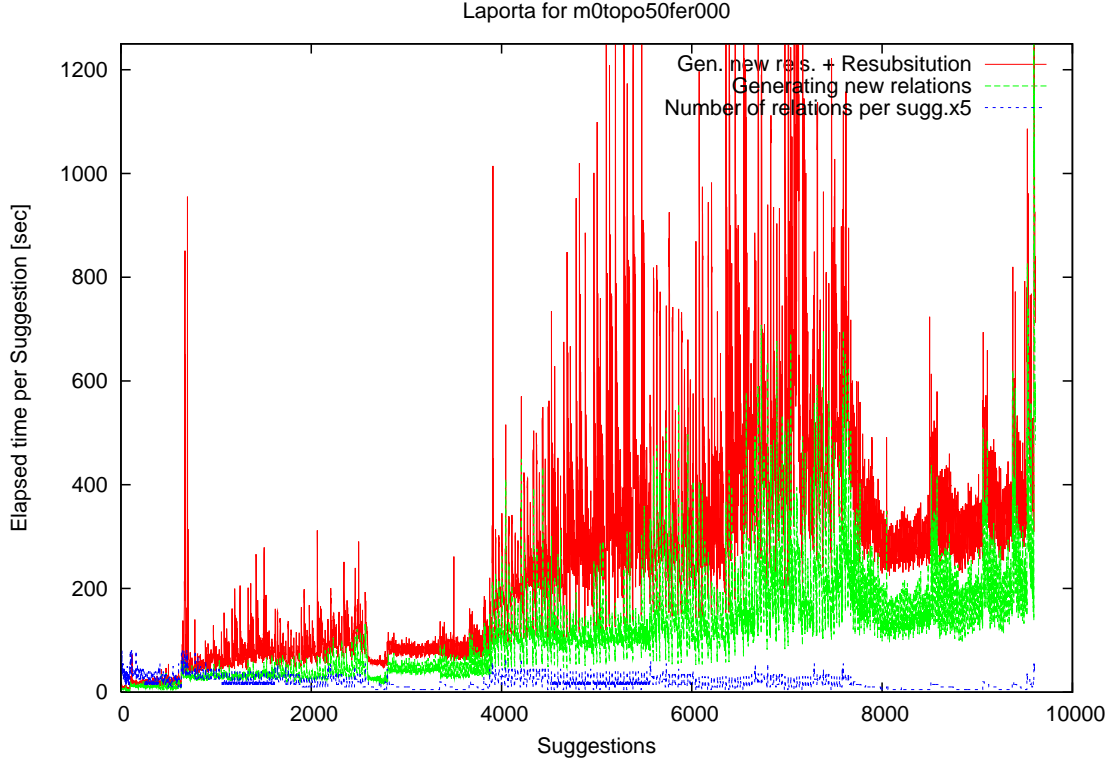


Figure A.4: Run-time behaviour for purely bosonic Spectacles topology: The red curve shows the overall CPU-time needed to process the i -th suggestion and possible re-substitutions. The green curve displays only the CPU-time to process the i -th suggestion and the blue curve stands for the number ($\times 5$) of new relations which are found during the i -th suggestion.

Let us try to get a rough estimation for the total amount of computing ressources we used for this project:

$$T \sim \underbrace{0.1 \times 3 \cdot 10^9}_{\sim 0.1 \times \text{Xeon}} \times \underbrace{14}_{\text{jobs}} \times \underbrace{2.6 \cdot 10^6}_{1 \text{ month}} \approx 10^{16} \text{ flop.}$$

A.5 Example Code

```

1 id I(fb(s1?,s2?,s3?,s4?,s5?,s6?),fc(sc1?,sc2?,sc3?),fq0(sq1?,sq2?,sq3?)) =
2 Ia(fb(s1,s2,s3,s4,s5,s6),fc(sc1,sc2,sc3),fq0(sq1,sq2,sq3))
3 -((p0)^(sq1)*(p0-q0)^(sq2)*(p0-r0)^(sq3))*
4 (Ia(fb(s1,s4,s5,s2,s3,s6),fc(sc1,mod_(sc2+sc1,2),mod_(sc3+sc1,2))));
5
6 id Ia(fb(s1?,s2?,s3?,s4?,s5?,s6?),fc(sc1?,sc2?,sc3?))*p0^s7*q0^s8*r0^s9 =
7 Ia(fb(s1,s2,s3,s4,s5,s6),fc(sc1,sc2,sc3),fq0(s7,s8,s9));

```

Listing A.1: Symmetry shown in Fig. 2.4 in FORM notation

```

1 id I(fb(s1?pos_,s2?pos_,s3?pos_,s4?pos_,s5?pos_,s6?pos_),fc(1,1,1),
2 fq0(sq1?,sq2?,sq3?)) =
3 ((-r0)^(sq1)*(q0-r0)^(sq2)*(p0-r0)^(sq3))*Ib(fb(s5,s4,s1,s6,s3,s2),fc(0,0,1));
4 *-----shift (fc(1,1,1) -> fc(0,0,1))-----*
5
6 id Ib(fb(s1?,s2?,s3?,s4?,s5?,s6?),fc(sc1?,sc2?,sc3?))*p0^sq1*q0^sq2*r0^sq3 =
7 I(fb(s1,s2,s3,s4,s5,s6),fc(sc1,sc2,sc3),fq0(sq1,sq2,sq3));

```

Listing A.2: Fermion shift $I_{...,1,1,1;...} \rightarrow I_{...,0,0,1;...}$ shown in Fig. 2.5 in FORM notation

```

1 id I(fb(s1?pos_,s2?pos_,s3?pos_,s4?neg0_,s5?pos_,s6?pos_),fc(sc1?,sc2?,sc3?),
2 fq0(sq1?,sq2?,sq3?))=
3 (-q0)^(sq2)*(-p0)^(sq3)*(-r0)^(sq1)*
4 (Id(fb(s3,s2,s1,s6,s5,s4),fc(sc3,sc2,sc1)));
5
6 id Id(fb(s1?,s2?,s3?,s4?,s5?,s6?),fc(sc1?,sc2?,sc3?))*p0^sq1*q0^sq2*r0^sq3 =
7 I(fb(s1,s2,s3,s4,s5,s6),fc(sc1,sc2,sc3),fq0(sq1,sq2,sq3));

```

Listing A.3: Shift $I_{1,1,1,0,1,1;...} \rightarrow I_{1,1,1,1,1,0;...}$ in FORM notation

```

1 id I(fb(s1?,s2?,s3?,s4?,s5?,s6?),fc(sc1?,sc2?,sc3?),fq0(sq1?,sq2?,sq3?)) =
2 +Ia(fb(-1+s1,s2,s3,1+s4,s5,s6),fc(sc1,sc2,sc3),fq0(sq1,sq2,sq3))*(-s4)
3 +Ia(fb(-1+s1,s2,s3,s4,1+s5,s6),fc(sc1,sc2,sc3),fq0(sq1,sq2,sq3))*(-s5)
4 +Ia(fb(1+s1,s2,s3,s4,s5,s6),fc(sc1,sc2,sc3),fq0(2+sq1,sq2,sq3))*(2*s1)
5 +Ia(fb(s1,-1+s2,s3,1+s4,s5,s6),fc(sc1,sc2,sc3),fq0(sq1,sq2,sq3))*(s4)
6 +Ia(fb(s1,s2,-1+s3,s4,1+s5,s6),fc(sc1,sc2,sc3),fq0(sq1,sq2,sq3))*(s5)
7 +Ia(fb(s1,s2,s3,1+s4,s5,s6),fc(sc1,sc2,sc3),fq0(1+sq1,1+sq2,sq3))*(-2*s4)
8 +Ia(fb(s1,s2,s3,1+s4,s5,s6),fc(sc1,sc2,sc3),fq0(2+sq1,sq2,sq3))*(2*s4)
9 +Ia(fb(s1,s2,s3,s4,1+s5,s6),fc(sc1,sc2,sc3),fq0(1+sq1,sq2,1+sq3))*(-2*s5)
10 +Ia(fb(s1,s2,s3,s4,1+s5,s6),fc(sc1,sc2,sc3),fq0(2+sq1,sq2,sq3))*(2*s5)
11 +Ia(fb(s1,s2,s3,s4,s5,s6),fc(sc1,sc2,sc3),fq0(sq1,sq2,sq3))*(-1-s5-s4-2*s1+d);
12 *-----IBP (dk1,k1)-----*

```

Listing A.4: Integration by parts relation in FORM notation

Acknowledgements

Ich möchte PD Dr. York Schröder für die Einführung in das interessante Gebiet der computergestützten Störungstheorie und der hervorragenden Betreuung während dieser Arbeit danken. Darüberhinaus danke ich Prof. Dr. Mikko Laine für die Begutachtung dieser Arbeit. Des weiteren gebührt mein Dank Dipl. Phys. Florian Kühnel für lebhafte Diskussionen während dieser Arbeit.

Zu guter Letzt danke ich meinen Eltern die mir jegliche Freiheiten während des Studiums gewährt haben.

Erklärung

Hiermit versichere ich, die vorliegende Arbeit selbstständig und mit keinen weiteren als den im Literaturverzeichnis angegebenen Hilfsmitteln angefertigt zu haben.

Bielefeld, 09.04.09

Bibliography

- [1] M. Veltman. SCHOONSCHIP. *CERN preprint*, 1967.
- [2] A.C. Hearn. REDUCE user’s manual Version 3.8. *RAND publication, Santa Monica*, 2004.
- [3] Chris A. Cole and Stephen Wolfram. SMP: A SYMBOLIC MANIPULATION PROGRAM. To be publ. in Proc. of 1981 ACM Symposium on Symbolic and ALgebraic Computation.
- [4] J.A.M.Vermaseren. *FORM version 3.2 Reference manual*. November 2007.
- [5] K. G. Chetyrkin and F. V. Tkachov. Integration by Parts: The Algorithm to Calculate beta Functions in 4 Loops. *Nucl. Phys.*, B192:159–204, 1981.
- [6] A. V. Smirnov and Vladimir A. Smirnov. Applying Groebner bases to solve reduction problems for Feynman integrals. *JHEP*, 01:001, 2006.
- [7] A. V. Smirnov and V. A. Smirnov. S-bases as a tool to solve reduction problems for Feynman integrals. *Nucl. Phys. Proc. Suppl.*, 160:80–84, 2006.
- [8] S. Laporta. High-precision calculation of multi-loop Feynman integrals by difference equations. *Int. J. Mod. Phys.*, A15:5087–5159, 2000.
- [9] Charalampos Anastasiou and Achilleas Lazopoulos. Automatic integral reduction for higher order perturbative calculations. *JHEP*, 07:046, 2004.
- [10] A. V. Smirnov. Algorithm FIRE – Feynman Integral REduction. 2008.
- [11] Gudrun Heinrich. Sector Decomposition. *Int. J. Mod. Phys.*, A23:1457–1486, 2008.
- [12] A. V. Smirnov and M. N. Tentyukov. Feynman Integral Evaluation by a Sector decomposition Approach (FIESTA). 2008.
- [13] Y. Schröder. Loops for Hot QCD. *Nucl. Phys. Proc. Suppl.*, B183:296–301, 2008.
- [14] J. I. Kapusta and C. Gale. *Finite-Temperature Field Theory Principles and Applications Second Edition*. Cambridge University Press, 2006.
- [15] L. F. Abbott. The Background Field Method Beyond One Loop. *Nucl. Phys.*, B185:189, 1981.
- [16] L. F. Abbott. Introduction to the Background Field Method. *Acta Phys. Polon.*, B13:33, 1982.

- [17] M. Laine. *Lecture notes: Quantum Field Theory*. University of Bielefeld, 2005.
- [18] Cheng-xing Zhai and Boris M. Kastening. The Free energy of hot gauge theories with fermions through g^{*5} . *Phys. Rev.*, D52:7232–7246, 1995.
- [19] Eric Braaten and Agustin Nieto. Free Energy of QCD at High Temperature. *Phys. Rev.*, D53:3421–3437, 1996.
- [20] David J. Gross, Robert D. Pisarski, and Laurence G. Yaffe. QCD and Instantons at Finite Temperature. *Rev. Mod. Phys.*, 53:43, 1981.
- [21] Andrei D. Linde. Infrared Problem in Thermodynamics of the Yang-Mills Gas. *Phys. Lett.*, B96:289, 1980.
- [22] Eric Braaten. Solution to the perturbative infrared catastrophe of hot gauge theories. *Phys. Rev. Lett.*, 74:2164–2167, 1995.
- [23] Paul H. Ginsparg. First Order and Second Order Phase Transitions in Gauge Theories at Finite Temperature. *Nucl. Phys.*, B170:388, 1980.
- [24] Thomas Appelquist and Robert D. Pisarski. High-Temperature Yang-Mills Theories and Three-Dimensional Quantum Chromodynamics. *Phys. Rev.*, D23:2305, 1981.
- [25] M. Laine. *Lecture notes: Basics of Thermal Field Theory*. University of Bielefeld, 2008.
- [26] Scott Chapman. A New dimensionally reduced effective action for QCD at high temperature. *Phys. Rev.*, D50:5308–5313, 1994.
- [27] K. Kajantie, M. Laine, K. Rummukainen, and Y. Schröder. The pressure of hot QCD up to $g^{*6} \ln(1/g)$. *Phys. Rev.*, D67:105008, 2003.
- [28] Michael E Peskin and Daniel V Schroeder. *An Introduction to Quantum Field Theory; 1995 ed.* Westview, 1995.
- [29] Biagio Lucini and Michael Teper. SU(N) gauge theories in 2+1 dimensions: Further results. *Phys. Rev.*, D66:097502, 2002.
- [30] P. Giovannangeli. Two loop renormalization of the magnetic coupling in hot QCD. *Phys. Lett.*, B585:144–148, 2004.
- [31] M. Laine and Y. Schröder. Two-loop QCD gauge coupling at high temperatures. *JHEP*, 03:067, 2005.
- [32] Paul M. Stevenson. Optimized Perturbation Theory. *Phys. Rev.*, D23:2916, 1981.
- [33] Su-zhou Huang and Marcello Lissia. The Relevant scale parameter in the high temperature phase of QCD. *Nucl. Phys.*, B438:54–66, 1995.
- [34] P. Nogueira. *An Introduction to QGRAF 3.0*. Lisboa.

- [35] Paulo Nogueira. Automatic Feynman graph generation. *J. Comput. Phys.*, 105:279–289, 1993.
- [36] A.J.P. Heck and J.A.M. Vermaseren. *FORM for Pedestrians*. Amsterdam, October 2000.
- [37] Y. Schröder. Unpublished, used for hep-ph/0503061.
- [38] Robert H. Lewis. *Fermat User’s Guide for Windows, Linux, Unix, and Mac OSX v3.5.8*. June 14, 2005.
- [39] M. Tentyukov and J. A. M. Vermaseren. Extension of the functionality of the symbolic program FORM by external software. *Comput. Phys. Commun.*, 176:385–405, 2007.
- [40] Peter Arnold and Cheng-Xing Zhai. The Three loop free energy for pure gauge QCD. *Phys. Rev.*, D50:7603–7623, 1994.
- [41] Peter Arnold and Cheng-Xing Zhai. The Three loop free energy for high temperature QED and QCD with fermions. *Phys. Rev.*, D51:1906–1918, 1995.
- [42] A. Gynther, M. Laine, Y. Schröder, C. Torrero, and A. Vuorinen. Four-loop pressure of massless $O(N)$ scalar field theory. *JHEP*, 04:094, 2007.
- [43] Wolfram Reasearch. Mathematica 6.0.